# South Dakota Granular Moisture-Density Curve Development and Dynamic Cone Penetrometer Implementation

## Study SD2023-02
## Final Report

**Provided by**

**Quality Engineering Solutions, Inc.**

**9930 Grubbs Road, Wexford, Pennsylvania 15090**

**June 2026**

# Disclaimer

The contents of this report, funded in part through grant(s) from the Federal Highway Administration, reflect the views of the authors who are responsible for the facts and accuracy of the data presented herein. The contents do not necessarily reflect the official views or policies of the South Dakota Department of Transportation, the State Transportation Commission, or the Federal Highway Administration. This report does not constitute a standard, specification, or regulation.

The South Dakota Department of Transportation gives public notice of its policy to uphold and assure full compliance with the non-discrimination requirements of Title VI of the Civil Rights Act of 1964 and related Nondiscrimination authorities. Title VI and related Nondiscrimination authorities stipulate that no person in the United States of America shall on the grounds of race, color, national origin, religion, sex, age, disability, income level or Limited English Proficiency be excluded from the participation in, be denied the benefits of, or be otherwise subjected to discrimination under any program or activity receiving Federal financial assistance.

Any person who has questions concerning this policy or wishes to file a discrimination complaint should contact the Department's Civil Rights Office at 605-773-3540.

# Technical Report Documentation Page

| | | |
|---|---|---|
| 1. Report No.<br>SD2023-02 | 2. Government Accession No. | 3. Recipient's Catalog No. |
| 4. Title and Subtitle<br>South Dakota Granular Moisture-Density Curve Development and Dynamic Cone Penetrometer Implementation. | | 5. Report Date<br>03/31/2026 |
| | | 6. Performing Organization Code<br>[ |
| 7. Author(s)<br>Mona Nobakht, Ph.D., P.E.<br>Carlos Cary, Ph.D., P.E. | | 8. Performing Organization Report No. |
| 9. Performing Organization Name and Address<br>Quality Engineering Solutions<br>9930 Grubbs Road, Wexford, Pennsylvania 15090 | | 10. Work Unit No. (TRAIS) |
| | | 11. Contract or Grant No. |
| 12. Sponsoring Agency Name and Address<br>South Dakota Department of Transportation<br>Office of Research<br>700 East Broadway Avenue<br>Pierre, SD 57501-2586 | | 13. Type of Report and Period Covered<br>Final Report |
| | | 14. Sponsoring Agency Code |
| 15. Supplementary Notes | | |

16. Abstract


The South Dakota Department of Transportation (SDDOT) currently estimates optimum moisture content (OMC) and maximum dry unit weight (MDUW) for granular materials using one-point Proctor tests together with the Ohio Highway Department (OHD) moisture–density family of curves. Because the OHD curves were developed using materials from outside South Dakota, their applicability to local granular materials is uncertain. This study redeveloped the SDDOT moisture–density family of curves using compaction data collected from South Dakota construction projects and evaluated the applicability of the Dynamic Cone Penetrometer (DCP) specification for compaction quality control.

A database of 294 compaction curves was compiled and analyzed to develop SDDOT moisture–density relationships. Regression analysis was used to estimate OMC and MDUW values, and a new family of curves was generated using Gaussian models. The curves were converted to wet unit weight relationships and expanded using a universal model to produce curves at 1-pcf density increments. Verification and validation analyses demonstrated improved prediction accuracy of the new SDDOT curves compared with the OHD curves. An Excel-based tool was also developed to automate the determination of compaction parameters from one-point Proctor test data. The applicability of the MnDOT DCP specification for SDDOT materials was evaluated using side-by-side field data, including DCP measurements, sand cone density tests, nuclear density gauge measurements, and proctor test results. The analysis showed generally good agreement between DCP-based compaction acceptance and density-based criteria. Optimization analysis identified adjustments to allowable Dynamic Penetration Index (DPI) and SEAT thresholds that improved agreement between the two methods. The study recommends adoption of the new SDDOT moisture–density curves, implementation of the automated Excel tool, and a three-year parallel implementation program to verify correct implementation and integration of the refined DCP specification with the new SDDOT moisture-density curves and to validate the combined field performance.


| | | | |
|---|---|---|---|
| 17. Key Words<br>Family of moisture-density curves, Dynamic Cone Penetrometer, compaction quality control, granular materials, one-point Proctor | | 18. Distribution Statement | |
| 19. Security Classification (of this report)<br>Unclassified | 20. Security Classification (of this page)<br>Unclassified | 21. No. of Pages<br>[Total number of pages] | 22. Price |

Form DOT F 1700.7 (8-72) Reproduction of completed page authorized

# South Dakota Granular Moisture-Density Curve Development and Dynamic Cone Penetrometer Implementation


*By*
Mona Nobakht, Ph.D., P.E.
Carlos, Cary, Ph.D., P.E. (Principal Investigator)
Quality Engineering Solutions (QES)


*Prepared for*
South Dakota Department of Transportation


June 2026

**Final Report**

SD2023-02

# Acknowledgments

This work was performed under the direction of the SD2023-02 Technical Panel:

| | | | |
|---|---|---|---|
| Jason Baker | Rapid City Area | Dave Huft | ITS |
| Thad Bauer | Research | Bryce Kampa | Geotechnical |
| Mike Border | Research | Donel Lemler | Region Materials |
| John DeBoer | Research | Jason Smith | Region Materials |
| Travor Diegel | Materials and Surfacing | Cliff Reuer | SDLTAP |
| Tom Grannes | Materials and Surfacing | Andy Vandel | Research |
| Gill Hedman | SDLTAP | Kirk Van Roekel | FHWA |

# Table of Contents

# List of Tables

# List of Figures

# List of Equations

# List of Abbreviations and Acronyms

DCP..................Dynamic Cone Penetrometer

DPI...................Dynamic Penetration Index

DUW................Dry Unit Weight

FP.....................False Positive

FN.....................False Negative

GN....................Grading Number

GUI...................Graphical User Interface

MAD.................Mean Absolute Deviation

MC....................Moisture Content

MDUW..............Maximum Dry Unit Weight

MnDOT..............Minnesota Department of Transportation

NDG...................Nuclear Density Gauge

NPA...................Negative Percent Agreement

OHD...................Ohio Highway Department

OMC..................Optimum Moisture Content

PPA....................Positive Percent Agreement

pcf......................Pounds per Cubic Foot

QES....................Quality Engineering Solutions

$R^2$.......................Coefficient of Determination

SDDOT..............South Dakota Department of Transportation

SEAT..................Dynamic Cone Penetrometer Seating Penetration

TP......................True Positive

TN.....................True Negative

VBA...................Visual Basic for Applications

WUW................Wet Unit Weight

# Executive Summary

## Problem Description

The South Dakota Department of Transportation (SDDOT) currently estimates optimum moisture content (OMC) and maximum dry unit weight (MDUW) for granular materials using one-point Proctor tests in combination with the Ohio Highway Department (OHD) moisture-density family of curves. Because the OHD curves were developed using materials from outside South Dakota, they may not accurately represent the compaction characteristics of granular materials commonly used in the state. Previous research conducted under projects SD2014-12 and SD2019-05 attempted to develop SDDOT-specific curves and evaluate the potential use of the Dynamic Cone Penetrometer (DCP) as a compaction quality control tool. However, limitations in the available datasets and the need for additional verification were identified.

During this study, systematic calculation errors were discovered in the dataset used to develop the earlier SDDOT curves, indicating the need for redevelopment using corrected and expanded data. In addition, the determination of compaction parameters from one-point Proctor tests requires multiple manual calculations which can introduce errors and inconsistencies. Further evaluation of the DCP specification was also needed before implementation. This study was conducted to redevelop the SDDOT moisture-density family of curves, develop an automated tool for determining compaction parameters, and evaluate and refine the DCP specification for South Dakota granular materials.

## Research Objectives

The objectives of this study were to:

- Perform an analysis of the moisture-density data supplied by SDDOT and refine the SDDOT moisture density family of curves.
- Analyze the proposed DCP specifications for agreement with the new moisture-density curves for subbase, base course, salvaged base course, and salvaged subbase materials.
- Develop DCP specifications specific to the granular materials used by the SDDOT.

## Task Descriptions

The research effort was conducted between February 2024 and March 2026 and consisted of several major tasks. First, a comprehensive database of moisture-density relationships was developed by compiling compaction curve data from previous research studies and new datasets provided by SDDOT. The compiled datasets were reviewed and subjected to data quality checks to remove duplicate records, resolve inconsistencies, and exclude unreliable data. During this process, systematic errors were identified in the SD2014-12 dataset, and those data were excluded from further analysis.

Regression analyses were then performed on the remaining compaction datasets to estimate optimum moisture content (OMC) and maximum dry unit weight (MDUW) for each curve. A quadratic spline function was used to determine these parameters accurately. The resulting datasets were grouped according to MDUW ranges, and statistical analyses were conducted to develop a new SDDOT family of moisture-density curves using a Gaussian regression model. The newly developed dry unit weight curves were subsequently converted to wet unit weight relationships to align with SDDOT practice and reduce the potential for calculation errors in field applications.

To facilitate practical use of the new curves, an Excel-based computational tool was developed using Visual Basic for Applications (VBA). The tool allows users to input either moisture-density values or raw Proctor test data, and it automatically determines the corresponding OMC and MDUW by comparing the data to the revised SDDOT family of curves.

The applicability of the MnDOT DCP specification was evaluated by analyzing side-by-side field test data, including DCP measurements, sand cone density tests, nuclear density gauge measurements, and Proctor test results. Compaction acceptability determined from the DCP specification was compared with relative compaction values calculated using both the OHD and the newly developed SDDOT moisture-density curves. Finally, optimization analyses were conducted to assess whether modifications to the existing DCP specification parameters could improve agreement between DCP-based and density-based compaction acceptance criteria.

## Findings and Conclusions

A total of 294 unique compaction curves were used to develop the new SDDOT family of curves. The redevelopment effort corrected deficiencies in the earlier SDDOT curves by eliminating overlapping curves, expressing the family in terms of wet unit weight, centering curve peaks on a fitted line of optimums, and developing a universal model that permits interpolation at 1-pcf increments. Compared with the original SDDOT family, the new system enables direct determination of OMC and MDUW from the curves, provides smooth transitions across the wet unit weight range, offers 1-pcf spacing rather than 2-pcf spacing, and covers a broader range of moisture contents.

Comparison with the OHD family of curves showed that the OHD line of optimum generally falls within the 95 percent prediction interval for South Dakota granular materials. However, outside the approximate MDUW range of 117 to 131 pcf, the OHD line deviates from the expected trend and tends to overestimate the required compaction. Statistical testing indicated a mean difference of 2.01 pcf between the OHD and SDDOT line-of-optimum relationships, confirming that the OHD curves generally require higher compaction levels than the new SDDOT curves.

Verification and validation analyses confirmed the improved performance of the new SDDOT curves. Verification using randomly selected four-point datasets showed lower mean absolute deviations in predicted OMC and MDUW for the SDDOT curves than for the OHD curves. Validation using 42 new compaction curves demonstrated that the SDDOT family of curves performed better than the OHD curves overall, with the 1-pcf SDDOT curves providing improved accuracy for MDUW and both the 1-pcf and 2-pcf SDDOT curves performing similarly for OMC while outperforming the OHD curves.

The Excel-based tool developed under this project successfully automates moisture-density calculations for SDDOT granular materials by matching one-point Proctor results with the nearest curve from the newly developed 1-pcf SDDOT family of curves. Analysis showed that the tool effectively identifies appropriate moisture-density relationships and provides an accurate estimation of OMC and MDUW. Optional checks against four-point tolerances in the SDDOT Materials Manual and against the OHD curves enhance the reliability of the tool, and the program satisfies the functional requirements of the project as an efficient alternative to manual calculations.

The MnDOT DCP-based compaction specification showed generally good agreement with density-based compaction adequacy when evaluated using the new SDDOT curves. For the 2023–2025 dataset of non-recycled materials with grading number (GN) between 3.1 and 4.5, the DCP specification agreed with the relative density assessment 81 percent of the time when relative density was calculated using the SDDOT curves. The DCP specification underestimated compaction adequacy in 17 percent of cases and falsely predicted adequate compaction in 2 percent of cases. For salvaged materials evaluated using the test strip method, agreement was 80 percent, with 10 percent underestimation and 10 percent overestimation. Compared with the OHD curves, use of the new SDDOT curves resulted in fewer cases in which the DCP specification falsely predicted adequate compaction.

Refinement of the DCP specification showed that targeted adjustments to the Dynamic Penetration Index (DPI) and SEAT thresholds could improve agreement between DCP-based and density-based compaction acceptance for South Dakota granular materials while maintaining the overall structure of the MnDOT specification. Specifically, optimization analysis indicated that the maximum allowable DPI should be increased from 10 to 13 for materials with GN between 3.6 and 4.0 and moisture content (MC) less than 5 percent, and the maximum allowable SEAT should be increased from 45 to 50 for materials with GN between 3.6 and 4.0 and MC between 5 percent and 8 percent. All other thresholds remain unchanged. For the datasets included in the optimization analysis, these modifications improved agreement with the relative density criteria from 87 percent to 91 percent for the 2023–2025 database and from 76 percent to 79 percent for the 2019 database. Additional datasets containing a greater number of failed relative density cases would support further refinement of the specification.

## Recommendations

The recommendations presented in this summary are based on the findings and conclusions of this study related to the development of the new SDDOT moisture–density family of curves and the evaluation of the DCP specification for compaction quality control of granular materials. These recommendations are intended to assist SDDOT in implementing the results of this research and improving current compaction evaluation practices:

- It is recommended that SDDOT adopt the newly developed SDDOT moisture–density family of curves for determining OMC and MDUW of granular base and subbase materials.
- To ensure the ongoing reliability and accuracy of these curves, it is recommended that SDDOT periodically review and update the curves as additional compaction data become available, preferably at five-year intervals. Periodic updates would help ensure that the curves continue to reflect the characteristics of granular materials used in construction projects across the state.
- It is recommended that SDDOT implement the Excel-based tool developed in this study to automate the determination of OMC and MDUW from one-point Proctor test data.
- It is recommended that SDDOT collect DCP data side by side with relative density data for a three-year parallel implementation period to support validation and further refinement of the DCP specification.
- During the parallel implementation period, it is recommended that SDDOT continue using relative density, determined using the new SDDOT moisture–density family of curves, as the primary criterion for evaluating compaction adequacy of granular materials and collect the DCP data as a supplemental for validation purposes.
- It is recommended that SDDOT implement the refined DPI and SEAT threshold values identified in this study when adopting the DCP specification during the parallel implementation program.

# Chapter 1. Problem Description

Recent research efforts by the SDDOT aimed to improve current methods for the determination of target compaction parameters and compaction quality control of native granular materials. SDDOT currently relies on the OHD family of curves to estimate OMC and MDUW when performing one-point Proctor tests. These curves were developed using datasets from materials outside South Dakota and, therefore, may not accurately represent the compaction characteristics of granular materials commonly used in South Dakota construction projects.

The SDDOT Moisture-Density Family of Curves developed under research project SD2014-12 (Jones and Weber, 2019) showed potential for reducing the unnecessary construction costs resulting from the use of the OHD Moisture-Density Family of Curves, which tends to overestimate target compaction parameters. Follow-up research conducted under project SD2019-05 (Ghabchi, 2022) included a comprehensive field test program designed to verify the SDDOT Moisture-Density Family of Curves. Project SD2019-05 identified the need for refinement of the SDDOT Family of Curves to specifically address observed curve overlapping and to convert the curves using wet unit weight as a reference.

Rather than refinement, the need for redevelopment of the SDDOT Family of Curves arose in this study from the identification of systematic calculation errors in the original development. These errors, which were discovered during data compilation and cleansing, affected the accuracy of the moisture content and dry density values used in the original development of the curves. The revision of the SDDOT Moisture-Density Family of Curves intends to enhance the overall accuracy of the method by incorporating data that became available after project SD2014-12. Also, this revision should address the shortcomings identified in the SD2019-05 study.

Additionally, determining OMC and MDUW from one-point Proctor tests requires comparing the measured moisture and density values to the family of curves to identify the appropriate curve. This process involves multiple manual calculations and interpretation steps, which can be time-consuming and may introduce calculation or interpretation errors. The development of a computer program to automate the applicability of the SDDOT Moisture-Density Family of Curves and improve accuracy by minimizing operator induced variability was needed.

The SD2019-05 research project evaluated the potential use of the DCP as a compaction quality control tool for granular materials. Results from ten construction projects included in the study showed promising results for the use of the DCP as a compaction quality control device. However, the SD2019-05 project report recommended that additional verification be performed before the proposed draft DCP test specification could be considered for implementation in the field.

The DCP data collected during the SD2019-05 study, together with newer datasets obtained from the recent construction projects in South Dakota, should be evaluated using the new SDDOT family of curves developed in this study. The MnDOT DCP specification originally proposed in the SD2014-12 and SD2019-05 studies may require modification to better reflect the characteristics of South Dakota granular material.

# Chapter 2. Research Objectives

This chapter presents the objectives of the study and describes the research team's interpretation of each objective and the approach used to accomplish it. The objectives presented below were established at the beginning of the project to address the needs identified by the SDDOT related to improving the determination of compaction parameters and evaluating the applicability of the DCP testing for compaction quality control of granular materials.

## 2.1 Refinement of the SDDOT Moisture–Density Family of Curves

**Objective:** Perform an analysis of the moisture-density data supplied by the SDDOT and refine the SDDOT Moisture Density Family of Curves.

The redevelopment of the SDDOT Moisture-Density Family of Curves was necessary to incorporate additional Proctor test data that became available after the completion of earlier research projects and to address identified systematic calculation errors in the original development. The approach involved compiling moisture–density datasets from previous studies and newly available compaction test results. The datasets were reviewed for completeness and quality before being incorporated into a comprehensive database. Statistical and regression-based methods were then used to redevelop a family of moisture–density curves that better represent the compaction characteristics of granular materials used in South Dakota. The new SDDOT curves were also compared with the OHD moisture-density curves currently used by SDDOT to evaluate their relative performance.

In addition, the development of a computer-based tool was identified as a critical need to automate the determination of OMC and MDUW from one-point Proctor test results using the revised SDDOT family of curves. The approach involved implementing the revised moisture–density relationships into an Excel spreadsheet tool that allows users to input test data and automatically determine the appropriate compaction parameters. The tool was designed to simplify the analysis process, reduce calculation errors, and improve consistency in the determination of compaction parameters.

## 2.2 Evaluation of the DCP Specification and Assessment of Agreement Between DCP Acceptance Criteria and Relative Density Criteria

**Objective:** Analyze the proposed DCP specifications for acceptance agreement with the new moisture-density curves for subbase, base course, base course salvaged, and subbase salvaged.

There was a need to evaluate whether the DCP specification developed by the MnDOT can reliably indicate compaction adequacy for granular materials used in South Dakota. The approach involved compiling DCP test data from previous studies and newly available field datasets and comparing the compaction adequacy predicted by the DCP specification with compaction adequacy determined using relative density criteria. Relative density values were calculated using maximum dry unit weight values obtained from both the OHD and the newly developed SDDOT moisture–density family of curves. Statistical analyses were performed to quantify the level of agreement between the DCP-based acceptance criteria and the density-based compaction criteria.

## 2.3 Refinement of the DCP Specification

**Objective:** Develop the DCP specifications specific to the materials used by the SDDOT.

Refinement of the DCP specification proposed in the SD2014-12 and SD2019-05 studies would be needed if the analysis results indicated that improving the specification is feasible and would enhance its ability to represent the characteristics of South Dakota granular materials. The approach involved analyzing the compiled datasets to determine whether adjustments to the allowable DCP parameters could further optimize agreement with density-based compaction criteria while maintaining the overall structure of the specification.

# Chapter 3. Task Descriptions

This section documents the work completed by the research team between February 2024 and March 2026 to accomplish the project's objectives. The work is divided into ten tasks as described below.

## 3.1 Task 1: Meet with the Project's Technical Panel to Review the Project Scope and Work Plan

The project kick-off meeting was held virtually on February 16, 2024. The QES research team met with the project's technical panel to review the project scope and work plan. The research team delivered a presentation and addressed questions and comments from the technical panel. The research team's technical approach for completing the project tasks and meeting the research objectives was outlined, and additional details regarding data availability were discussed.

## 3.2 Task 2: Analyze the Moisture-Density Data Compiled by SDDOT from Past Construction Projects and Refine the SDDOT Moisture-Density Family of Curves

This task involved analyzing the moisture-density data compiled by SDDOT from past construction projects and using these data to redevelop the SDDOT Moisture-Density Family of Curves. The work began with the development of a master database by compiling available moisture-density datasets from previous research studies and additional compaction curves provided by SDDOT. The datasets were organized and subjected to data conditioning procedures that included removing duplicate records, addressing inconsistencies, and excluding unreliable data. These steps ensured that the database used for analysis contained consistent and representative compaction curves suitable for the redevelopment of the SDDOT Family of Curves.

Following preparation of the master database, regression analysis was conducted on individual compaction curves to estimate the OMC and MDUW for each dataset using a quadratic spline function. The resulting parameters were used to group the datasets according to MDUW ranges and to establish the line of optimums representing the relationship between OMC and MDUW for SDDOT granular materials. Regression analyses using non-linear functions were evaluated to determine an appropriate model for fitting the compaction data within each density range. Based on this evaluation, a Gaussian model was used to develop the SDDOT Family of Curves. The work also included the development of a global model to generate curves at different density increments and the verification and validation of the redeveloped curves using independent compaction datasets.

## 3.3 Task 3: Convert the SDDOT Family of Curves to Wet Unit Weight

After the analysis results were verified as satisfactory and approved by the technical panel, the final version of the refined SDDOT family of curves was produced by converting the dry unit weight-based moisture-density curves into wet unit weight-based relationships. This conversion was performed by dividing the dry unit weight values by one plus the corresponding moisture contents. The use of wet unit weights is intended to remove the potential for error in calculations by eliminating the additional step of computing dry unit weights. It also aligns with current practice in South Dakota.

## 3.4 Task 4: Prepare and Present for Approval of the Project's Technical Panel a Technical Memorandum that Summarizes the Findings of Tasks 2 & 3

The first technical memorandum was prepared and delivered to the project's technical panel for approval on September 9, 2024. It summarized the findings of Tasks 2 and 3 and included all relevant information necessary for the panel to conduct a comprehensive evaluation of the project's progress. The memorandum documented the analysis conducted to develop the new SDDOT family of curves.

## 3.5 Task 5: Develop an Excel Spreadsheet to Calculate OMC and MDUW Based on One-Point Proctor Test's Moisture and Density Information Utilizing the SDDOT Moisture-Density Family of Curves Approved by the Project's Technical Panel

The Excel spreadsheet was developed to automatically calculate MDUW and OMC from one-point proctor test moisture and density information by directly comparing the test data with the new SDDOT family of curves. The Excel spreadsheet makes use of the Visual Basic Application (VBA) Macro Programming tool to execute the computations while providing a user-friendly interface. Two data input modes were incorporated: 1) moisture and density information, and 2) raw proctor test information for calculation of moisture and density (i.e., weight of mold, weight of mold and specimen, etc.) Mode 2 is intended to minimize the potential for error from intermediate calculations to obtain moisture and density. Once data input is complete, a plot showing the one-point proctor moisture and wet density over the new SDDOT family of curves will be displayed on the screen by clicking a button, and the program automatically selects the curve nearest to the plotted point and determines the corresponding MDUW and OMC. In addition, optional verification checks are built into the code to evaluate compliance with prediction tolerances in the SDDOT Materials Manual and to compare results with the Ohio Highway Department family of curves.

## 3.6 Task 6: Prepare and Present for Approval of the Project's Technical Panel a Technical Memorandum that Summarizes the Suggested Changes to the Moisture-Density Curves and Present the Excel Spreadsheet Developed in Task 5

The second memorandum was submitted to the project's technical panel on January 29, 2025. The document included the changes made to the original SDDOT family of curves. It also presented the Excel program developed by the research team under Task 5 for the automated calculation of OMC and MDUW utilizing the new SDDOT family of curves approved by the project's technical panel.

## 3.7 Task 7: Analyze the DCP, Sand Cone, and Nuclear Density Gauge Side-by-Side Test Data Supplied by SDDOT for Agreement with the New Moisture-Density Curves

The purpose of this task was to evaluate the agreement between the DCP-based compaction acceptance criteria and the actual relative compaction levels achieved using the new SDDOT moisture-density curves, thereby assessing the applicability of the MnDOT DCP specification for SDDOT granular materials. The analysis used data from project sites included in the SD2019-05 study as well as more recent SDDOT field data collected between 2023 and 2025. Relative compaction was calculated by dividing in-situ densities from sand cone and nuclear density gauge tests by the corresponding target

MDUW values. For the 2023-2025 datasets, target MDUW values were determined using one-point Proctor test results and both the new SDDOT and the OHD family of moisture-density curves, following SD 104, Method 4 (SDDOT, 2015b). For the SD2019-05 study, one-point Proctor tests were not available. Therefore, the available four-point test data were used to determine target MDUW values per SD 104, Method 3 (SDDOT, 2015b).

The required data for assessing the DCP-based compaction criteria (including field MC, Grading Number (GN), and the measured SEAT and DPI values) were provided by SDDOT for the 2023-2025 database and extracted from the SD2019-05 study for the 2019 database. DCP-based compaction acceptability was then determined using the MnDOT DCP Specification (MnDOT, 2025) and compared with the compaction acceptability based on the relative density values calculated by using both the OHD and the new SDDOT moisture-density curves.

## 3.8 Task 8: Develop the DCP Specifications for Subbase, Base Course, Base Course Salvaged, and Subbase Salvages Specific to SDDOT Based on the Results of Task 7

The adequacy of the available data for developing a new DCP specification was evaluated in this task. Based on the level of agreement between the MnDOT DCP specification and the relative compaction results from Task 7, the analysis indicated that there was potential for improvement in the current specification. However, given the GN range of the materials included in the database, refining and optimizing the existing DCP specification was deemed more appropriate than developing an entirely new specification.

Accordingly, an optimization analysis was conducted to evaluate the current DPI and SEAT threshold values and identify potential modifications that could improve the agreement between DCP-based and relative density-based compaction acceptance. Following the optimization process, a statistical analysis was performed to compare the performance of the current specification with that of the refined specification.

## 3.9 Task 9: In Conformance with Guidelines for Performing Research for the South Dakota Department of Transportation, Prepare a Final Report Summarizing the Research Methodology, Findings, Conclusions, and Recommendations

A comprehensive final report has been prepared by the research team in accordance with SDDOT's guidelines for performing research. The report documents all aspects of the project, including the detailed research methodology, study findings, and a summary of conclusions and recommendations. It also includes the user manual for the Excel program developed to automate the calculation of OMC and MDUW from one-point proctor test moisture and density information. The report is subject to revision as needed to incorporate comments and feedback provided by the project's technical panel.

## 3.10 Task 10: Make an Executive Presentation to the SDDOT Research Review Board at the Conclusion of the Project

Upon completion of the research effort, the project research team will prepare and deliver an executive presentation to the SDDOT Research Review Board online. The presentation will cover all the work conducted under the research tasks and summarize the results, critical findings, conclusions, and recommendations.

# Chapter 4. Findings and Conclusions

This section describes in detail the analysis conducted and presents the corresponding findings and research products. The content is organized into four subsections to align with the objectives of the study:

## 4.1 Analysis of the Moisture-Density Data Compiled by SDDOT From Past Construction Projects and Refinement of the SDDOT Family of Curves

This section presents the analysis conducted to redevelop the SDDOT family of compaction curves using the available moisture–density data compiled from past construction projects. The work includes the development of the new curves, comparison with the OHD family of curves currently used by SDDOT, and verification of the accuracy of the newly developed curves. The procedures, analyses, and resulting findings associated with this effort are described in the following subsections:

### 4.1.1 Compiling the Master Database and Conditioning the Data

The initial step in developing the family of moisture-density curves was to build a master database by aggregating all available compaction curve datasets. These datasets included those used in previous studies as well as additional data collected after completion of the SD2014-12 project. Since the original moisture-density data from SD2014-12 were not available in Excel format, the research team extracted 471 moisture-density datasets embedded in charts from the SD2014-12 final report provided by SDDOT in Word format. Moisture-density data for an additional 10 compaction curves were extracted from the SD2019-05 final report (provided in PDF format) and converted to Excel format. SDDOT also supplied 291 new compaction curves, summarized in the four-point density sheets (DOT-40 forms) from the Aberdeen, Mitchell, Pierre, and Rapid City regions. All datasets were processed and organized into a unified Excel-based master database.

Data cleansing was then conducted on the master database to improve its quality by removing duplicates, addressing missing values, and correcting inconsistencies. During this process, the team identified 105 duplicates between the new data provided by SDDOT and the SD2014-12 study. These duplicated records shared the same Sample IDs (MST#) but contained different moisture content and dry density values. A quality check on 10% of these duplicates revealed a systematic calculation error in the SD2014-12 dataset: the tare weight had not been subtracted from the total weight of the dry sample plus tare, resulting in incorrect dry unit weight and moisture content values. As a result, the SD2014-12 data were deemed questionable and, after consulting with SDDOT, were excluded from further analysis. Additionally, seven more duplicates with different Sample IDs but identical moisture and density values were identified and removed. The final master database used for the redevelopment of the SDDOT Family of Curves, presented in Appendix A, includes 294 unique compaction curves.

### 4.1.2 Regression Analysis of Individual Compaction Curves

To identify the OMC and MDUW for each compaction curve, a detailed regression analysis was performed on the 294 compaction data sets. Several candidate functions were evaluated using the adjusted coefficient of determination ($R^2$) as the primary criterion for model selection. Among the functions tested, the quadratic spline function provided the best fit.

A quadratic spline function is a piecewise second-degree polynomial used to interpolate a set of data points while maintaining continuity in both the curve and its slope. This ensures there are no abrupt changes in the function or its rate of change between data points. The data range is divided into smaller intervals, each represented by its own quadratic equation, producing a smooth overall curve. The quadratic spline function provides a superior fit compared with other models and effectively captures the essential characteristics of the compaction curves, enabling accurate determination of OMC and MDUW for each dataset. Figure 1 illustrates an example of a quadratic spline fitted to a four-point moisture-density dataset, where the X-axis represents moisture content and the Y-axis represents dry unit weight. The estimated OMC and MDUW values for all 294 compaction curves are presented in Appendix A.

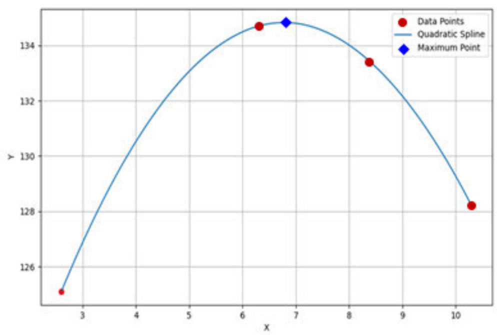


**2.6 ≤ x < 7.35**: Y= 0.0*(x-2.6)^2 + 128.2*(x-2.6) +133.7089

**7.35 ≤ x < 10.3**: Y= 0.0*(x-7.35)^2 + 0.0*(x-7.35) + 128.2

**OMC** = 6.8%
**MDUW** = 134.8

**Figure 1. Example of a Quadratic Spline Fit to a Sample**

### 4.1.3 Development of the SDDOT Family of Curves

After determining the OMC and MDUW for all compaction curves in the master database, the datasets were grouped by maximum dry unit weight in 2-pcf intervals. This categorization resulted in the 14 distinct groups illustrated in Figure 2 (see table in Appendix A for data values). Each group is labeled by an MDUW range in pcf. For example, the "MDUW 114-116" group includes all data from compaction curves with MDUW between 114 and 116 pcf.

The number of compaction curves in each group is provided in Table 1. The compaction curve counts for the first two groups indicate that there is insufficient data to reliably represent MDUW ranges below 118 pcf. Average MDUW and OMC values for each group are also summarized in Table 1 and plotted in Figure 3. Regression analysis was then performed on the plotted data to fit a function, and a fitted OMC was calculated for each group as a function of the average MDUW. The fitted OMC values were used, rather than the average OMC values, to establish the line of optimums for SDDOT granular materials. When developing the family curves, each curve must be centered on this line of optimums. This approach provides a smooth line of optimums, ensures seamless transition between curves, and minimizes the potential for curve overlap.

For the next step, a regression analysis was performed to identify the most suitable model for fitting all compaction test data points within each group. Several non-linear functions, such as the Gaussian, Lorentzian, Logistic, and Extreme Value models, were evaluated. These models were selected because their flexible regression parameters allow precise control over key curve attributes, including peak height (representing the average MDUW for each increment), peak position on the horizontal axis (representing the fitted OMC), and the width or steepness of the curve around the peak. This flexibility is essential for rationally capturing granular material behavior when developing the family of compaction curves.

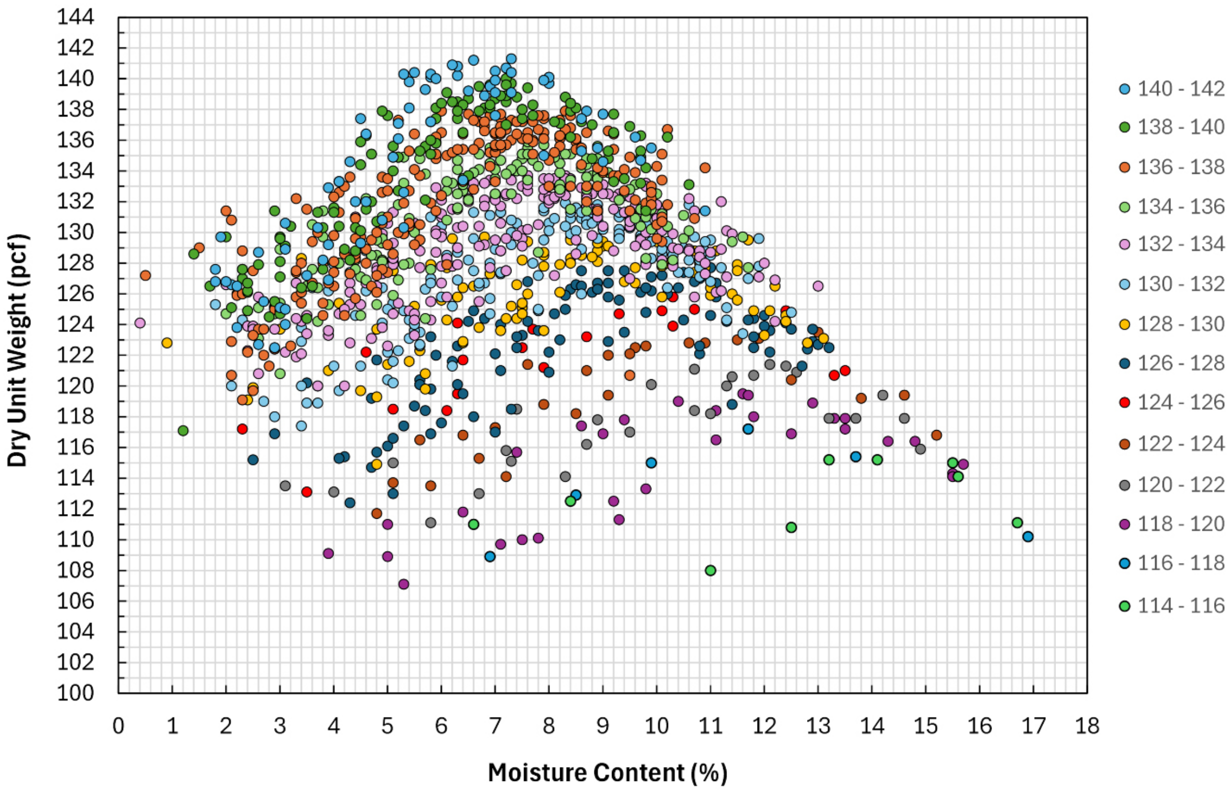


**Figure 2. Datasets Grouped by MDUW in 2-pcf intervals (See table in Appendix A for data values)**

**Table 1. Incremental MDUW and OMC Values**

| MDUW Range (pcf) | Dataset Counts | Average MDUW (pcf) | Average OMC (%) | Fitted OMC (%) |
|---|---|---|---|---|
| 114-116 | 2 | 115.4 | 13.96 | 13.50 |
| 116-118 | 1 | 117.2 | 11.85 | 12.71 |
| 118-120 | 6 | 119.2 | 11.55 | 11.92 |
| 120-122 | 6 | 121.3 | 11.77 | 11.17 |
| 122-124 | 6 | 123.3 | 10.84 | 10.55 |
| 124-126 | 5 | 125.0 | 9.60 | 10.07 |
| 126-128 | 23 | 127.0 | 9.84 | 9.53 |
| 128-130 | 22 | 129.2 | 9.07 | 9.03 |
| 130-132 | 37 | 131.1 | 8.64 | 8.61 |
| 132-134 | 52 | 133.1 | 8.06 | 8.23 |
| 134-136 | 33 | 134.9 | 7.75 | 7.90 |
| 136-138 | 52 | 137.0 | 7.57 | 7.56 |
| 138-140 | 29 | 139.1 | 7.26 | 7.24 |
| 140-142 | 18 | 141.0 | 6.99 | 6.98 |

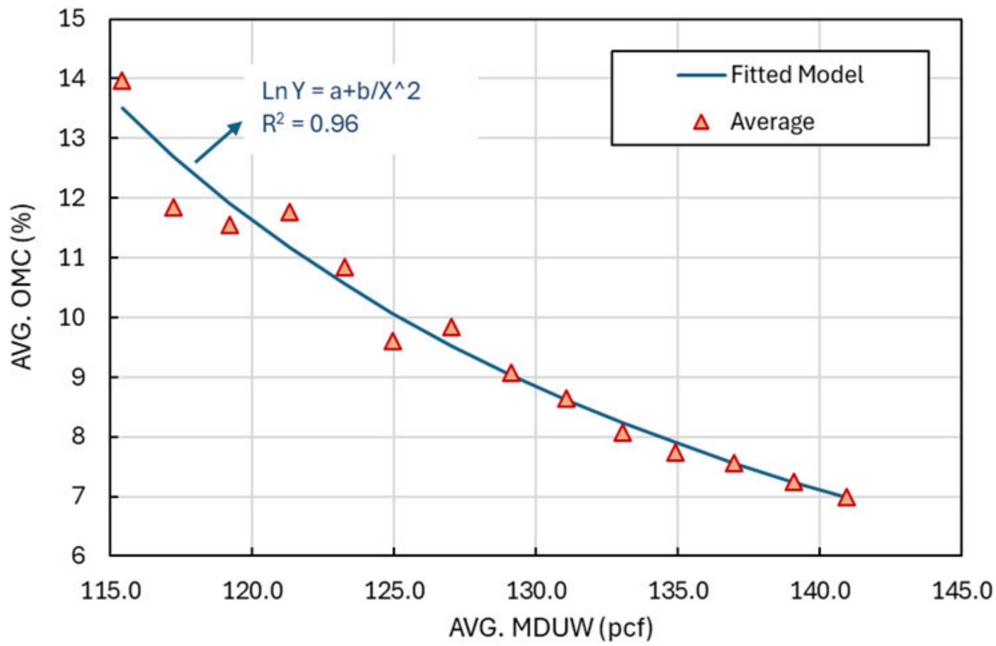


**Figure 3. OMC- MDUW Line of Optimums**

Of all the functions evaluated, the four-parameter Gaussian was chosen as the final fitting function, as it yielded the highest adjusted $R^2$ value. The Gaussian mathematical function reads as follows:

$$\mathbf{Y = a + b\,exp(-0.5(\frac{X-c}{d})^2)}$$

Where:

X = moisture content, %
Y= dry unit weight, pcf
a, b, c and d = regression coefficients

**Equation 1. The Gaussian Mathematical Function**

A set of constraints was established for the regression analysis to ensure rational and meaningful results. These constraints are as follows:

- Peak height or position in the vertical axis: the sum of parameters a and b represents the peak height of the model and was fixed to the average MDUW of each incremental group shown in Table 1.
- Peak position in the horizontal axis: parameter *c* represents the OMC and was set equal to the fitted OMC of each incremental group.
- Shape parameters: parameters *d* and *a* were defined as functions of the fitted OMC and are expressed mathematically as follows:

$$\mathbf{a} = \mathbf{0.26} \times \mathbf{OMC}^2 - \mathbf{8.35} \times \mathbf{OMC} + \mathbf{172.5}$$

$$\mathbf{d} = -\mathbf{0.013} \times \mathbf{OMC}^2 + \mathbf{0.37} \times \mathbf{OMC} + \mathbf{0.292}$$

**Equation 2. Formulation of Parameters *a* and *d* as a Function of OMC**

By implementing these constraints and using the fitted OMC for each group, the Gaussian model ensures a precise representation of the compaction curves, facilitates smooth transition across different MDUW intervals, and provides a robust fit to the data.

The newly developed family of curves (in terms of dry unit weight) is presented in Figure 4, with the corresponding data points color-coded by group (see table in Appendix A for data values). The adjusted $R^2$ value for each curve is shown in the figure, and the sets of regression coefficients for each increment are summarized in Table 2. In Figure 4, the adjusted $R^2$ values are generally greater than 0.5, which is considered satisfactory given the inherent variability in moisture-density relationship data. This indicates that the Gaussian model adequately explains the observed variance for more than half of the data. However, the adjusted $R^2$ values for the 114-116 and 128-130 pcf MDUW ranges fall below 0.5. These two datasets are shown in Figure 5. The 114-116 pcf range contains only two compaction test datasets, and as noted earlier, the database lacks sufficient data within this range, which contributes to the lower adjusted $R^2$ value. Additional moisture-density datasets within this MDUW range would improve the model's goodness of fit.

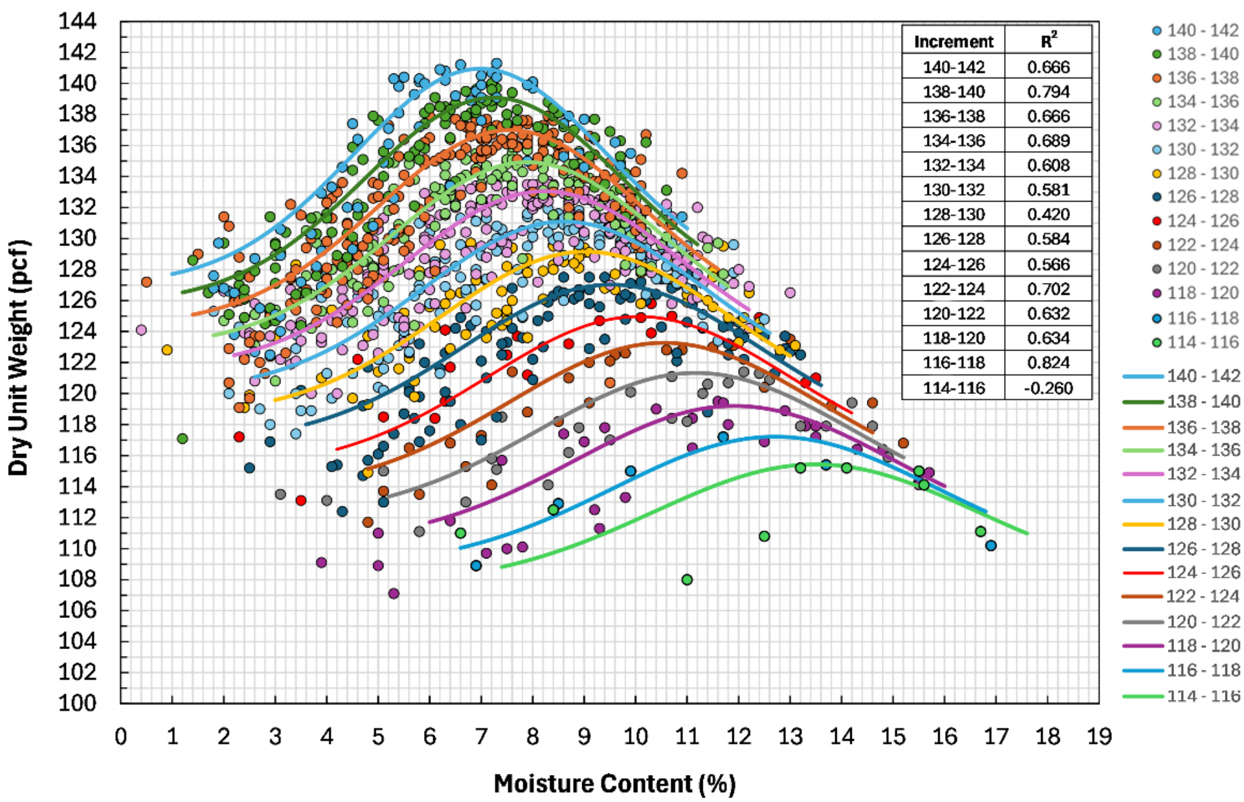


**Figure 4. Dry Unit Weight Family of Curves (See table in Appendix A for data values)**

**Table 2. Model Regression Coefficients for each MDUW Increment**

| MDUW Range | a | b | c | d |
|---|---|---|---|---|
| 114-116 | 107.61 | 7.84 | 13.50 | 3.16 |
| 116-118 | 108.77 | 8.45 | 12.71 | 3.14 |
| 118-120 | 110.26 | 8.95 | 11.92 | 3.10 |
| 120-122 | 111.98 | 9.35 | 11.17 | 3.05 |
| 122-124 | 113.61 | 9.67 | 10.55 | 3.00 |
| 124-126 | 115.04 | 9.93 | 10.07 | 2.94 |
| 126-128 | 116.77 | 10.26 | 9.53 | 2.88 |
| 128-130 | 118.51 | 10.64 | 9.03 | 2.81 |
| 130-132 | 120.06 | 11.04 | 8.61 | 2.75 |
| 132-134 | 121.55 | 11.50 | 8.23 | 2.69 |
| 134-136 | 122.93 | 11.99 | 7.90 | 2.63 |
| 136-138 | 124.39 | 12.60 | 7.56 | 2.57 |
| 138-140 | 125.79 | 13.29 | 7.24 | 2.51 |
| 140-142 | 126.99 | 13.97 | 6.98 | 2.46 |

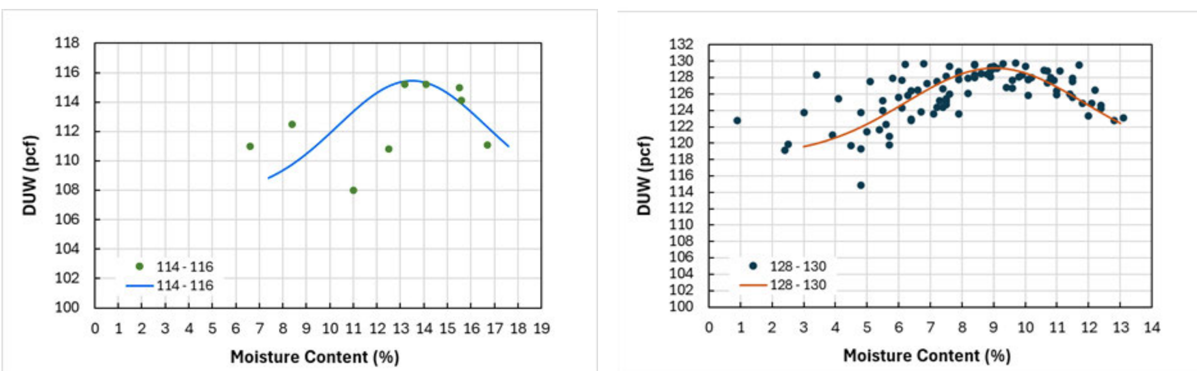


**Figure 5. 114-116 and 128-130 Curves**

For the 128-130 pcf MDUW range, the moisture-density data are more scattered and show greater variability, resulting in a lower adjusted $R^2$ value compared with other ranges. This increased variability may reflect heterogeneous material characteristics within this interval, potentially due to differences in granular material types (e.g. highly variable gravel-to-sand ratios) or other factors not fully captured by the model.

The newly developed family of curves, referred to as the SDDOT Family of Curves, was converted to wet unit weight by multiplying the dry unit weight values by one plus the corresponding moisture content. The resulting SDDOT Family of Curves in terms of wet unit weight are shown in Figure 6. These curves are truncated at five points below OMC and four points above OMC to cover a practical range of field compaction conditions for granular materials.

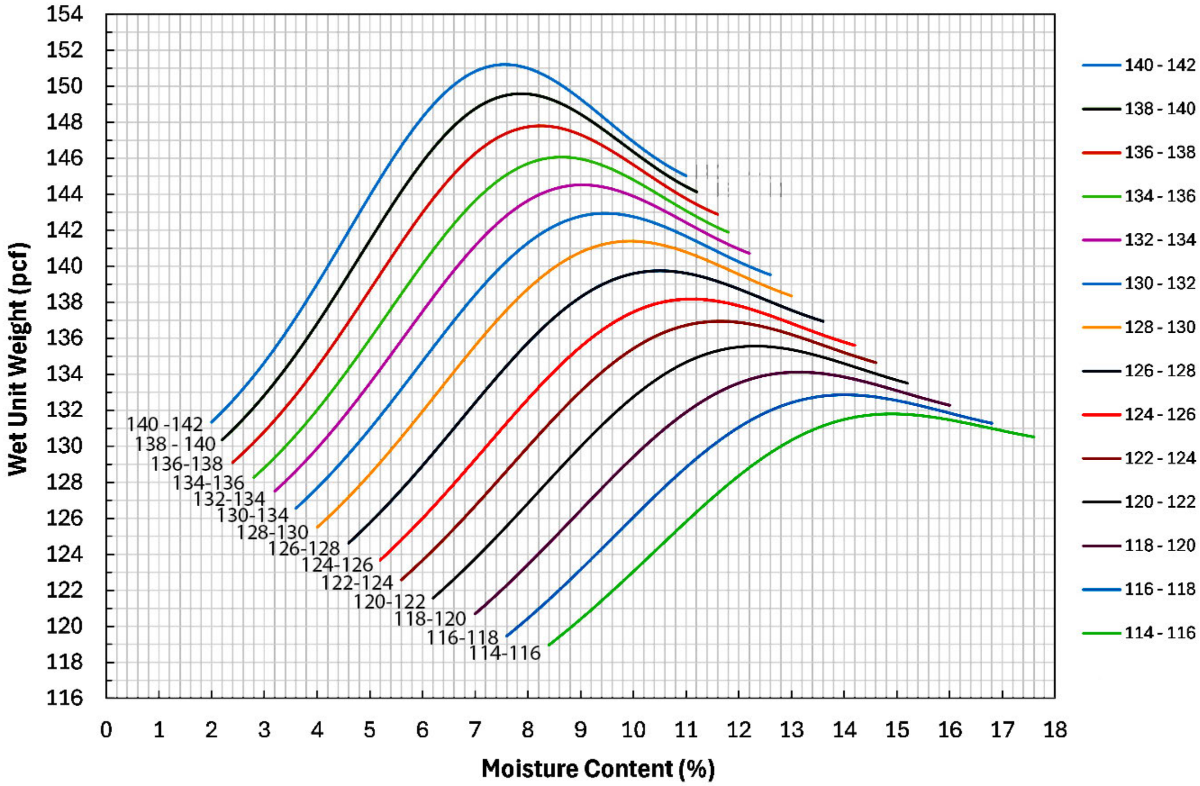


**Figure 6. SDDOT Wet Unit Weight Curves**

### 4.1.4 Comparison with the OHD Family of Curves

SDDOT currently compares four-point compaction test data with the OHD typical moisture-density curves to determine target compaction parameters. Section 4.1.4.1 presents an analysis to evaluate the adequacy of the OHD Family of Curves for use with SDDOT granular materials.

In addition, Section 4.1.4.2 presents a statistical analysis to quantify the magnitude of the differences between the line of optimums derived from the OHD and SDDOT families of curves. Section 4.1.4.3 provides a verification analysis to assess the accuracy of the newly developed SDDOT Family of Curves.

#### 4.1.4.1 Adequacy of the OHD Curves for Application to SDDOT Granular Materials

To assess the adequacy of the OHD Family of Curves for application to SDDOT granular materials, a prediction interval was developed to represent the range in which 95% of the MDUW values for South Dakota granular materials are expected to fall. If the OHD line of optimums lies within this 95% interval, the OHD Family of Curves can be considered potentially valid for use with South Dakota's granular base and subbase materials.

Creating this prediction interval requires the underlying data to be approximately normally distributed. Therefore, histograms were generated for all MDUW and OMC values using the 294 unique moisture-density datasets provided by SDDOT. These histograms, shown in Figures 7 and 8, indicate that although the dry unit weight data exhibit a slight rightward skew, they are reasonably consistent with a normal distribution.

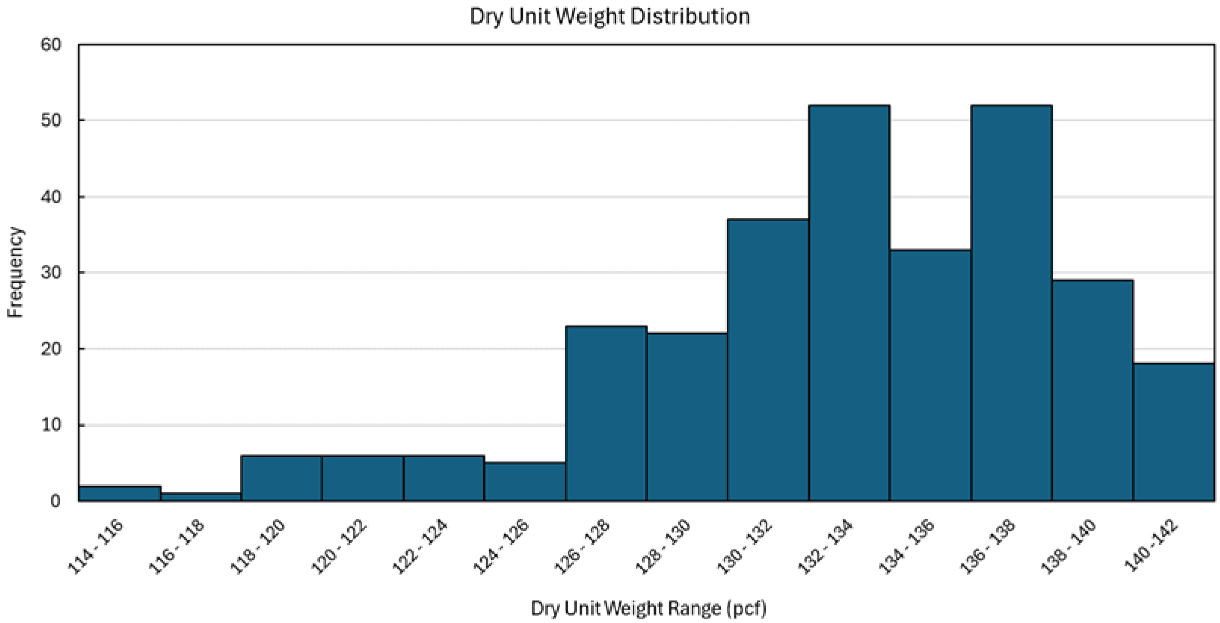


**Figure 7. MDUW Distribution**

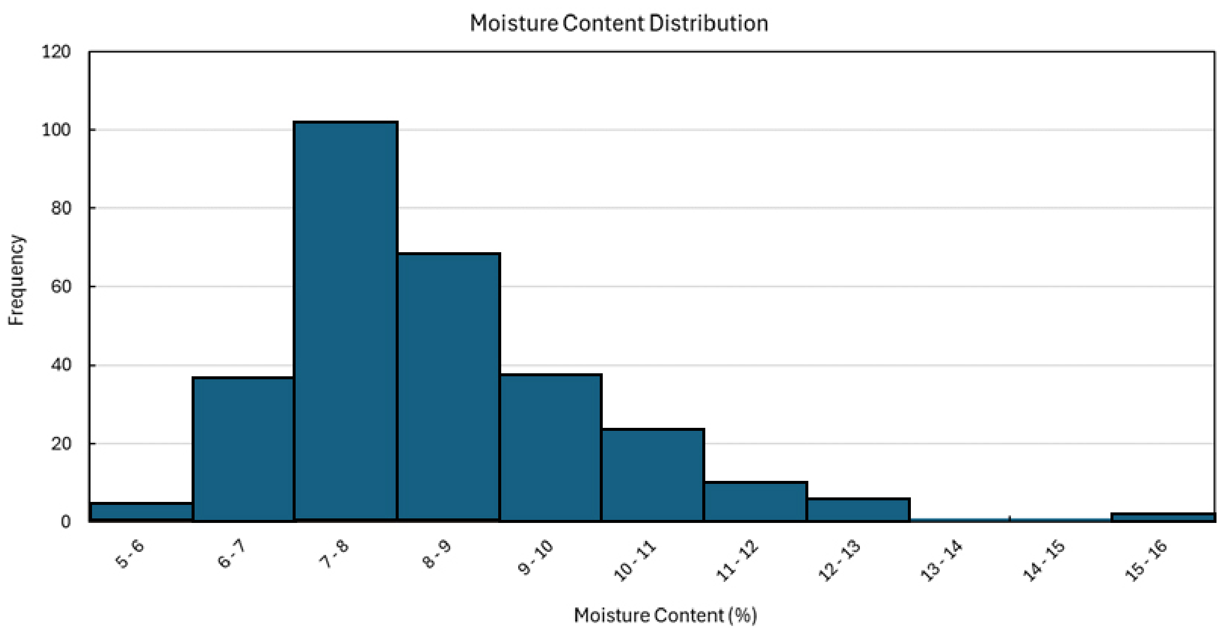


**Figure 8. OMC Distribution**

The OMC and MDUW values for all 294 compaction curves in the master database, estimated using the quadratic spline method (as described in Section 4.1.2), were plotted in Figure 9. A regression analysis was then performed to fit a function to the data, shown as the red line in the figure. The prediction interval was calculated using Equation 3, and the yellow bounds in Figure 9 illustrate the expected variability, providing a benchmark for comparison with the OHD Family of Curves.

$$Y_p = Y \pm t_\alpha SE\sqrt{(1 + \frac{1}{n} + \frac{(X - X_m)^2}{SS_{XX}})}$$

Where:

*Yp* = calculated interval boundaries for MDUW
*Y* = known MDUW from fitted function
$t_\alpha$ = alpha level (1.96 for a 95% confidence)
*SE* = standard error (*SE* = 3.19)
*n* = number of data points (*n* =294)
$SS_{XX}$ = sum of squared error ($SS_{XX}$ =758.71)
*X* = known OMC from fitted function
$X_m$= mean OMC ($X_m$= 8.41)

**Equation 3. Prediction Interval Formula**

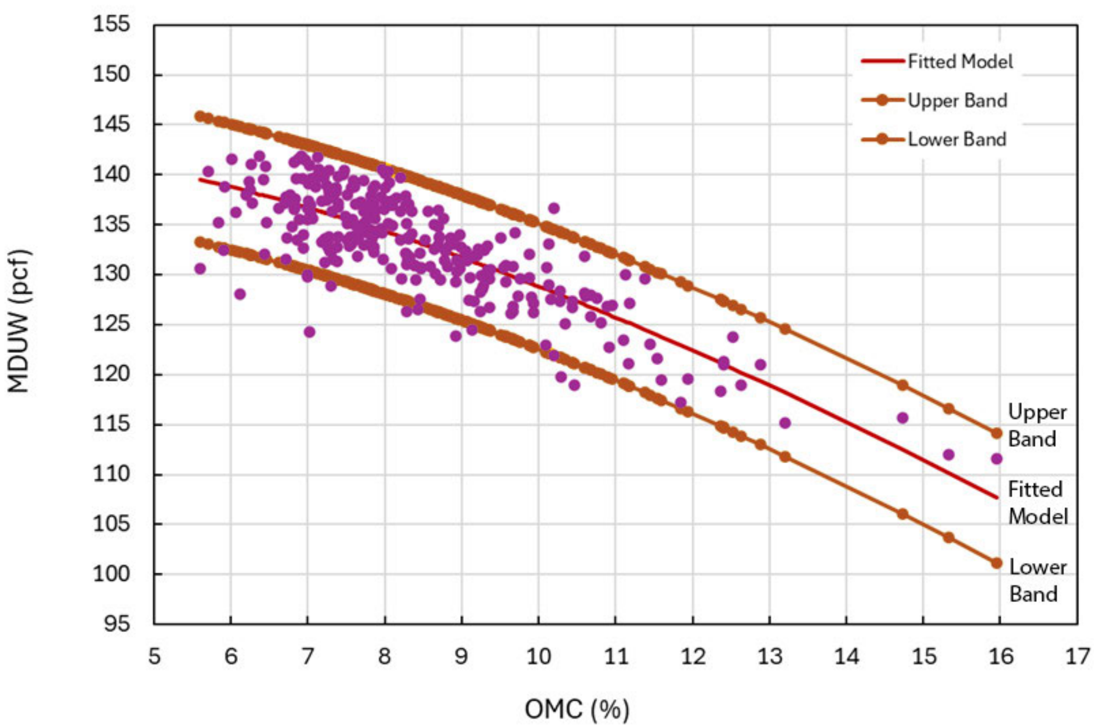


**Figure 9. 95% Prediction Interval for SDDOT Granular Materials**

In Figure 10, the OHD line of optimums is plotted over the prediction interval to assess the potential validity of the OHD Family of Curves for use with South Dakota's granular base and subbase materials. The plot shows that the OHD line of optimums falls within the prediction interval, suggesting that the OHD curves may be valid for use with South Dakota's granular materials. The OHD line of optimums closely follows the fitted regression line for dry unit weight values between approximately 117 and 131 pcf, indicating that materials within this range may be accurately represented by the OHD curves.

Outside this range, however, the OHD line deviates upward from the fitted regression line, suggesting a tendency to overestimate MDUW for South Dakota granular materials. Therefore, while the OHD Family of Curves may be applicable to some extent, caution should be exercised when applying these curves to materials with maximum dry unit weights outside the 117-131 pcf range.

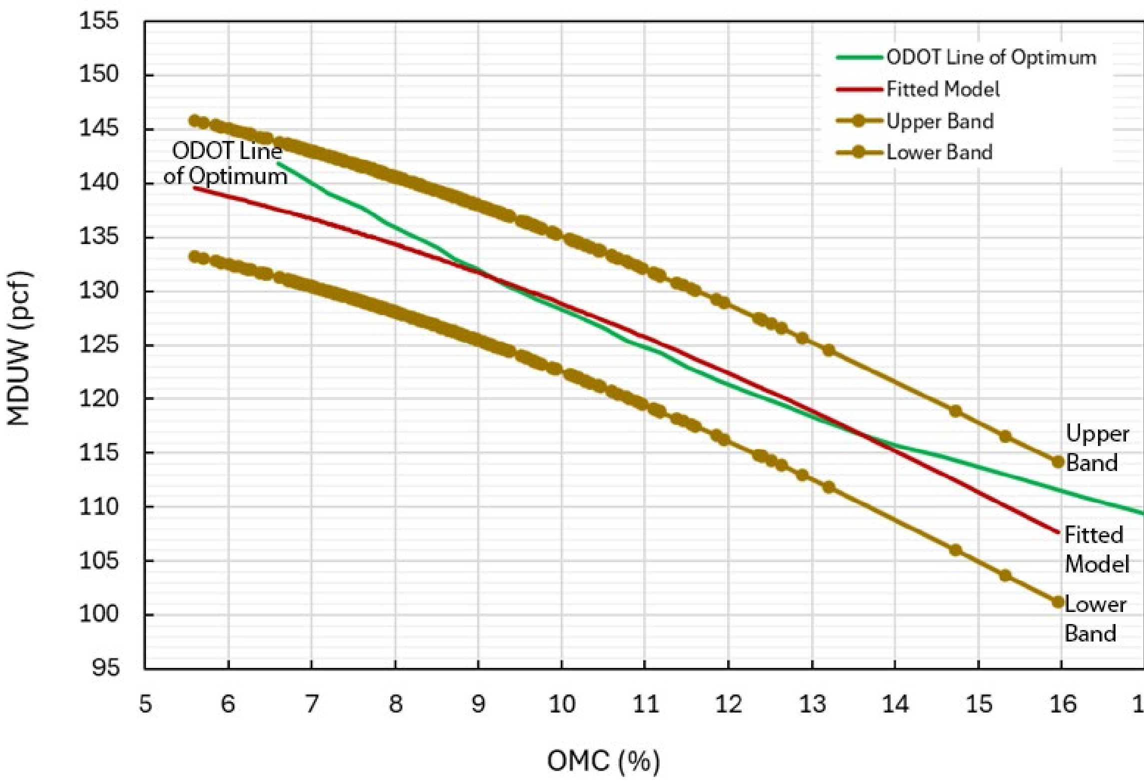


**Figure 10. Line of Optimums Plotted within the 95 Percent Prediction Interval**

### 4.1.4.2 Lines of Optimums Comparison

This section presents the statistical analysis conducted to quantify the magnitude of the difference between the OHD and SDDOT lines of optimums. As shown in Figure 11, a noticeable difference exists between the two lines. This difference was statistically evaluated for both significance and magnitude. Visual inspection also suggests that the OHD Family of Curves may overestimate compaction.

According to Section 3.4E of the SDDOT Materials Manual, Method 104 (SDDOT, 2015b), if the maximum density determined from the OHD Family of Curves deviates by more than ±3 pcf from the four-point range, the Region Materials Engineer should be contacted. Accordingly, Figure 11 includes dotted lines representing the ±3 pcf limits relative to the line of optimums derived from the SDDOT four-point compaction data. The OHD line of optimums falls mostly within these bounds.

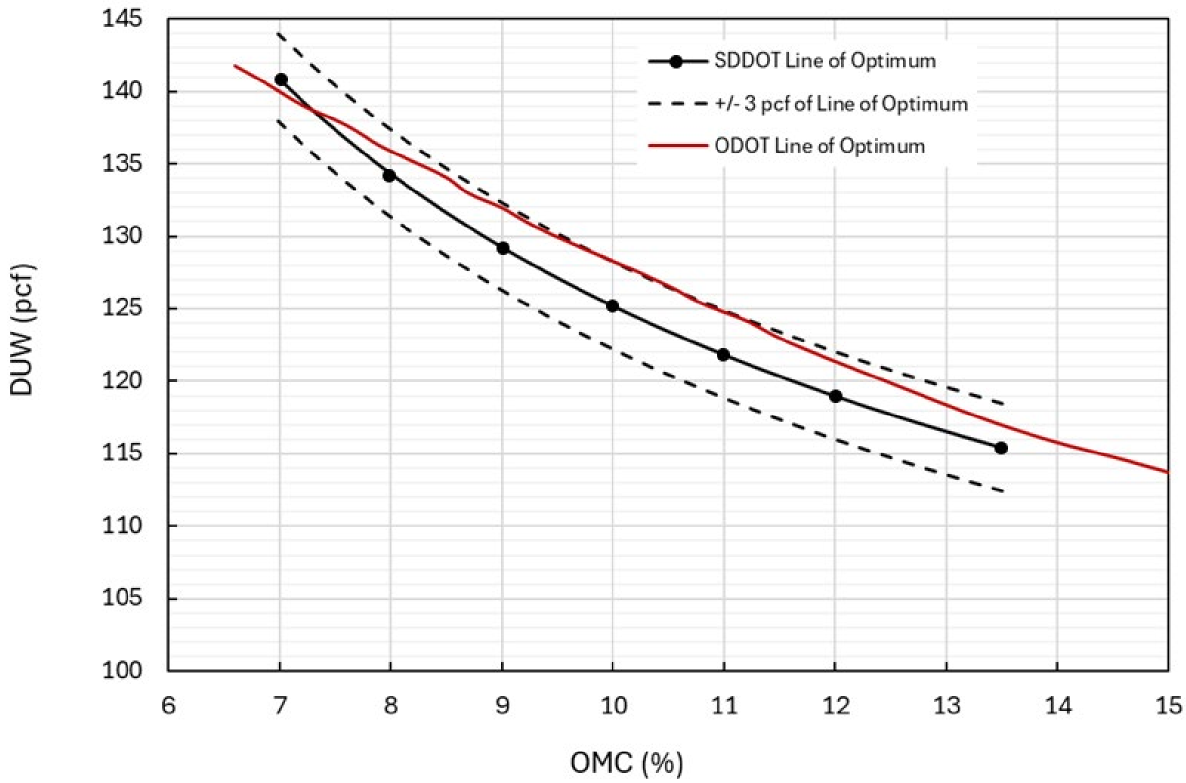


**Figure 11. Ohio and SDDOT Line of Optimums**

A standard t-test was used to determine whether a significant difference exists between the OHD and SDDOT lines of optimums. Dry unit weights along each line of optimums were obtained at randomly selected moisture contents, and the differences in maximum dry unit weights were averaged and statistically compared to zero. The hypotheses shown in Equation 4 were used to evaluate whether the mean difference, $\mu$, was statistically significant.

$$H_0: \mu = 0$$

$$H_1: \mu \neq 0$$

**Equation 4. Hypotheses for the t-test**

The null hypothesis, $H_0$, states that the average difference is not significantly different from zero at a 95% confidence level. The analysis aimed to disprove the null hypothesis by providing evidence of a significant difference. Table 3 shows the moisture contents and dry unit weights sampled, along with the calculated differences in dry unit weight between the two lines of optimums. The sampled moisture contents ranged from 7.2 to 13.5%, and the observed differences in dry unit weight ranged from -0.28 to 3.15 pcf. The mean difference of 2.01 pcf was found to be statistically different from zero at the 95% confidence level. The resulting t-statistic of 4.72 fell within the rejection region, defined by ±2.45. Therefore, the null hypothesis was rejected, indicating that, on average, the OHD line of optimums may overestimate the level of compaction required for South Dakota granular materials. Table 4 summarizes the test statistics.

**Table 3. Samples Used for Lines of Optimums Comparison**

| Predictor Values Moisture Content, % | OHD Dry Density Line of Optimums (Maximum Dry Unit Weight, pcf) | SDDOT Line of Optimums (Maximum Dry Unit Weight, pcf) | Difference in Maximum Dry Unit Weight, (pcf) |
|---|---|---|---|
| 7.2 | 139.1 | 139.38 | -0.28 |
| 8.5 | 134.1 | 131.65 | 2.45 |
| 9.3 | 130.7 | 127.97 | 2.73 |
| 10.5 | 126.6 | 123.45 | 3.15 |
| 11.9 | 121.7 | 119.26 | 2.44 |
| 12.7 | 119.3 | 117.25 | 2.05 |
| 13.5 | 117 | 115.44 | 1.56 |

**Table 4. t-Test Statistics**

| Mean Difference (pcf) | Sample Standard Deviation (pcf) | Number of Samples | T-Statistic | Rejection Region |
|---|---|---|---|---|
| 2.01 | 1.13 | 7 | 4.72 | $t < -2.45$ or $t > 2.45$ |

### 4.1.4.3 SDDOT Family of Curves Verification and Accuracy Assessment

The accuracy of the newly developed SDDOT Family of Curves was assessed through a verification analysis conducted on a 5% sample of randomly selected compaction curves (four-point datasets). The one-point moisture-density method was applied to predict OMC and MDUW using individual data points from each compaction curve. In this approach, each data point was evaluated independently to estimate OMC and MDUW based on both the OHD and SDDOT families of curves. For the fifteen samples selected for verification, the predicted OMC and MDUW values were then compared with the actual values obtained from the four-point Proctor test, and the mean absolute deviations (MAD) were calculated.

According to Section 3.4E of the SDDOT Materials Manual, Method 104 (SDDOT, 2015b), a second one-point test is required when the moisture in the one-point determination deviates more than 2% below or 1% above the predicted optimum moisture. Therefore, any data point that did not meet this requirement was excluded from the verification analysis. Table 5 presents an example of the analysis for one of the selected samples (Sample ID 2336937). The top and bottom rows were excluded from the MAD calculation based on the moisture content deviation criteria. For this sample, the SDDOT curves produced a MAD of 1.2% for OMC and 2.1 pcf for MDUW relative to the Proctor test results. These deviations are 18% and 10% lower, respectively, than those obtained from the OHD Family of Curves, indicating that the SDDOT curves predict OMC and MDUW more accurately for this sample.

Table 6 summarizes the MAD values calculated based on the OHD and SDDOT families of curves for all 15 verification samples. The overall average MADs for OMC and MDUW from both curve sets are shown in the last row of the table. For both parameters, the SDDOT curves yield lower average MAD values than the OHD curves, indicating that the SDDOT curves provide higher prediction accuracy.

**Table 5. Example of OMC and MDUW Predictions using OHD and SDDOT Curves**

| Standard Proctor | | Standard Four-Point Proctor Data | | | SDDOT Curves' Predicted Values | | | OHIO Curves' Predicted Values | | | SDDOT Absolute Deviation | | OHIO Absolute Deviation | |
|---|---|---|---|---|---|---|---|---|---|---|---|---|---|---|
| OMC (%) | MDUW (pcf) | Moisture (%) | DUW (pcf) | WUW (pcf) | OMC (%) | MDUW (pcf) | Curve | OMC (%) | MDUW (pcf) | Curve | OMC (%) | MDUW (pcf) | OMC (%) | MDUW (pcf) |
| 6.7 | 137.13 | 5 | 133.5 | 140.2 | 7.2 | 139.1 | 138-140 | 7.2 | 139.1 | B | | | | |
| | | 7.1 | 136.9 | 146.6 | 7.6 | 137.0 | 136-138 | 7.6 | 137.7 | b | 0.9 | 0.1 | 0.9 | 0.6 |
| | | 8.7 | 133.0 | 144.6 | 8.2 | 133.1 | 132-134 | 8.7 | 133 | d | 1.5 | 4.1 | 2.0 | 4.1 |
| | | 10.1 | 130.7 | 143.9 | 8.2 | 133.1 | 132-134 | 8.2 | 135.2 | c | | | | |
| **Mean Absolute Deviations** | | | | | | | | | | | 1.2 | 2.1 | 1.5 | 2.3 |

**Table 6. Summary of Accuracy Assessment on the Verification Dataset**

| Sample ID | SDDOT Curves | | OHD Curves | | Comparison | |
|---|---|---|---|---|---|---|
| | MAD - OMC | MAD - MDUW | MAD - OMC | MAD - MDUW | Lowest MAD for OMC | Lowest MAD for MDUW |
| 1030404 | 0.23 | 0.89 | 0.26 | 3.04 | SDDOT | SDDOT |
| 2336937 | 1.19 | 2.11 | 1.45 | 2.35 | SDDOT | SDDOT |
| 2311842 | 0.20 | 0.02 | 0.15 | 0.85 | OHD | SDDOT |
| 2301402 | 0.84 | 1.44 | 1.12 | 2.40 | SDDOT | SDDOT |
| 1430197 | 0.69 | 1.05 | 0.69 | 0.70 | SDDOT | OHD |
| 2372590 | 0.02 | 0.84 | 0.33 | 1.11 | SDDOT | SDDOT |
| 2318769 | 0.62 | 2.33 | 0.79 | 1.50 | SDDOT | OHD |
| 1464795 | 1.09 | 1.97 | 1.25 | 1.80 | SDDOT | OHD |
| 2245289 | 0.50 | 0.13 | 0.47 | 2.27 | OHD | SDDOT |
| 2338094 | 2.17 | 4.09 | 2.64 | 3.49 | SDDOT | OHD |
| 2343745 | 1.65 | 2.04 | 0.78 | 0.60 | OHD | OHD |
| 2365416 | 0.74 | 0.22 | 0.31 | 1.42 | OHD | SDDOT |
| 2295345 | 0.12 | 0.93 | 0.45 | 1.90 | SDDOT | SDDOT |
| 2080343 | 1.78 | 3.12 | 1.63 | 2.61 | OHD | OHD |
| 1077254 | 1.62 | 0.60 | 1.87 | 1.52 | SDDOT | SDDOT |
| **Average** | **0.90** | **1.45** | **0.95** | **1.84** | **SDDOT** | **SDDOT** |

Table 6 shows that the SDDOT curves predict the OMC more accurately than the OHD curves for 10 of the 15 samples. For MDUW, the SDDOT curves show higher accuracy for 9 samples, whereas the OHD curves predict MDUW more accurately for 6 samples. Overall, these results indicate that the SDDOT Family of Curves generally provides better predictions of OMC and MDUW for South Dakota's granular base and subbase materials compared with the OHD Family of Curves, supporting their use for local applications.

### 4.1.5 Development of the Global Model

The SDDOT Family of Curves described in Section 4.4 was developed at 2-pcf increments. The purpose of this section is to build upon that work and develop a universal function that allows interpolation of a family of curves at any desired increment (e.g., 1 pcf).

As mentioned in Section 4.1.3, the Gaussian model was fitted to the incremental data groups, and a set of constraints was applied to the model coefficients for the regression analysis. Specifically, the sum of parameters a and b was set equal to the MDUW for each increment; parameter c was set equal to the fitted OMC for each increment, and parameters a and d were defined as functions of OMC, as shown in Equation 5. Substituting these constraints into the Gaussian model presented in Equation 1 yields the following universal function:

$$\boldsymbol{DUW} = \left(\mathbf{0.26} \times \boldsymbol{OMC}^{\mathbf{2}} - \mathbf{8.35} \times \boldsymbol{OMC} + \mathbf{172.5}\right) + \Big(\boldsymbol{MDUW} - \left(\mathbf{0.26} \times \boldsymbol{OMC}^{\mathbf{2}} - \mathbf{8.35} \times \boldsymbol{OMC} + \mathbf{172.5}\right)\Big) \times \mathbf{exp}\left(-\mathbf{0.5} \times \left(\frac{\boldsymbol{MC}-\boldsymbol{OMC}}{(-\mathbf{0.013}\times\boldsymbol{OMC}^{\mathbf{2}}+\mathbf{0.37}\times\boldsymbol{OMC}+\mathbf{0.292})\times\mathbf{1.1}}\right)^{\mathbf{2}}\right.$$

Where:

DUW= dry unit weight, pcf
MC= moisture content, %
OMC = optimum moisture content, %
MDUW= maximum dry unit weight, pcf

**Equation 5. Universal Function for DUW**

The universal function was fitted to the 294 compaction datasets and produced an adjusted $R^2$ value of 0.87, indicating a good overall fit. By inputting the OMC and MDUW of interest into the universal function, the dry unit weight can be calculated as a function of moisture content, allowing an entire moisture-density curve to be generated. The line of optimums established in Section 4.1.3 and shown in Figure 3 can then be used to determine the corresponding OMC and MDUW at any desired increment.

Using this approach, a family of curves was developed at 1-pcf increments in terms of dry unit weight (Figure 12). This alternative family of curves covers a MDUW range from 114 to 142 pcf. The dry unit weight family of curves was then converted to wet unit weight curves (Figure 13) by multiplying each dry unit weight value by one plus its corresponding moisture content.

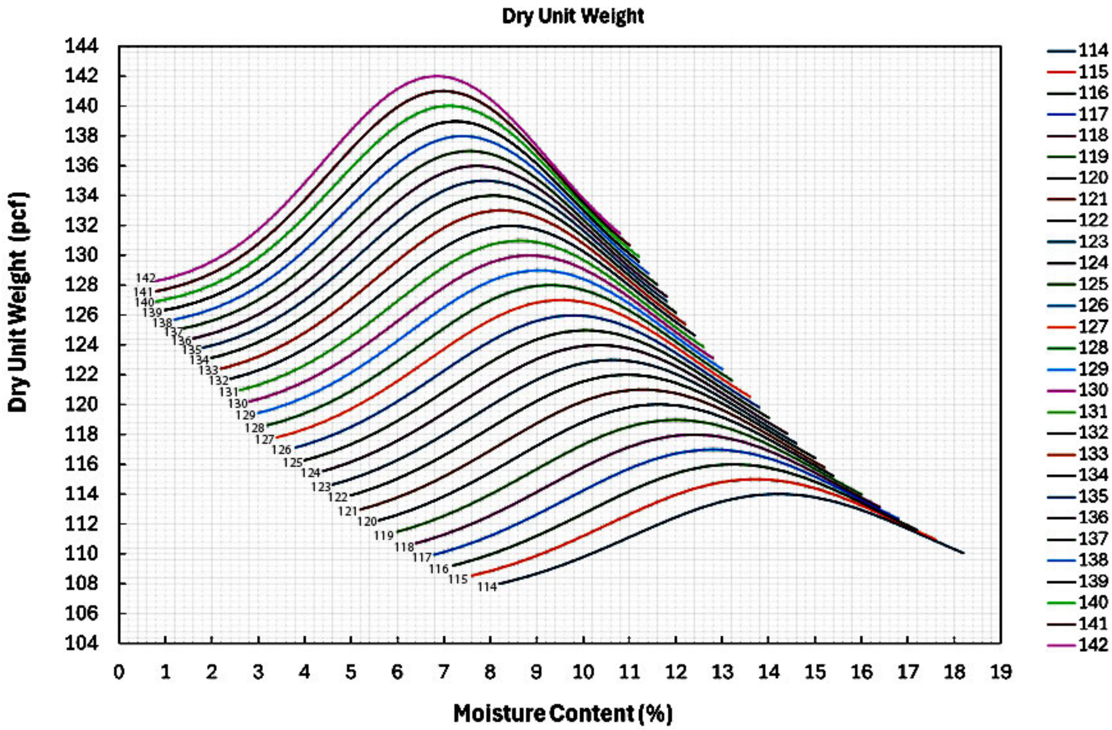


**Figure 12. SDDOT Dry Unit Weight Family of Curves in 1-pcf Increments**

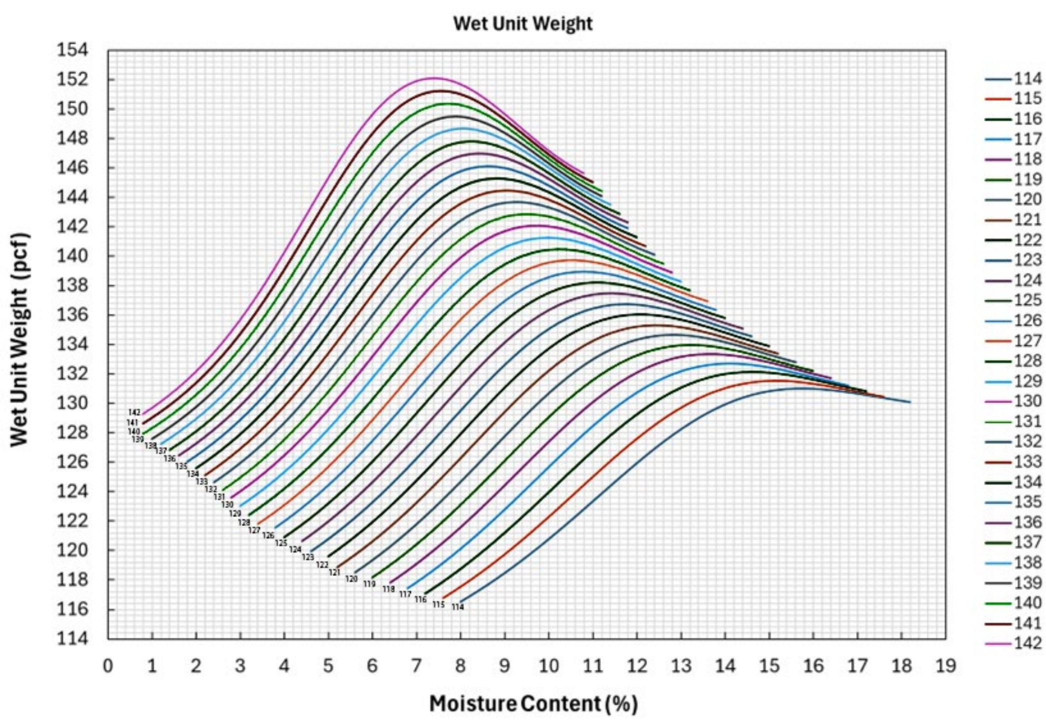


**Figure 13. SDDOT Wet Unit Weight Family of Curves in 1-pcf Increments**

### 4.1.6 Validation of the New Family of Curves

The accuracy of the SDDOT Family of Curves was validated using new datasets that were not involved in curve development. The validation process evaluated whether the SDDOT curves generalize well to new, unseen data and are not overfitted to the initial development dataset. Successful validation increases confidence that the curves will perform reliably in real-world applications.

A total of 42 new compaction curves from four-point density sheets (Form DOT-40) were provided by SDDOT. These datasets were cleaned and prepared for validation and are included in Appendix B. The same procedure described in Section 4.1.4.3 was followed: the one-point moisture-density method was applied to predict OMC and MDUW for individual data points using the OHD curves, the 2-pcf SDDOT curves, and the 1-pcf SDDOT curves. The predicted values were compared with the actual OMC and MDUW from the four-point Proctor tests, and MAD values were calculated for both compaction parameters. As noted in Section 4.5.3, data points that did not satisfy the moisture content criteria of Section 3.4E of the SDDOT Materials Manual were excluded, resulting in 38 usable samples. MAD values for OMC and MDUW were calculated for each curve set and are presented in Table 7, which shows the curve set providing the lowest deviation in both three-way and pairwise comparisons.

The columns titled *Comparison of Three Curves* identify the curve set with the lowest MAD when considering all three families of curves. The pairwise comparison columns (OHD vs 2-pcf SDDOT, OHD vs 1-pcf SDDOT, and 1-pcf vs 2-pcf SDDOT) indicate which curve performs better for each parameter.

For OMC, 2-pcf SDDOT curves provide the lowest deviation most frequently (36.84%) among the three curve sets. In pairwise comparisons, the 2-pcf SDDOT curves outperform the OHD curves 60.53% of the time, and the 1-pcf SDDOT curves also outperform the OHD curves 60.53% of the time. When comparing the two SDDOT curve sets directly, the 2-pcf curves produce lower deviation 52.63% of the time.

For MDUW, 1-pcf SDDOT curves most frequently yield the lowest deviation (42.11%) among the three curve sets. In pairwise comparisons, the 2-pcf SDDOT curves show lower deviation than the OHD curves 60.53% of the time, while the 1-pcf SDDOT curves outperform the OHD curves 65.79% of the time. Between the two SDDOT curve sets, the 1-pcf curves show lower deviation 63.16% of the time.

Overall, the 2-pcf SDDOT Family of Curves performs best for predicting OMC, whereas the 1-pcf SDDOT Family of Curves performs best for predicting MDUW. If a single curve set were to be selected based on combined performance for both OMC and MDUW, the 1-pcf SDDOT curves could be considered superior overall due to their strong performance in MDUW prediction.

**Table 7. Performance Comparison of the SDDOT 2-pcf, SDDOT 1-pcf, and OHD Families of Curves**

| Sample ID | SDDOT 2-pcf Curves | | SDDOT 1-pcf Curves | | OHD Curves | | Comparison of Three Curves | | Comparison of OHD & 2-pcf SDDOT | | Comparison of OHD & 1-pcf SDDOT | | Comparison of 1-pcf & 2-pcf SDDOT | |
|---|---|---|---|---|---|---|---|---|---|---|---|---|---|---|
| | MD* OMC | MD* MDUW | MD* OMC | MD* MDUW | MD* OMC | MD* MDUW | Best Curve-OMC | Best Curve-MDUW | Best Curve-OMC | Best Curve-MDUW | Best Curve-OMC | Best Curve-MDUW | Best Curve-OMC | Best Curve-MDUW |
| 2390119 | 0.84 | 0.87 | 0.61 | 0.23 | 0.15 | 0.47 | OHD | 1-pcf SDDOT | OHD | OHD | OHD | 1-pcf SDDOT | 1-pcf SDDOT | 1-pcf SDDOT |
| 2400445 | 0.83 | 3.86 | 1.04 | 3.14 | 0.88 | 0.54 | 2-pcf SDDOT | OHD | 2-pcf SDDOT | Ohio | OHD | OHD | 2-pcf SDDOT | 1-pcf SDDOT |
| 2402606 | 0.37 | 0.26 | 0.26 | 0.50 | 0.10 | 1.30 | OHD | 2-pcf SDDOT | OHD | 2-pcf SDDOT | OHD | 1-pcf SDDOT | 1-pcf SDDOT | 2-pcf SDDOT |
| 2395185 | 0.91 | 4.23 | 1.19 | 3.20 | 0.88 | 1.20 | OHD | OHD | OHD | OHD | OHD | OHD | 2-pcf SDDOT | 1-pcf SDDOT |
| 2416173 | 0.97 | 1.42 | 0.92 | 1.50 | 1.09 | 2.00 | 1-pcf SDDOT | 2-pcf SDDOT | 2-pcf SDDOT | 2-pcf SDDOT | 1-pcf SDDOT | 1-pcf SDDOT | 1-pcf SDDOT | 2-pcf SDDOT |
| 2413907 | 1.22 | 2.55 | 1.14 | 2.50 | 1.60 | 3.15 | 1-pcf SDDOT | 1-pcf SDDOT | 2-pcf SDDOT | 2-pcf SDDOT | 1-pcf SDDOT | 1-pcf SDDOT | 1-pcf SDDOT | 1-pcf SDDOT |
| 2400552 | 0.79 | 0.98 | 1.00 | 1.00 | 1.26 | 1.70 | 2-pcf SDDOT | 2-pcf SDDOT | 2-pcf SDDOT | 2-pcf SDDOT | 1-pcf SDDOT | 1-pcf SDDOT | 2-pcf SDDOT | 2-pcf SDDOT |
| 2390640 | 0.07 | 0.63 | 0.17 | 0.91 | 0.35 | 1.19 | 2-pcf SDDOT | 2-pcf SDDOT | 2-pcf SDDOT | 2-pcf SDDOT | 1-pcf SDDOT | 1-pcf SDDOT | 2-pcf SDDOT | 2-pcf SDDOT |
| 2395860 | 1.53 | 0.70 | 1.51 | 0.80 | 1.14 | 0.20 | OHD | OHD | OHD | OHD | OHD | OHD | 1-pcf SDDOT | 2-pcf SDDOT |
| 2410583 | 0.21 | 0.18 | 0.24 | 0.03 | 0.53 | 1.68 | 2-pcf SDDOT | 1-pcf SDDOT | 2-pcf SDDOT | 2-pcf SDDOT | 1-pcf SDDOT | 1-pcf SDDOT | 2-pcf SDDOT | 1-pcf SDDOT |
| 2409672 | 0.29 | 1.65 | 0.11 | 0.75 | 0.18 | 1.35 | 1-pcf SDDOT | 1-pcf SDDOT | OHD | OHD | 1-pcf SDDOT | 1-pcf SDDOT | 1-pcf SDDOT | 1-pcf SDDOT |
| 2392228 | 0.45 | 1.04 | 0.58 | 0.50 | 0.14 | 1.00 | OHD | 1-pcf SDDOT | OHD | OHD | OHD | 1-pcf SDDOT | 2-pcf SDDOT | 1-pcf SDDOT |
| 2404911 | 0.16 | 0.59 | 0.34 | 0.26 | 0.12 | 0.96 | OHD | 1-pcf SDDOT | OHD | 2-pcf SDDOT | OHD | 1-pcf SDDOT | 2-pcf SDDOT | 1-pcf SDDOT |

| Sample ID | SDDOT 2-pcf Curves | | SDDOT 1-pcf Curves | | OHD Curves | | Comparison of Three Curves | | Comparison of OHD & 2-pcf SDDOT | | Comparison of OHD & 1-pcf SDDOT | | Comparison of 1-pcf & 2-pcf SDDOT | |
|---|---|---|---|---|---|---|---|---|---|---|---|---|---|---|
| | MD* OMC | MD* MDUW | MD* OMC | MD* MDUW | MD* OMC | MD* MDUW | Best Curve-OMC | Best Curve-MDUW | Best Curve-OMC | Best Curve-MDUW | Best Curve-OMC | Best Curve-MDUW | Best Curve-OMC | Best Curve-MDUW |
| 2419984 | 0.05 | 2.65 | 0.04 | 2.61 | 0.08 | 0.39 | 1-pcf SDDOT | OHD | 2-pcf SDDOT | OHD | 1-pcf SDDOT | OHD | 1-pcf SDDOT | 1-pcf SDDOT |
| 2413595 | 1.14 | 3.97 | 1.18 | 4.02 | 1.41 | 3.60 | 2-pcf SDDOT | OHD | 2-pcf SDDOT | OHD | 1-pcf SDDOT | OHD | 2-pcf SDDOT | 2-pcf SDDOT |
| 2419324 | 0.17 | 1.16 | 0.01 | 0.31 | 0.14 | 1.69 | 1-pcf SDDOT | 1-pcf SDDOT | Ohio | 2-pcf SDDOT | 1-pcf SDDOT | 1-pcf SDDOT | 1-pcf SDDOT | 1-pcf SDDOT |
| 2410531 | 0.84 | 0.28 | 0.58 | 1.43 | 0.57 | 1.27 | OHD | 2-pcf SDDOT | OHD | 2-pcf SDDOT | OHD | OHD | 1-pcf SDDOT | 2-pcf SDDOT |
| 2420067 | 0.32 | 0.77 | 0.24 | 0.50 | 0.71 | 1.15 | 1-pcf SDDOT | 1-pcf SDDOT | 2-pcf SDDOT | 2-pcf SDDOT | 1-pcf SDDOT | 1-pcf SDDOT | 1-pcf SDDOT | 1-pcf SDDOT |
| 2414295 | 0.67 | 1.95 | 0.69 | 2.00 | 1.14 | 2.40 | 2-pcf SDDOT | 2-pcf SDDOT | 2-pcf SDDOT | 2-pcf SDDOT | 1-pcf SDDOT | 1-pcf SDDOT | 2-pcf SDDOT | 2-pcf SDDOT |
| 2416366 | 0.56 | 2.70 | 0.40 | 3.69 | 0.52 | 1.99 | 1-pcf SDDOT | OHD | OHD | OHD | 1-pcf SDDOT | OHD | 1-pcf SDDOT | 2-pcf SDDOT |
| 2391011 | 0.14 | 0.54 | 0.20 | 0.50 | 0.63 | 1.53 | 2-pcf SDDOT | 1-pcf SDDOT | 2-pcf SDDOT | 2-pcf SDDOT | 1-pcf SDDOT | 1-pcf SDDOT | 2-pcf SDDOT | 1-pcf SDDOT |
| 2406521 | 0.12 | 0.57 | 0.12 | 0.57 | 0.08 | 0.13 | OHD | OHD | OHD | OHD | OHD | OHD | 2-pcf SDDOT | 1-pcf SDDOT |
| 2389811 | 0.52 | 1.01 | 0.68 | 0.09 | 0.83 | 1.29 | 2-pcf SDDOT | 1-pcf SDDOT | 2-pcf SDDOT | 2-pcf SDDOT | 1-pcf SDDOT | 1-pcf SDDOT | 2-pcf SDDOT | 1-pcf SDDOT |
| 2387741 | 0.40 | 0.00 | 0.42 | 0.10 | 0.49 | 1.90 | 2-pcf SDDOT | 2-pcf SDDOT | 2-pcf SDDOT | 2-pcf SDDOT | 1-pcf SDDOT | 1-pcf SDDOT | 2-pcf SDDOT | 2-pcf SDDOT |
| 2405743 | 0.89 | 0.73 | 0.73 | 0.36 | 0.93 | 0.74 | 1-pcf SDDOT | 1-pcf SDDOT | 2-pcf SDDOT | 2-pcf SDDOT | 1-pcf SDDOT | 1-pcf SDDOT | 1-pcf SDDOT | 1-pcf SDDOT |
| 2414351 | 0.52 | 1.24 | 0.53 | 1.16 | 0.52 | 0.14 | OHD | OHD | OHD | OHD | OHD | OHD | 2-pcf SDDOT | 1-pcf SDDOT |
| 2409289 | 0.06 | 0.62 | 0.23 | 0.18 | 0.44 | 0.68 | 2-pcf SDDOT | 1-pcf SDDOT | 2-pcf SDDOT | 2-pcf SDDOT | 1-pcf SDDOT | 1-pcf SDDOT | 2-pcf SDDOT | 1-pcf SDDOT |

| Sample ID | SDDOT 2-pcf Curves | | SDDOT 1-pcf Curves | | OHD Curves | | Comparison of Three Curves | | Comparison of OHD & 2-pcf SDDOT | | Comparison of OHD & 1-pcf SDDOT | | Comparison of 1-pcf & 2-pcf SDDOT | |
|---|---|---|---|---|---|---|---|---|---|---|---|---|---|---|
| | MD* OMC | MD* MDUW | MD* OMC | MD* MDUW | MD* OMC | MD* MDUW | Best Curve-OMC | Best Curve-MDUW | Best Curve-OMC | Best Curve-MDUW | Best Curve-OMC | Best Curve-MDUW | Best Curve-OMC | Best Curve-MDUW |
| 2409599 | 0.89 | 0.97 | 0.82 | 0.50 | 1.38 | 1.22 | 1-pcf SDDOT | 1-pcf SDDOT | 2-pcf SDDOT | 2-pcf SDDOT | 1-pcf SDDOT | 1-pcf SDDOT | 1-pcf SDDOT | 1-pcf SDDOT |
| 2418452 | 0.06 | 0.20 | 0.06 | 0.24 | 0.32 | 1.04 | 1-pcf SDDOT | 2-pcf SDDOT | 2-pcf SDDOT | 2-pcf SDDOT | 1-pcf SDDOT | 1-pcf SDDOT | 1-pcf SDDOT | 2-pcf SDDOT |
| 2388175 | 0.57 | 0.71 | 0.72 | 0.28 | 0.91 | 0.02 | 2-pcf SDDOT | OHD | 2-pcf SDDOT | OHD | 1-pcf SDDOT | OHD | 2-pcf SDDOT | 1-pcf SDDOT |
| 2391204 | 0.73 | 0.27 | 0.57 | 0.72 | 0.38 | 0.42 | OHD | 2-pcf SDDOT | OHD | 2-pcf SDDOT | OHD | OHD | 1-pcf SDDOT | 2-pcf SDDOT |
| 2418113 | 0.15 | 0.43 | 0.15 | 0.44 | 0.19 | 1.14 | 1-pcf SDDOT | 2-pcf SDDOT | 2-pcf SDDOT | 2-pcf SDDOT | 1-pcf SDDOT | 1-pcf SDDOT | 1-pcf SDDOT | 2-pcf SDDOT |
| 2406238 | 0.47 | 4.35 | 0.64 | 3.40 | 0.50 | 2.20 | 2-pcf SDDOT | OHD | 2-pcf SDDOT | OHD | OHD | OHD | 2-pcf SDDOT | 1-pcf SDDOT |
| 2404487 | 0.68 | 0.52 | 0.68 | 0.52 | 0.64 | 0.18 | OHD | OHD | OHD | OHD | OHD | OHD | 2-pcf SDDOT | 1-pcf SDDOT |
| 2420069 | 0.32 | 0.77 | 0.14 | 0.13 | 0.41 | 1.13 | 1-pcf SDDOT | 1-pcf SDDOT | 2-pcf SDDOT | 2-pcf SDDOT | 1-pcf SDDOT | 1-pcf SDDOT | 1-pcf SDDOT | 1-pcf SDDOT |
| 2420070 | 0.32 | 0.77 | 0.34 | 0.87 | 1.01 | 1.17 | 2-pcf SDDOT | 2-pcf SDDOT | 2-pcf SDDOT | 2-pcf SDDOT | 1-pcf SDDOT | 1-pcf SDDOT | 2-pcf SDDOT | 2-pcf SDDOT |
| 2413637 | 0.00 | 1.07 | 0.32 | 0.29 | 0.01 | 1.01 | 2-pcf SDDOT | 1-pcf SDDOT | 2-pcf SDDOT | OHD | OHD | 1-pcf SDDOT | 2-pcf SDDOT | 1-pcf SDDOT |
| 2414461 | 0.63 | 0.74 | 0.47 | 0.18 | 0.33 | 1.02 | OHD | 1-pcf SDDOT | OHD | 2-pcf SDDOT | OHD | 1-pcf SDDOT | 1-pcf SDDOT | 1-pcf SDDOT |

Note: *MD stands for Mean Deviation

Additionally, the absolute deviations between the predicted and actual OMC and MDUW values obtained from the Proctor tests were calculated for each individual data point and are provided in Appendix C. The overall average deviations for the validation database are summarized in Table 8. As shown in the table, 1-pcf and 2-pcf SDDOT families of curves provide nearly the same accuracy for predicting OMC, and both outperform the OHD Family of Curves. For MDUW, the 1-pcf SDDOT curves provide better accuracy than both the 2-pcf SDDOT curves and the OHD curves.

**Table 8. Overall Average of Deviations for Three Moisture-Density Curves**

| Prediction Curves | Total Average of Deviations | |
|---|---|---|
| | OMC | MDUW |
| SDDOT 2-pcf Curves | 0.54 | 1.25 |
| SDDOT 1-pcf Curves | 0.55 | 1.1 |
| OHD | 0.67 | 1.37 |

### 4.1.7 Summary of the Changes Made to the Original SDDOT Family of Curves

Under project SD2019-05, several drawbacks of the original SDDOT family of curves developed in project SD2014-12 were identified as areas for improvement. These issues, outlined in Chapter 6 of the SD2019-05 report, included overlapping curves and the need to convert the curves to wet unit weight (WUW). Converting to WUW would eliminate the calculations required to derive DUW and reduce the potential for computational errors. The SD2023-02 project was initiated to address these issues and refine the original SDDOT family of curves by incorporating new data. However, during data compilation and verification, the research team identified systematic calculation errors in the original curve set development. The primary error occurred because the tare weight had not been subtracted from the combined dry sample and tare weight, resulting in incorrect DUW and MC values. Consequently, the scope of Task 2 in SD2023-02 shifted from refining the original curves to completely redeveloping them.

The SD2023-02 research team incorporated the recommendations from SD2019-05 into the redevelopment effort, particularly addressing the overlapping curves and redefining the curves in terms of the WUW-MC relationship. As described earlier, the line of optimums was fitted to the average MDUW and OMC values of each curve in the new family. The peaks of the new curves were then centered on this line of optimums, creating smooth transitions between curves and minimizing overlap. This approach also enables direct determination of target compaction parameters from the curves themselves, in contrast to the SD2014-12 approach, where the curves only defined boundaries between DUW increments and target parameters were provided for each increment separately in tabular form.

Another major improvement was the development of a universal model to describe the moisture-density relationship for SDDOT granular materials using a Gaussian function. This enhancement allows interpolation of the family of curves at 1-pcf increments, greatly improving prediction accuracy. Figure 14 illustrates the original SDDOT family of curves alongside the newly developed curves, and Table 9 summarizes the key differences between them.

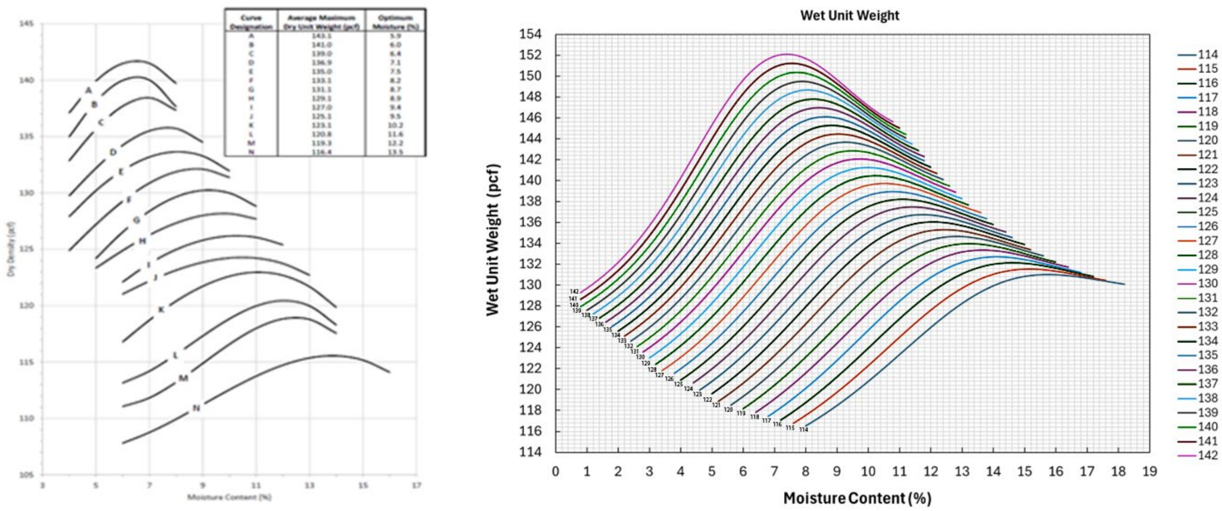


**Figure 14. Original SDDOT Family of Curves (a) versus New Family of Curves (b)**

**Table 9. Comparison of Characteristics Between the Original and New SDDOT Family of Curves**

| Curve Characteristics | New SDDOT Curves | Original SDDOT Curves |
|---|---|---|
| Described in terms of Wet Unit Weight | Yes | No |
| Target compaction parameters (i.e., OMC and MDUW) directly obtained from the curves | Yes | No |
| Curves are parallel and transition smoothly across the entire Wet Unit Weight range (i.e., no presence of curve overlapping) | Yes | No |
| Family of curves is described using a universal model | Yes | No |
| Dry Unit Weight increments between curves | 1 pcf | 2 pcf |
| Total number of curves | 29 | 14 |
| Moisture Content range covered by curves | 0.8% - 18.2% | 4%-16% |

## 4.2 Excel Program Development for Automated Calculation of OMC and MDUW

The Excel spreadsheet is an automated tool for determining the OMC and MDUW of SDDOT granular materials. It calculates these parameters using moisture and density information from a one-point Proctor test by plotting the test data on the 1-pcf SDDOT family of curves and selecting the closest curve. The 1-pcf SDDOT family of curves was developed using 294 unique moisture-density relationships for SDDOT granular base and subbase materials, as detailed earlier in this report.

The Excel tool uses Visual Basic for Applications (VBA) macro programming for computation and visualization. A Graphical User Interface (GUI) is incorporated to facilitate user input. The tool includes two data-input modes: Mode 1, which requires one-point Proctor test results (i.e., MC and WUW), and Mode 2, which requires the raw one-point Proctor test data used to calculate MC and WUW. Mode 2 is intended to minimize potential errors arising from intermediate manual calculations.

Once data input is complete, the algorithm checks the user input against the list of SDDOT 1-pcf curves to find a match within ±0.02 for MC and ±0.01 for WUW. If a curve is found, it is added to a list of potential matches; if not, the algorithm incrementally broadens the search by ±0.01 until a match is found or until the WUW range exceeds 1.1. After compiling potential matches, the algorithm removes duplicates that may occur if a curve meets both the moisture and density tolerances independently. If only one curve remains, the algorithm outputs the curve's details. If multiple curves are found, it selects the curve with the closest moisture content match. If no curves match, the algorithm outputs "Curve Not Found.". The selected curve is then visualized on a graph displayed in the GUI.

### 4.2.1 Operating Instructions

For proper operation, the tool requires Microsoft Excel (version 2016 or later) with VBA enabled. VBA Macros must be activated to ensure that the tool's calculations run correctly. Instructions for enabling VBA macros and operating the Excel program are provided in the following sections.

#### 4.2.1.1 Main Dashboard

To set up the tool, first open the Excel file and, if prompted, select "Enable Content" to activate VBA macros. If macros remain disabled, it can be enabled by navigating to File > Options > Trust Center > Trust Center Settings > Macro Settings and selecting "Enable all macros." As shown in Figure 15, the tool's main dashboard (i.e., the "Main" tab in the Excel file) provides access to all functionalities, where the Mode 1 and Mode 2 buttons open separate forms for data entry and analysis.

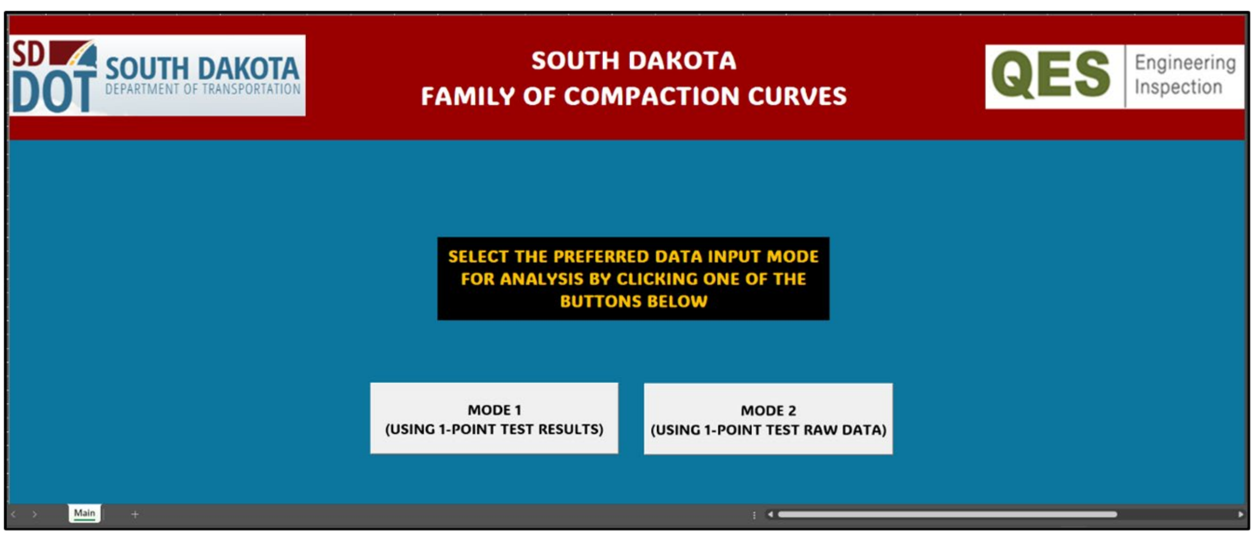


**Figure 15. Main Dashboard for Selecting the Preferred Data Input Mode**

#### 4.2.1.2 Data Input Mode 1 – Using One-Point Test Results

If Mode 1 is the preferred data input mode, click the **MODE 1** button on the main dashboard. This opens the Mode 1 interface (Figure 16), which is designed for quick calculations using one-point Proctor test data. In this mode, enter the Moisture Content (%) and Wet Unit Weight (pcf) into the corresponding fields.

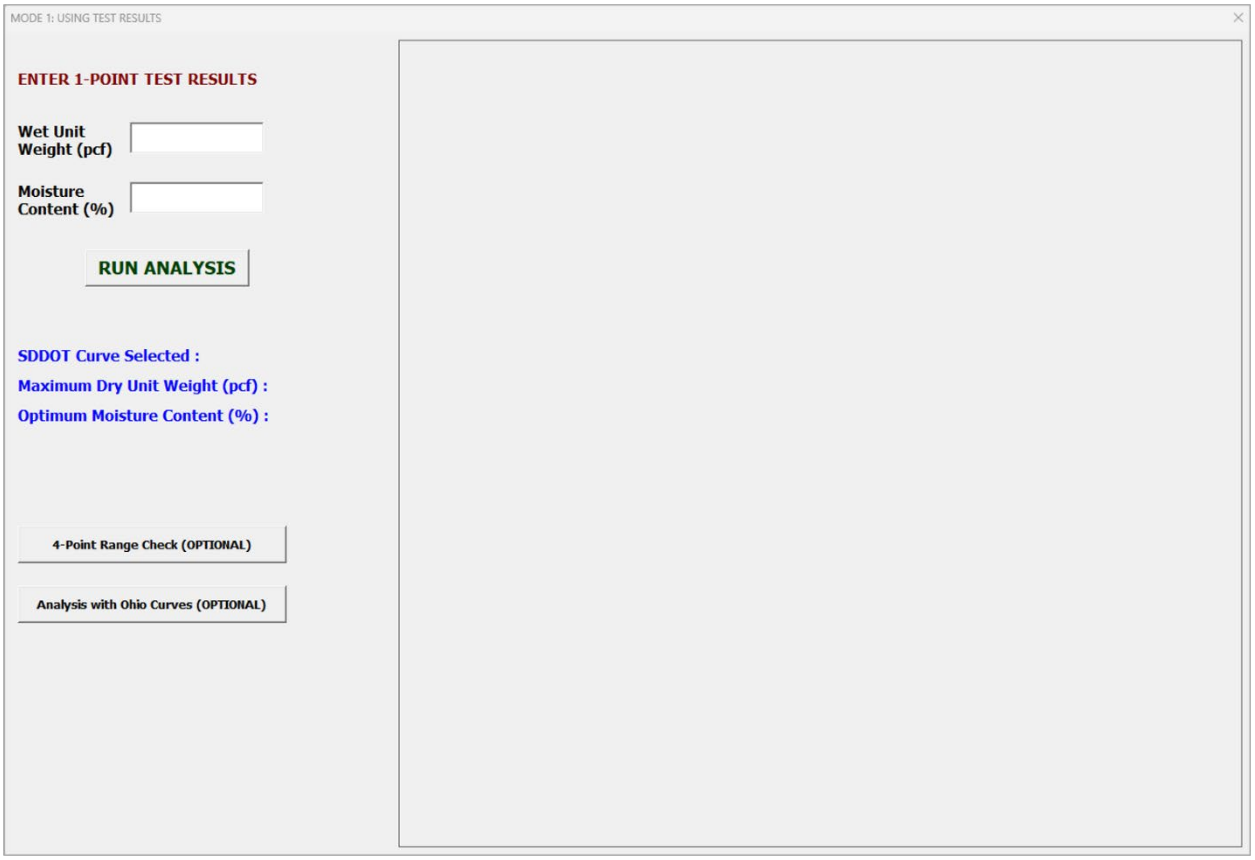


**Figure 16. Mode 1 Interface (blank)**

After entering the data, click the **RUN ANALYSIS** button to initiate the calculation. The tool will then determine the nearest matching curve and display the corresponding OMC and MDUW on the form (Figure 17). In accordance with Section 3.4E of the SDDOT Materials Manual, if the one-point moisture content deviates by more than 2 percentage points below or 1 percentage point above the OMC of the selected curve, a warning will appear indicating that another one-point test is required (Figure 18). If the tool cannot identify a matching curve, a "Curve Not Found" message will be shown.

The form includes two optional check buttons. When the **4-Point Range Check (OPTIONAL)** button is selected, a prompt window appears (Figure 19) for entering the four-point MDUW. The tool evaluates whether the MDUW from the selected curve differs by more than ±3 pcf from the user-entered four-point MDUW. If the tolerance is met, a **PASS** message is displayed, confirming compliance with the acceptable range (Figure 20). If the tolerance is not met, a **WARNING** message appears, indicating that the selected curve's MDUW is outside the ±3 pcf limit (Figure 21). In accordance with Section 3.4E of the SDDOT Materials Manual, the region's Materials Engineer should be consulted when this requirement is not met.

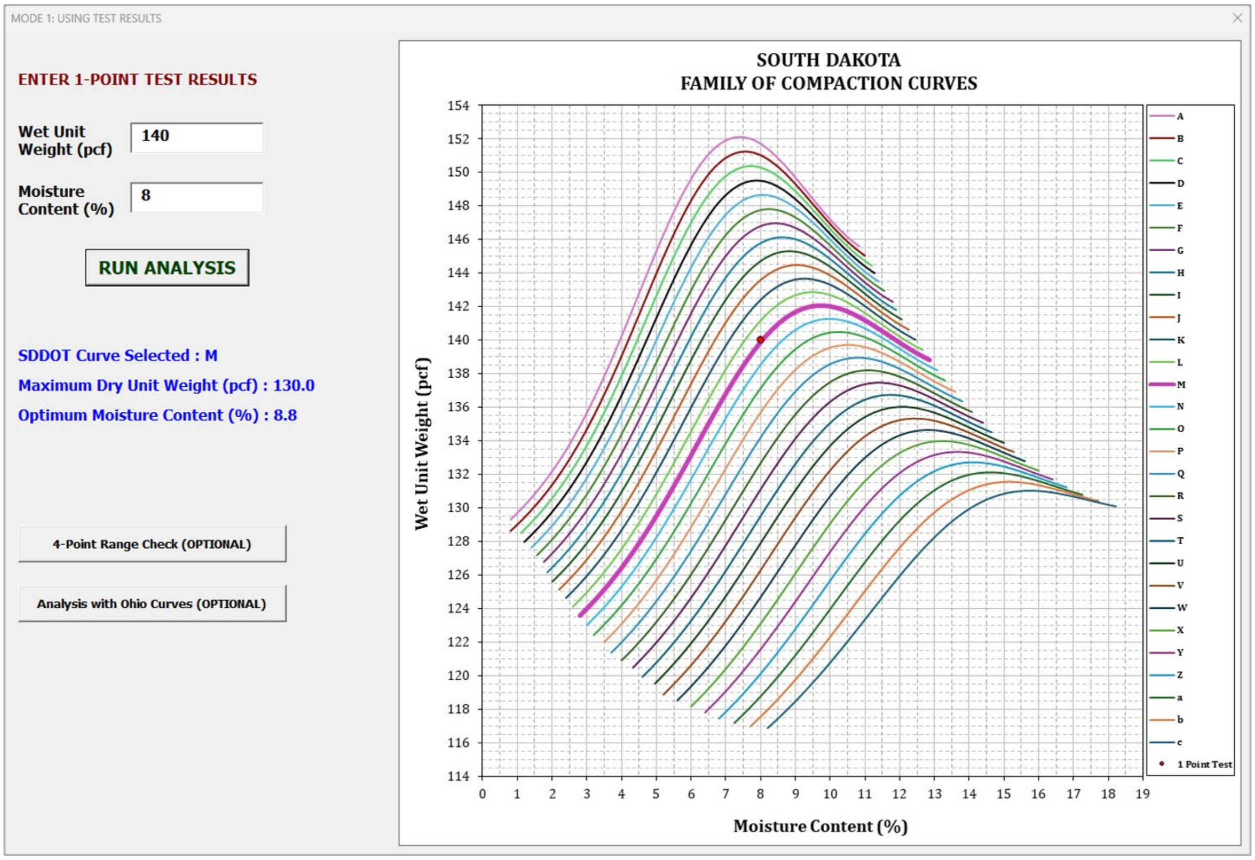


**Figure 17. Output Results in Mode 1 Interface**

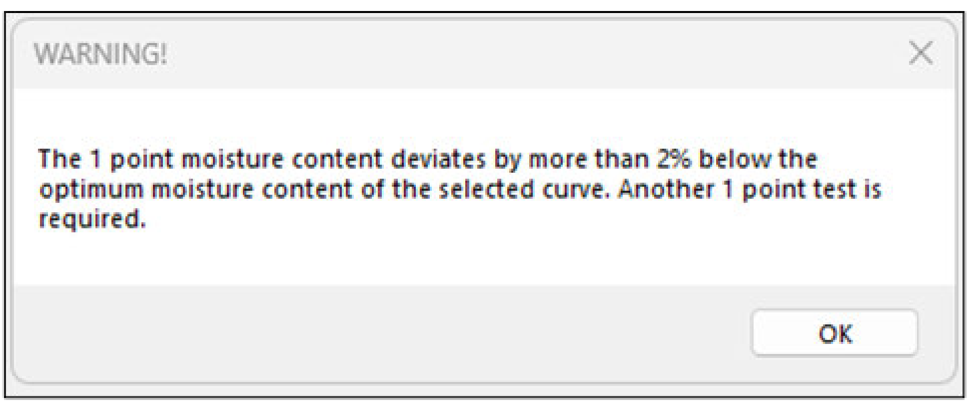


**Figure 18. Moisture Content Deviation Check Message**

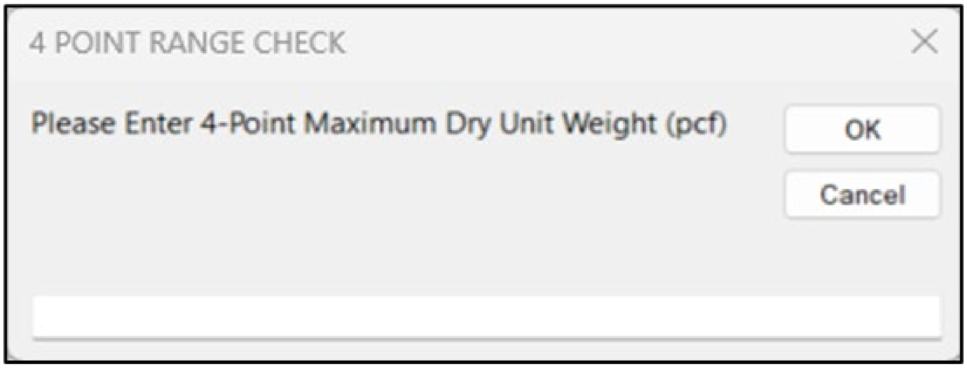


**Figure 19. Data Entry Window for Four-Point Range Check**

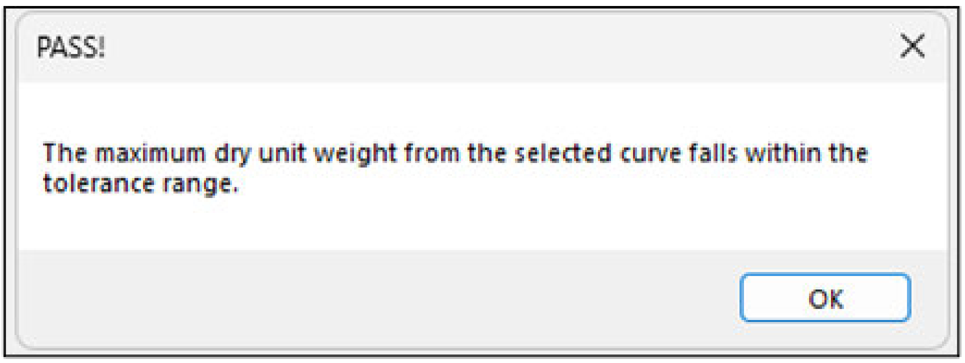


**Figure 20. Four-Point Range Check PASS Message**

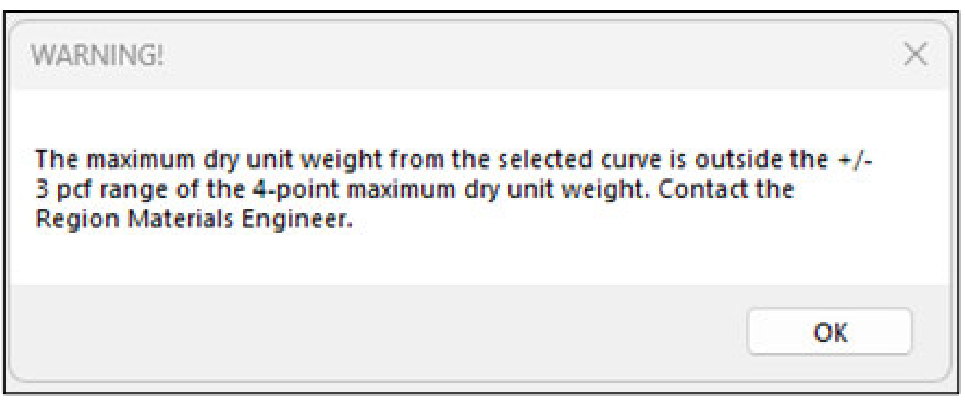


**Figure 21. Four-Point Range Check WARNING Message**

To determine OMC and MDUW using the Ohio Highway Department's (OHD) typical moisture-density curves, the user may click the **Analysis with Ohio Curves (OPTIONAL)** button. This action opens a prompt window (Figure 22) that displays the nearest OHD curve and the associated OMC and MDUW values.

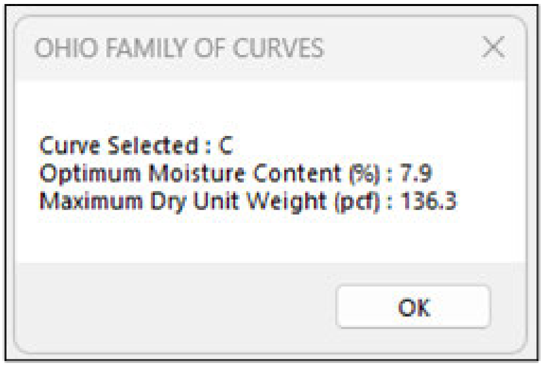


**Figure 22. Results of Analysis with Ohio Curves**

#### 4.2.1.3 Data Input Mode 2 – Using One-Point Test Raw Data

If Mode 2 is the preferred data input mode, click the **MODE 2** button on the main dashboard. This action opens the Mode 2 interface (Figure 23). In this mode, raw data, including the Mold and Specimen Weight, Mold Weight, Mold Factor, Can and Wet Material Weight, Can and Dry Material Weight, and Can Weight, should be entered into the corresponding fields.

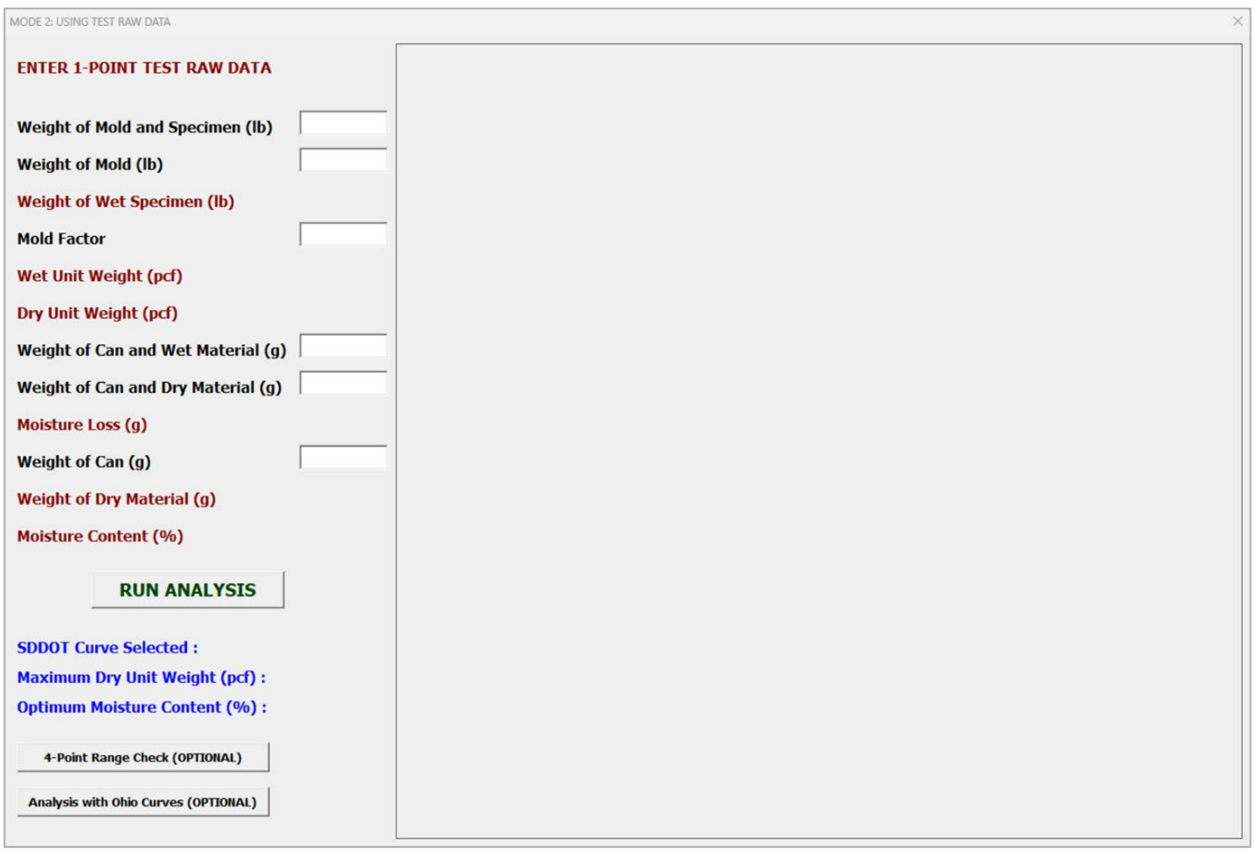


**Figure 23. Mode 2 Interface (blank)**

Once the data is entered, click the **RUN ANALYSIS** button to begin the calculation. The tool will compute Wet Specimen Weight, Wet Unit Weight, Dry Unit Weight, Moisture Loss, Dry Material Weight, and Moisture Content. It will then identify the nearest matching curve and display the corresponding OMC and MDUW on the form (Figure 24).

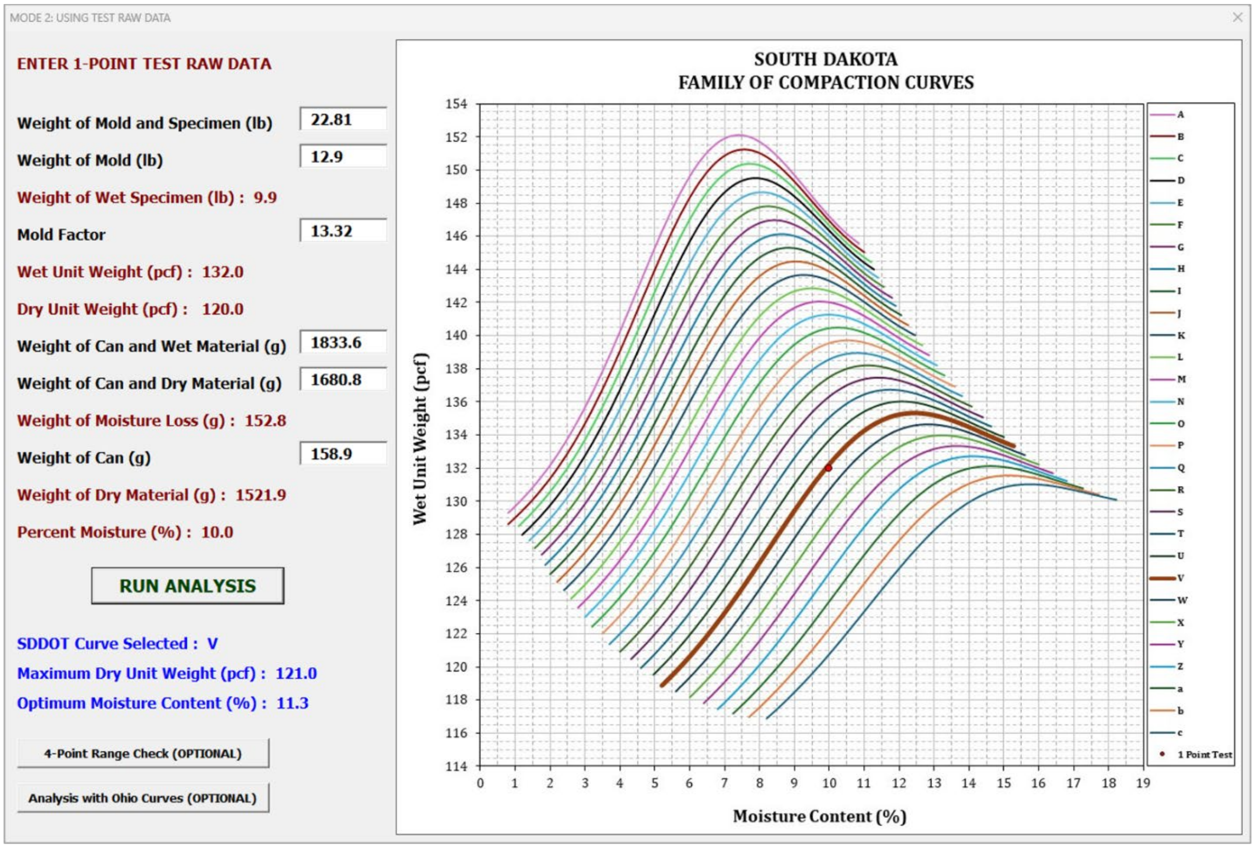


Figure 24. Output Results in Mode 2 Interface

Similar to Mode 1, the Mode 2 interface provides optional checks for comparing the one-point MDUW selected from the 1-pcf SDDOT family of curves with the four-point MDUW range and with the Ohio family of compaction curves. Additionally, if the one-point moisture content deviates by more than 2 percentage points below or 1 percentage point above the OMC of the selected curve, a warning message will appear recommending that another one-point test be performed.

### 4.2.2 Other Tabs in the Excel Spreadsheet

In addition to the Main tab, the Excel tool includes five supporting tabs: *Mode 1 Input, Mode 2 Input, Updated Query, Wet-1-pcf Updated, and Ohio Query*. These tabs are reserved for internal calculations and macro-driven data management. They are not intended for direct user interaction but provide essential background data to ensure accurate computations and efficient program performance. Each tab stores predefined data, intermediate outputs, or specific configuration parameters used by the macros in the Mode 1 and Mode 2 interfaces to generate moisture-density curves, select the appropriate curve, and apply regional standards. To safeguard these internal components, these tabs are hidden.

## 4.3 Analysis of DCP, Sand Cone, and Nuclear Density Gauge Side-by-Side Test Data Supplied by SDDOT for Agreement with the New Moisture-Density Curves

The SDDOT specifies compaction control procedures for granular materials in Section 260.3 of the Standard Specifications for Roads and Bridges (SDDOT, 2015a). Base course material must be compacted to at least 97 percent of the maximum dry density. The maximum dry density is determined using SDDOT Method SD 104, Method 4 (SDDOT, 2015b), which is closely related to AASHTO T 272-18 (AASHTO, 2022a).

SDDOT Method SD 104, Method 4 uses a one-point determination procedure, which provides a more rapid estimate of the target density compared with the four-point compaction test specified in AASHTO T99 (AASHTO, 2022b). In this method, a single specimen is compacted at approximately optimum moisture content in a 6-in mold, following procedures similar to those described in AASHTO T 99 (AASHTO, 2022b). The wet density and moisture content of the specimen are then determined and plotted within a family of compaction curves. The curve that most closely matches the measured wet density and moisture content is selected as the representative curve for the material, and the corresponding dry density from that curve is adopted as the target density.

SDDOT currently requires a one-point determination for each in-place density test to establish an individual target density for that specific test location. The material used for the one-point test is obtained from the material removed from, or immediately adjacent to, the test hole. If the moisture content of the one-point test deviates from the optimum moisture content of the selected curve by more than 2 percentage points below optimum or 1 percentage point above optimum, a second one-point test must be conducted. The additional test must be performed at or closer to the optimum moisture content and within the tolerances specified in SD 104 (SDDOT, 2015b).

The SDDOT is considering adopting the DCP specification developed and used by the MnDOT for quality control and acceptance of compaction in granular base materials (MnDOT, 2025). The MnDOT acceptance criteria for the DCP specification are presented in Table 10. According to these criteria, the Dynamic Penetration Index (DPI), moisture content (MC), gradation number (GN), and SEAT value are used to determine the acceptability of a compacted base layer.

**Table 10. DCP Specification for Base Compaction Acceptance (MnDOT, 2025)**

| GN | MC | Maximum Allowable SEAT, mm | Maximum Allowable DPI, mm | Test Layer, in |
|---|---|---|---|---|
| 3.1 – 3.5 | < 5 | 40 | 10 | 4 - 6 |
| | 5.0 – 8.0 | 40 | 12 | |
| | > 8 | 40 | 16 | |
| 3.6 – 4.0 | < 5 | 40 | 10 | 4 - 6 |
| | 5.0 – 8.0 | 45 | 15 | |
| | > 8 | 55 | 19 | |
| 4.1 – 4.5 | < 5 | 50 | 13 | 5 - 6 |
| | 5.0 – 8.0 | 60 | 17 | |
| | > 8 | 70 | 21 | |
| 4.6 – 5.0 | < 5 | 65 | 15 | 6 -12 |
| | 5.0 – 8.0 | 75 | 19 | |
| | > 8 | 85 | 23 | |
| 5.1 – 5.5 | < 5 | 85 | 17 | 7 - 12 |
| | 5.0 – 8.0 | 95 | 21 | |
| | > 8 | 105 | 25 | |
| 5.6 – 6.0 | < 5 | 100 | 19 | 8 - 12 |
| | 5.0 – 8.0 | 115 | 24 | |
| | > 8 | 125 | 28 | |

SEAT (mm) refers to the penetration of the DCP cone in the granular base as a result of two initial blows, and DPI is the penetration index value (mm/blow). SEAT and DPI are determined from the following equations:

$$SEAT = A - B$$

Where:

A = penetration reading after two initial blows (mm)
B = penetration reading before two blows (mm)

**Equation 6. SEAT**

$$DPI = \frac{(A - B)}{3}$$

Where:

A = penetration reading after five blows (mm)
B = penetration reading after two blows (mm)

**Equation 7. Dynamic Penetration Index**

The GN values are calculated from the sieve analysis information according to the following equation:

$$GN = \frac{25mm + 19mm + 9.5mm + 4.75mm + 2.0mm + 425\mu m + 75\mu m}{100}$$

Where:

Sive sizes = percent passing each sieve

**Equation 8. GN Formula**

The agreement between the DCP-based compaction acceptance criteria and the relative compaction levels determined using the new SDDOT moisture–density curves and the OHD curves was evaluated in this section. This analysis was conducted to assess the applicability of the DCP-based specification as a compaction acceptance method for granular materials.

The analysis utilized data provided by SDDOT from 2023 and 2025 construction projects, along with data from project sites included in the SD2019-05 study. The 2023–2025 database served as the primary dataset because it contains all required inputs, including field MC, GN, DPI, SEAT value, in-situ density (from sand cone or nuclear gauge tests), and one-point Proctor test results (one-point density and moisture content).

In contrast, the 2019 database used in the SD2019-05 study does not include one-point test results. Under current SDDOT practice, as confirmed by the project technical team, a one-point test is performed at each test location to estimate the MDUW and OMC for the materials. Relative compaction is then calculated by dividing the in-situ density by the MDUW obtained from the one-point test. However, in the SD2019-05 study, due to the absence of one-point test data for each DCP test location, a single representative four-point Proctor test was used to determine the MDUW for all DCP test locations at each project site.

Because of this difference in testing procedures and to maintain consistency with current SDDOT practice, the research team decided not to merge the 2019 database with the newer database. Instead, the agreement between the DCP specification and the compaction levels determined using the OHD curves and the new SDDOT family of curves was evaluated separately for each database. This approach ensures a consistent comparison within each database while avoiding potential bias introduced by differences in testing procedures and data completeness.

The 2023–2025 database includes 66 datasets. One-point test results were available for 56 datasets, while the remaining 10 correspond to salvaged materials for which test strip data were provided. The OHD family of curves could be applied to 53 of the 56 datasets with one-point test results to estimate MDUW and OMC. The remaining three datasets were excluded because their one-point MC values deviated from the OMC by more than the allowable limits (i.e., more than 2 percentage points below or 1 percentage point above), consistent with the SDDOT Materials Manual, Method 104. Using the new SDDOT family of curves, MDUW could be determined for 42 datasets; the remaining 14 were excluded for exceeding the same MC deviation limits.

Sand cone in-situ density test results were available for 48 datasets, while nuclear density gauge measurements were available for the remaining eight datasets. Relative compaction was calculated by dividing the in-situ density, determined from either the sand cone test or the nuclear gauge, by the corresponding MDUW values. The agreement between the DCP-based compaction acceptance and the relative density-based compaction acceptance (i.e., 97% of maximum dry density) using the new SDDOT family of curves was evaluated for all 56 datasets. A similar evaluation was conducted using the OHD family of curves, and the results from the two curve systems were compared. The detailed analysis of agreement for the 2023-2025 datasets using the new SDDOT curves (42 datasets) and the OHD curves (56 datasets) is presented in Appendix D.

As noted earlier, one-point Proctor test results were not available for the SD2019-05 study database. In that study, nine different virgin base material types were tested. For each material type, DCP tests were performed at nine locations. The MDUW and OMC for each material type were determined from a single four-point Proctor test conducted in accordance with SDDOT Materials Manual Method 104, Method 3. Relative compaction for each dataset was then calculated by dividing the in-situ density by the MDUW obtained from the four-point test. As with the 2023–2025 database, MDUW values were also estimated using the new SDDOT family of curves and the OHD family of curves separately. The agreement between the DCP-based and the relative density-based compaction acceptance criteria using both the curve families was then evaluated, as detailed in Appendix D.

To evaluate the effectiveness of the DCP specification in predicting compaction adequacy, the variation of DPI and SEAT values with respect to the achieved relative density was analyzed. The analysis was conducted for two categories:

- cases where the achieved compaction was adequate (relative density ≥ 97%), and
- cases where the achieved compaction was inadequate (relative density < 97%).

For each sample in the database, the difference between the measured DPI and the maximum allowable DPI (ΔDPI), as well as the difference between the measured SEAT and the maximum allowable SEAT (ΔSEAT), was calculated. The maximum allowable SEAT and DPI values are functions of GN and MC, as specified in Table 10. Accordingly, compaction is considered acceptable under the DCP specification only when both ΔSEAT and ΔDPI are less than zero.

Similarly, the difference between the in-situ relative density and the minimum acceptable relative density of 97% was calculated for each dataset. Compaction is considered adequate when the relative density differential (ΔDensity) is greater than or equal to zero. Figure 25 presents the variations of ΔSEAT and ΔDPI for the 2023–2025 database for all cases of adequate compaction based on the OHD family of curves. Samples located in Quadrant IV represent cases where compaction is also adequate according to the DCP specification. The circle radii represent ΔDensity, with larger radii indicating higher relative density above the 97% threshold. Quadrants I, II, and III represent cases where the DCP specification falsely indicates inadequate compaction. It can be observed that the SEAT parameter more effectively identifies adequately compacted bases compared with the DPI parameter, as only one sample with adequate relative density lies to the right of the ΔSEAT = 0 line.

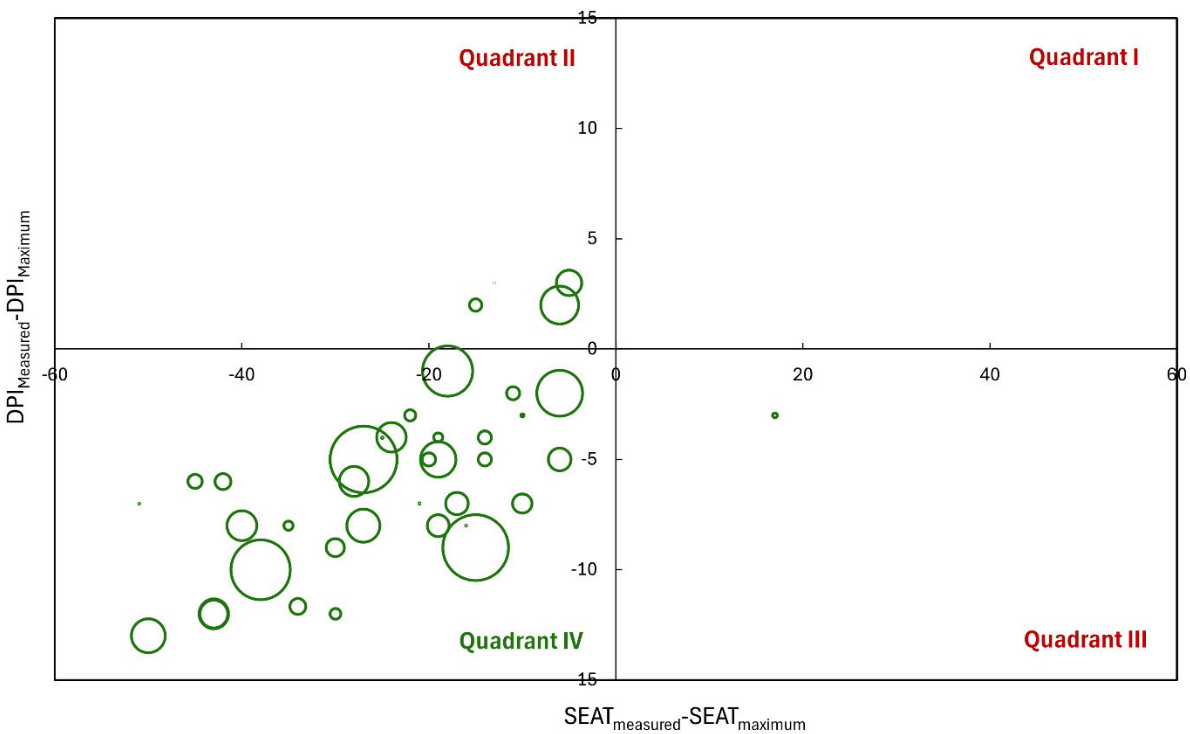


**Figure 25. Variations of ΔSEAT and ΔDPI with Achieved Relative Density in Excess of 97% Using OHD Family of Curves**

Figure 26 presents the variations of ΔSEAT and ΔDPI for the 2023–2025 database, where the achieved relative density is less than 97% based on the OHD family of curves (inadequate compaction). Data points located in Quadrants I, II, and III represent cases where the DCP specification correctly identifies inadequate compaction. In this figure, the circle radii again represent ΔDensity, with larger radii indicating a greater deviation below the 97% relative density threshold. Quadrant IV represents cases where the DCP specification falsely indicates adequate compaction.

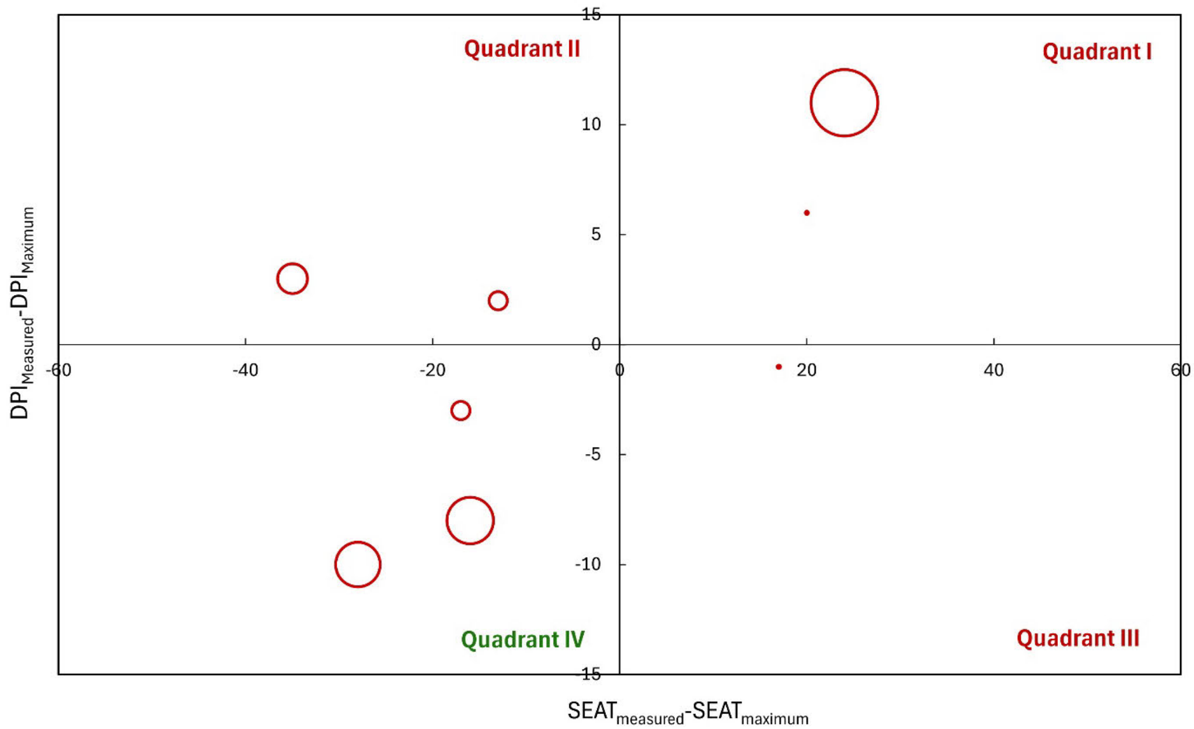


**Figure 26. Variations of ΔSEAT and ΔDPI with Achieved Relative Density Short of 97% using OHD Family of Curves**

Overall, using the OHD family of curves to determine relative density, the DCP specification shows 83% agreement with the relative density assessment. The DCP specification underestimates compaction quality in 9% of cases and falsely predicts adequate compaction in 8% of cases.

The same analysis described earlier was conducted for the 2023–2025 database using the new SDDOT family of curves to calculate relative density, and the results are presented in Figures 27 and 28. The results indicate that the compaction adequacy determined using the DCP specification agrees with the relative compaction assessment in 81% of the cases. The DCP specification underestimates compaction quality in 17% of the cases and falsely predicts adequate compaction in 2% of the cases.

The overall level of agreement between the DCP specification and relative compaction is similar for both OHD and SDDOT curves. However, the new SDDOT family of curves appears to be more conservative in identifying compaction adequacy and is less likely to falsely predict adequate compaction.

The SD2019-05 study database was also analyzed to assess the agreement between the compaction adequacy predicted by the DCP specification and the relative density values. The statistics from the analyses conducted for both the 2019 and the 2023–2025 databases are summarized in Table 11. The results indicate that, for the 2019 database, the DCP specification shows a slightly better agreement with the relative density values when the new SDDOT family of curves is used.

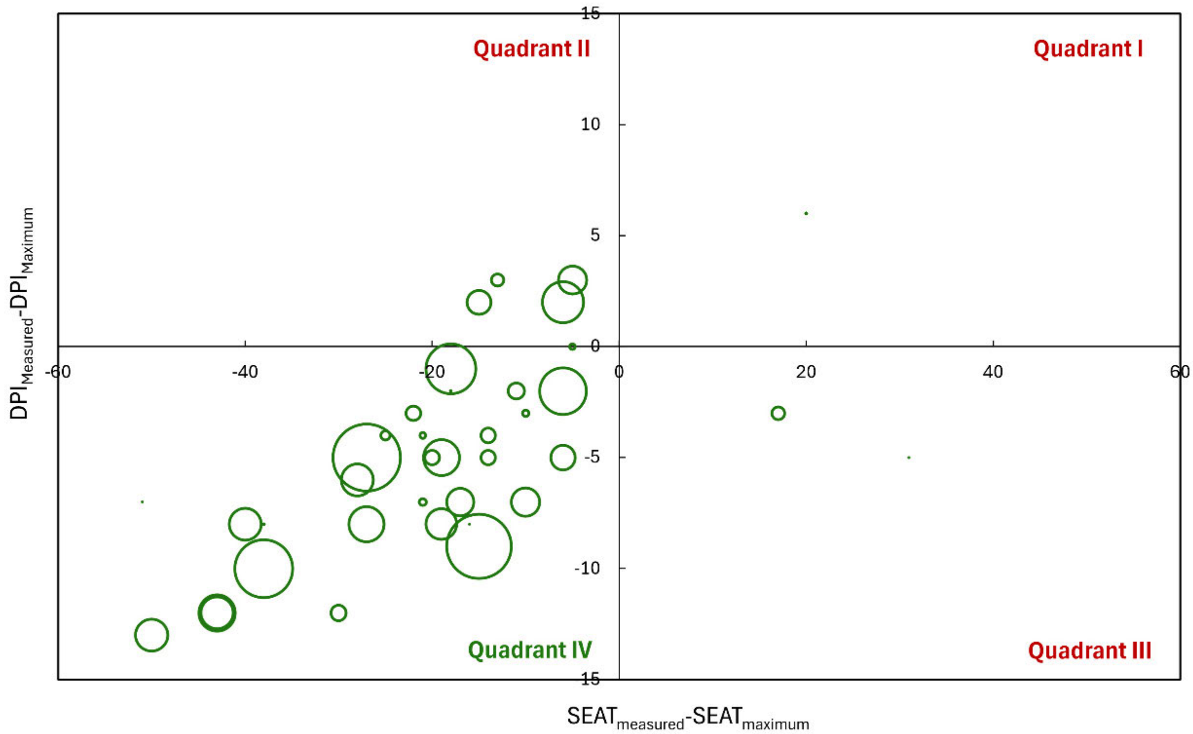


**Figure 27. Variations of ΔSEAT and ΔDPI with Achieved Relative Density in Excess of 97% Using the New SDDOT Family of Curves**

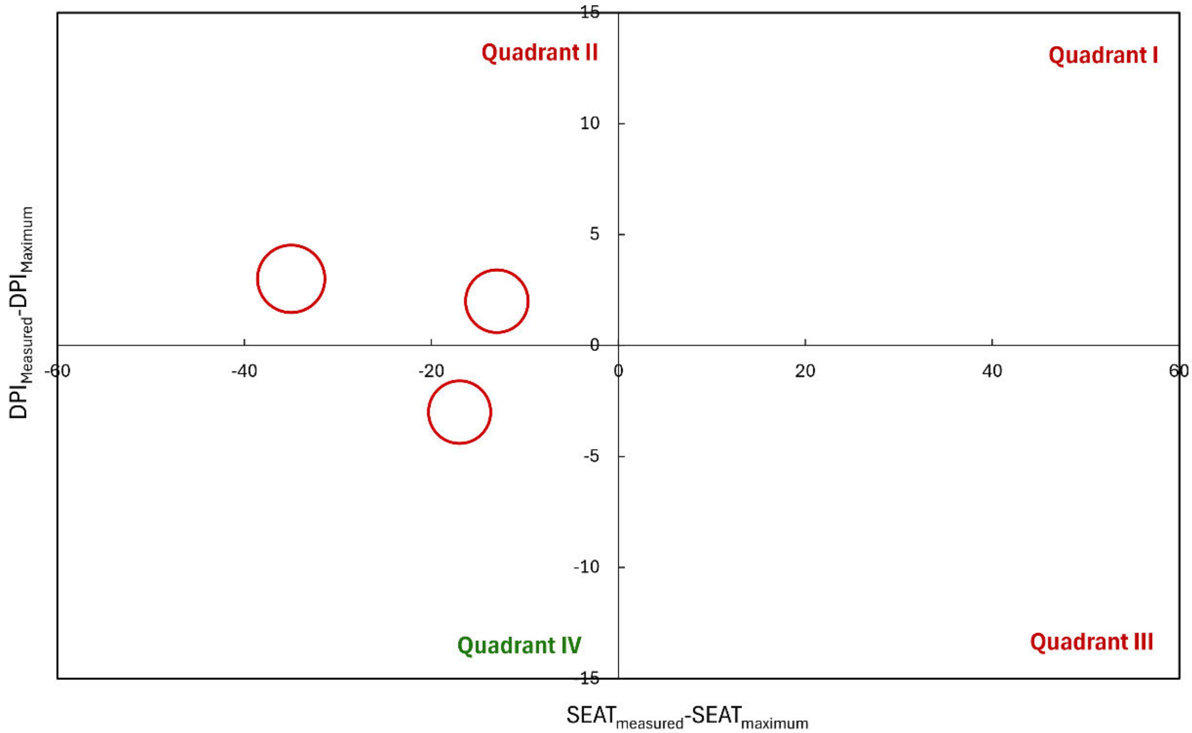


**Figure 28. Variations of ΔSEAT and ΔDPI with Achieved Relative Density Short of 97% using the New SDDOT Family of Curves**

**Table 11. Comparison of DCP Compaction Specification with Relative Density Determined from OHD Curves, SDDOT Curves, and Test Strip Data**

| Database | DCP Specification versus Relative Density | Using OHD Curves | Using SDDOT Curves | Using Test Strip Data |
|---|---|---|---|---|
| 2023-2025 | DCP agrees with Relative Density | 83% | 81% | NA |
| | DCP underestimates compaction | 9% | 17% | NA |
| | DCP overestimates compaction | 8% | 2% | NA |
| 2019 | DCP agrees with Relative Density | 65% | 68% | NA |
| | DCP underestimates compaction | 17% | 18% | NA |
| | DCP overestimates compaction | 19% | 14% | NA |
| 2023-2025 Salvaged Materials | DCP agrees with Relative Density | NA | NA | 80% |
| | DCP underestimates compaction | NA | NA | 10% |
| | DCP overestimates compaction | NA | NA | 10% |

It should be noted that one-point test results were not available for individual DCP test locations in the 2019 database. Instead, the relative compaction for all test locations within a given material type was calculated using the MDUW obtained from a single four-point Proctor test conducted on a representative sample. This approach differs from the standard SDDOT practice for determining the relative density of granular materials. According to Section 260.3 of the SDDOT Standard Specifications (SDDOT, 2015a), the MDUW should be determined for each individual sample at the construction site using a one-point Proctor test. This procedure ensures that variations in the supplied materials are captured. Therefore, in this study, greater emphasis was placed on the results obtained from the 2023-2025 database, as these data were collected in accordance with current SDDOT practice.

The 2023–2025 database included 10 salvaged base material datasets. According to SDDOT Materials Manual Method SD 219 (SDDOT, 2015c), the test strip method is used to determine the target dry density for salvaged materials, and each compacted layer is required to achieve at least 95% of this target. For the salvaged materials included in the database, SDDOT provided the target density, in-situ density, MC, GN, and the corresponding DCP test results. The compaction adequacy predicted by the DCP specification was compared with the actual relative density of these materials. As summarized in Table 11, the DCP specification agrees with the relative density assessment in 80% of cases, underestimates compaction in 10%, and falsely predicts adequate compaction in 10%.

Based on the observed results, the MnDOT DCP-based compaction specification shows good agreement with the in-situ relative density determined using the new SDDOT family of curves and the test strip method. Compared with the OHD curves, using the new SDDOT curves results in fewer cases where the DCP specification falsely predicts adequate compaction (i.e., overestimates compaction). However, there remains potential to further improve the overall level of agreement, as discussed in the following section.

## 4.4 Refinement of the MnDOT DCP Specification for SDDOT Granular Materials

The 2023-2025 database of both virgin and salvaged base materials was initially used for refining the MNDOT DCP specification in this study. The GN values of the materials in this database were primarily between 3.6 and 4.5, corresponding to the second and third GN ranges in Table 10. Only five samples had GN values between 3.1 and 3.5 (i.e., first GN range in Table 10), which is insufficient to justify modifications of the existing DPI and SEAT thresholds for this GN range. The limited number of samples in the first range also suggests that granular materials with GN values greater than 4.6 (i.e., fourth through sixth GN ranges in Table 10) may exist within the state but are not represented in the available data. Because the current DCP specification is intended to apply across a broad range of GN values, any updated specification should maintain this applicability. Consequently, while the available data support potential modifications to the DPI and SEAT thresholds for the second and third GN ranges in Table 10, the overall structure of the specification should continue to accommodate a wider range of GN values.

Prior to conducting the analysis, the research team reviewed the MnDOT methodology used to develop the DCP specification. This approach is based on regression analysis, in which envelope planes are fitted to measured DPI and SEAT values from test locations that meet the required relative density (Dai and Kremer, 2006). These planes are expressed as linear functions of GN and MC. The equations defining the envelope planes are provided below.

$$DPI = 4.76 \times GN + 1.68 \times MC - 14.4$$

$$SEAT = 36.8 \times GN + 4.12 \times MC - 124$$

**Equation 9. DPI and SEAT Functions Fitted to MnDOT Database**

It can be observed that the DPI and SEAT functions increase with increasing GN and MC, as the coefficients of these variables in Equation 8 are positive. This trend is consistent with expected material behavior. As the GN value increases, indicating a finer material, the DPI and SEAT values are expected to increase. Similarly, as MC increases, the frictional resistance between particles decreases, resulting in higher DPI and SEAT values. It should be noted that the materials in the MnDOT database cover a wide range of GN values (3.1 to 6.0). As a result, the increasing linear relationship between DPI, SEAT, and GN was effectively captured in the regression equations.

To develop the current specification, the MnDOT research team divided the GN and MC ranges into smaller intervals, as shown in Table 10. The DPI and SEAT thresholds (i.e., maximum allowable values) for each interval were then determined by substituting the midpoint values of the corresponding GN and MC ranges into the DPI and SEAT equations.

In this study, the research team followed the MnDOT approach to perform a regression analysis on the 2023-2025 database and fit envelop planes to the measured DPI and SEAT values from test locations that meet the required relative density. Figures 29 and 30 illustrate the fitted planes. The equations representing the planes fitted to the SDDOT data are presented below.

$$DPI = 24.42 - 3.89 \times GN + 0.17 \times MC$$

$$SEAT = 120.76 - 23.5 \times GN + 0.37 \times MC$$

**Equation 10. DPI and SEAT Functions Fitted to SDDOT Database**

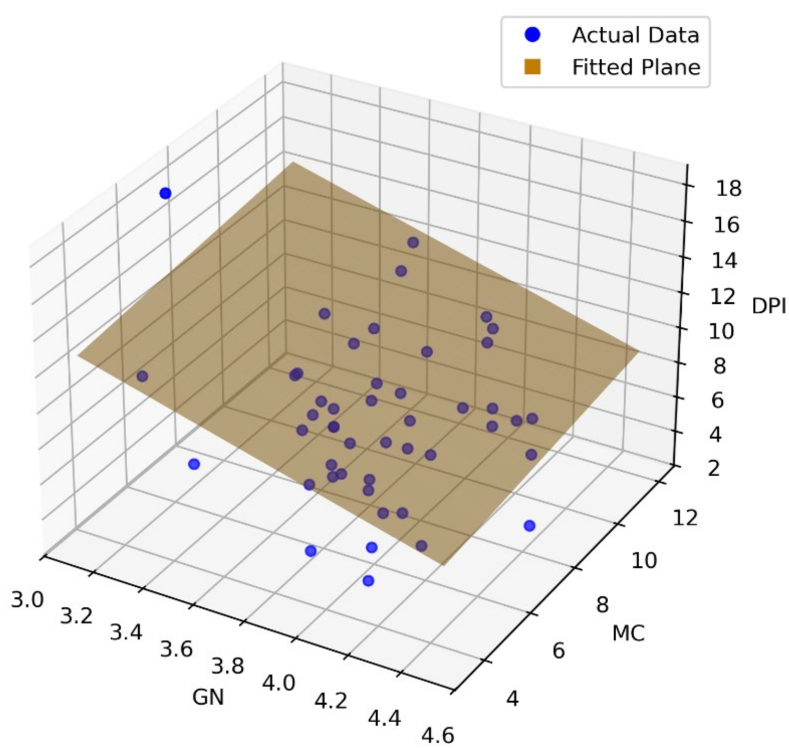


**Figure 29. Envelope Plane Fitted to DPI Values as a Function of MC and GN**

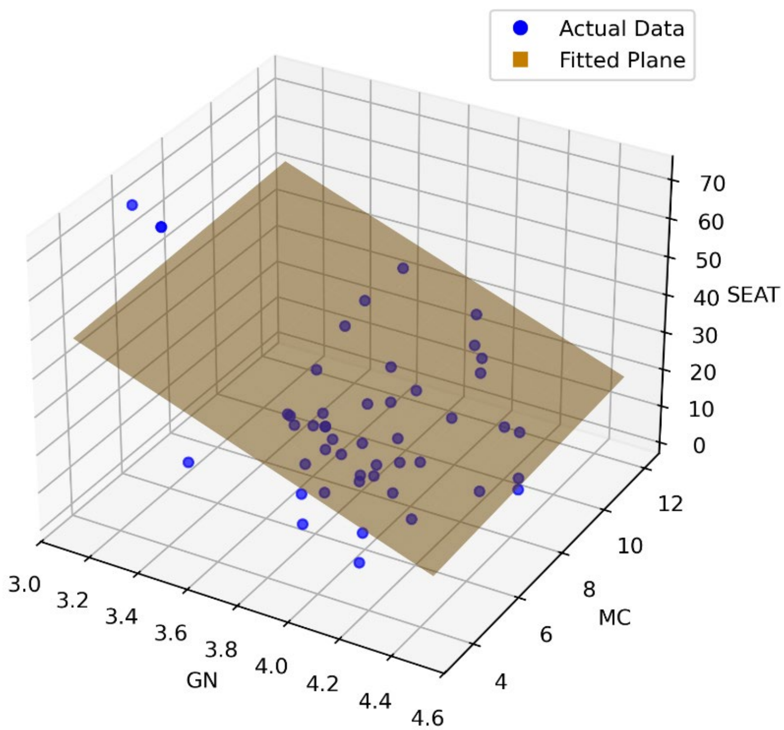


**Figure 30. Envelope Plane Fitted to SEAT Values as a Function of MC and GN**

As shown in the fitted equations and Figures 29 and 30, the DPI and SEAT relationships with GN in the SDDOT database do not exhibit an increasing trend. This behavior is inconsistent with the expected material response. The coefficient of determination ($R^2$) for the DPI and SEAT regression equations are 0.14 and 0.29, respectively, indicating weak relationships. These values are considerably lower than those obtained for the MnDOT database, where the corresponding $R^2$ values are 0.65 and 0.66.

One possible explanation for this discrepancy is the limited range of GN values in the SDDOT database. GN values in this dataset range only from 3.6 to 4.5, which may not be representative of the full range of material gradations. When the GN range is restricted, the underlying trend may not be clearly captured. In contrast, the MnDOT database covers a wider GN range (approximately 3.0 to 6.0), allowing the expected increasing trend to be more clearly observed. Figure 31 illustrates the relationship between DPI and GN in the MnDOT database, where this trend becomes apparent when the full GN range is considered. However, if the analysis in Figure 31 were limited to the narrow GN range of 3.6-4.5 represented in the SDDOT database, the increasing trend initially observed across the full GN range would no longer be evident.

Figure 34 shows the relation between DPI and GN in the SDDOT database. The DPI values exhibit high variability with respect to GN. If the current specification thresholds were updated using the DPI and SEAT equations presented in Equation 9, the allowable DPI and SEAT limits within the second and third GN ranges of Table 10 would decrease as GN increases. This outcome contradicts the expected trend and would create inconsistencies with the allowable limits in other GN ranges. As discussed earlier, the overall structure of the specification should accommodate a broader range of GN values and remain consistent with expected performance trends. For this reason, the research team decided not to use the regression equations fitted to the SDDOT database and instead adopted an alternative approach.

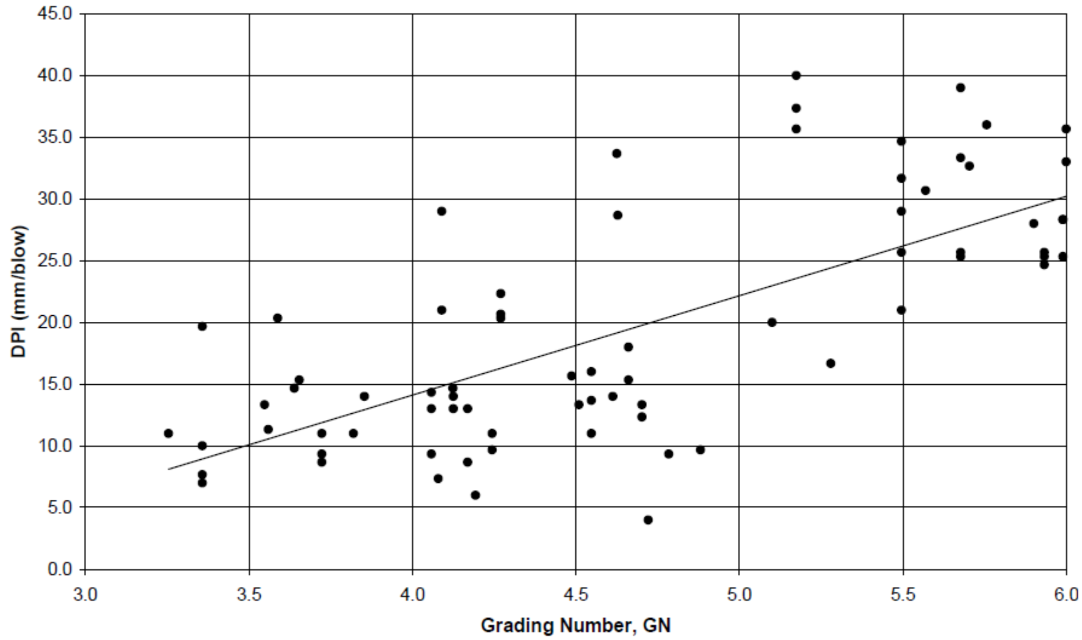


**Figure 31. DPI versus GN in MnDOT Database (add reference)**

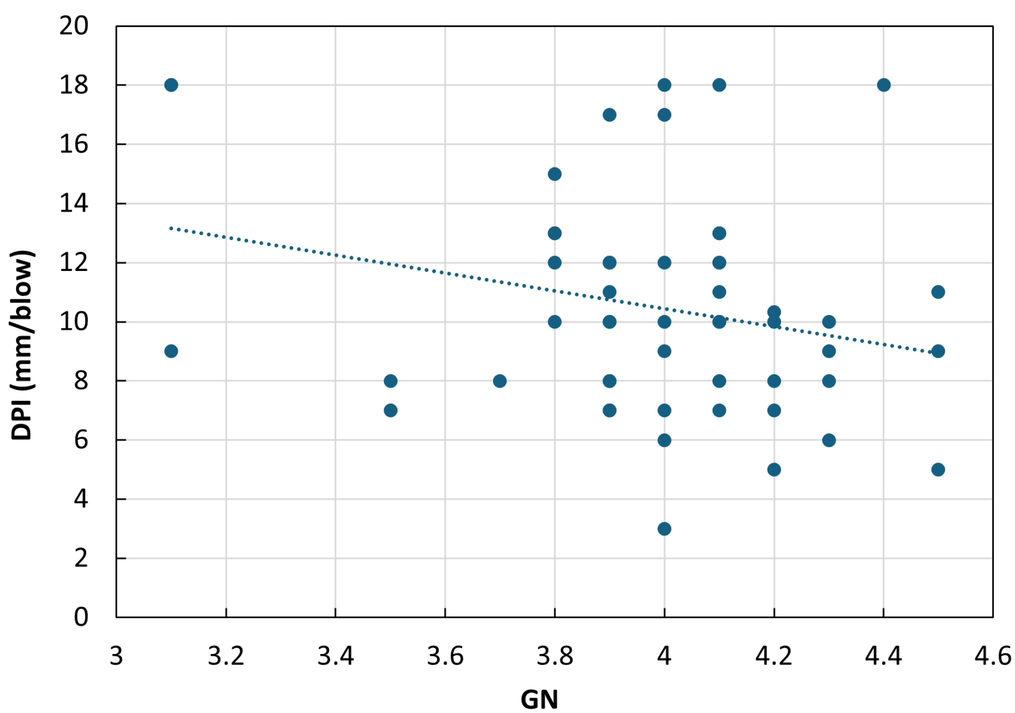


**Figure 32. DPI versus GN in SDDOT Database**

The MnDOT DPI and SEAT functions shown in Equation 8 provide a suitable basis for updating the allowable DPI and SEAT thresholds, as they reasonably represent the expected relationship among DPI, SEAT, GN, and MC. Figures 33 and 34 present the MnDOT DPI and SEAT planes plotted together with the 2023–2025 SDDOT datasets that meet the relative density requirements. These planes generally envelop the dataset, with the exception of a few outliers.

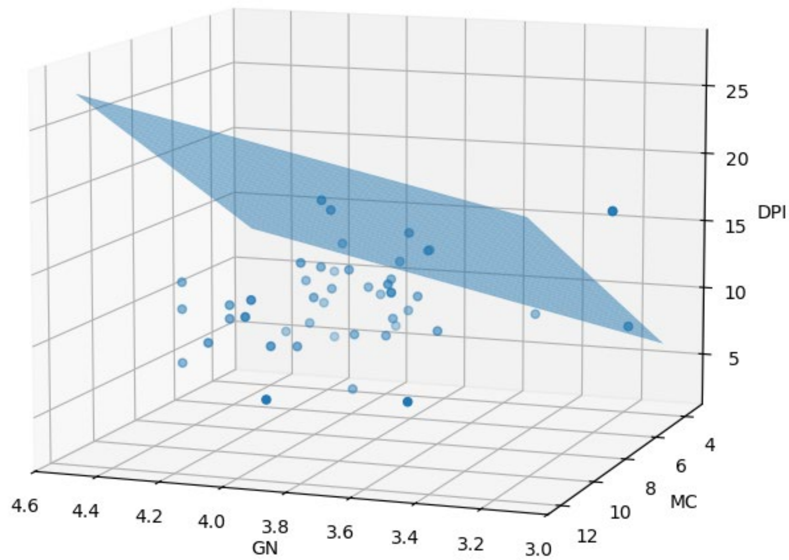


**Figure 33. The MnDOT DPI Plane on the 2023-2025 SDDOT Datasets**

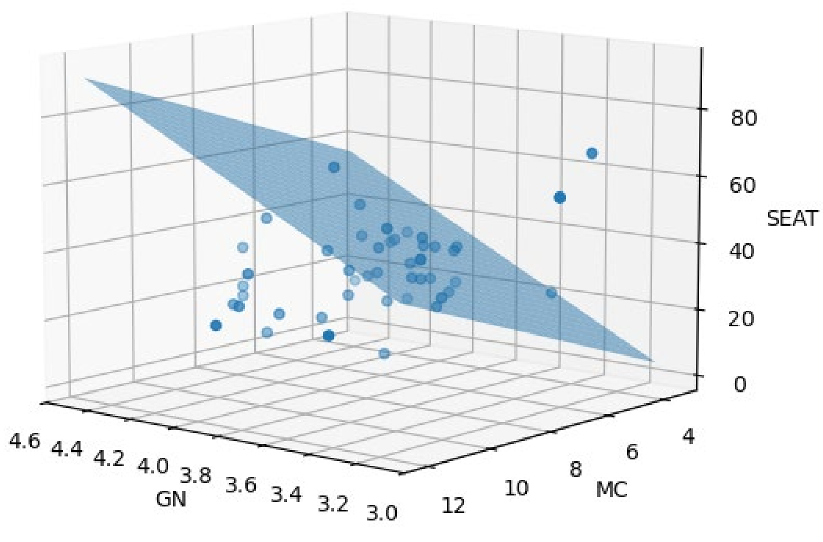


**Figure 34. The MnDOT SEAT Plane on the 2023-2025 SDDOT Datasets**

As mentioned earlier, to discretize the envelope plane fitted to the MnDOT data and develop the current MnDOT DCP specification, the MnDOT research team substituted the midpoint values of the corresponding GN and MC ranges into the DPI and SEAT equations (Equation 9). Figure 35 schematically illustrates this discretization process for the DPI plane. For each GN range in the current DCP specification, using the midpoint values results in a single constant threshold rather than a continuous planar relationship. Consequently, for approximately half of the points with GN and MC values greater than the midpoint, the threshold underestimates the allowable DPI, while for the remaining points below the midpoint, the threshold overestimates the allowable DPI. However, this behavior is inherent to the discretization process, in which a continuous relationship is approximated using discrete threshold values.

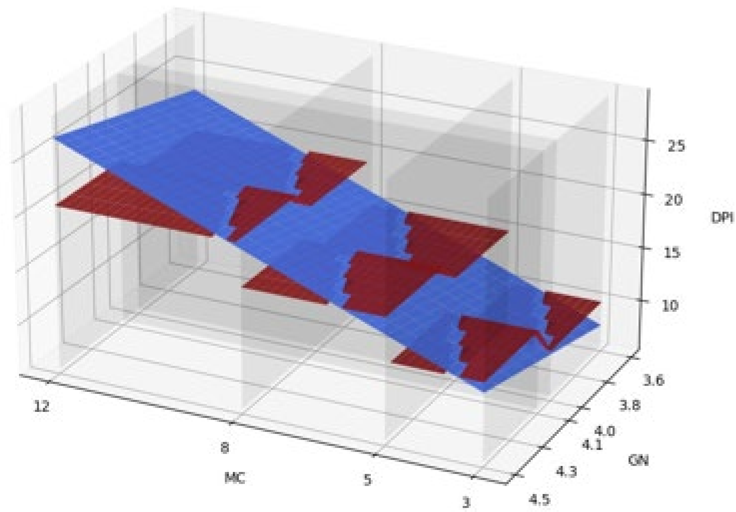


**Figure 35. Discretization of the MNDOT DPI Plane**

Instead of selecting midpoint values of the GN and MC ranges to determine allowable thresholds, an optimization analysis can be performed to identify DPI and SEAT thresholds that better represent SDDOT granular materials and improve agreement with compaction adequacy determined using relative density criteria. The objective of the optimization is to maximize agreement between DCP-based compaction adequacy and the relative compaction criteria.

The analysis is focused on the second and third GN ranges in Table 10, as these ranges contained sufficient data for meaningful evaluation. For each GN–MC subcategory, the 95$^{th}$ percentile of DPI and SEAT values for test locations meeting the relative density requirement and the 5$^{th}$ percentile of DPI and SEAT values for test locations failing the relative density requirement were calculated. These percentile values were used to define the feasible range of candidate threshold values.

As noted in the previous section, the research team initially preferred to use only the 2023–2025 database to evaluate the current DCP specification and develop potential improvements. However, this dataset contained only four test locations with inadequate compaction (i.e., relative density <97% for non-recycled materials and <95% for salvaged materials), which was insufficient to support meaningful modifications of the existing DPI and SEAT thresholds. Therefore, the 2019 database was combined with the 2023–2025 database to create a master database for further analysis, resulting in a total of 124 datasets.

The optimization analysis evaluated all candidate DPI and SEAT threshold values within the defined percentile-based bounds to identify the combination that maximized agreement between the DCP specification and the relative density criteria. The search space was further constrained by the MnDOT DPI and SEAT planes. When percentile values were not available for a specific GN-MC subcategory, the corresponding minimum or maximum value derived from the MnDOT fitted plane was used as the lower or upper bound.

In addition, if the percentile range did not include the current specification threshold, the corresponding bound was extended to the minimum or maximum value of the fitted plane within the applicable GN–MC increment so that the current threshold value was included in the optimization analysis. The optimization was performed simultaneously across all GN–MC increments. Agreement was defined as cases in which the DCP specification correctly predicted passing or failing compaction conditions consistent with the relative density requirements. Two constraints were imposed during the optimization process:

1. The DPI and SEAT thresholds must not decrease with increasing GN or MC, ensuring consistency with the expected physical relationship between DCP response, material gradation, and moisture content.
2. If multiple threshold values result in the same maximum level of agreement:
    - If the current specification threshold lies within this set of equally performing thresholds, it is retained to avoid unnecessary modification of the specification.
    - If the current specification threshold does not lie within this set, the threshold closest to the current specification value is selected.

This approach allows the specification to be updated using the available SDDOT datasets in the second and third GN ranges, while preserving the overall structure of the existing specification so that it remains applicable to a broader range of GN values that may occur in future construction projects.

Tables 12 and 13 summarize the results of the optimization analysis conducted on the available data. The last column of each table presents the recommended modifications to the DPI and SEAT thresholds. As shown, modifications are recommended for two GN–MC ranges.

**Table 12. Optimization Analysis Inputs and Results for DPI**

| GN Range | MC Range (%) | 95th Percentile DPI (Passed) | 5th Percentile DPI (Failed) | Current DPI | MnDOT Min. DPI | MnDOT Max. DPI | Tested Range | Recommended DPI |
|---|---|---|---|---|---|---|---|---|
| 3.6–4.0 | <5 | 13 | 16 | **10** | 8 | 13 | 8-16 | **13** |
| | 5-8 | 16 | 13 | 15 | 11 | 18 | 13-16 | 15 |
| | >8 | 15 | - | 19 | 16 | 25 | 15-25 | 19 |
| 4.1–4.5 | <5 | 12 | 11 | 13 | 10 | 15 | 11-15 | 13 |
| | 5-8 | 13 | 13 | 17 | 14 | 20 | 13-20 | 17 |
| | >8 | 15 | 18 | 21 | 19 | 27 | 15-27 | 21 |

**Table 13. Optimization Analysis Inputs and Results for SEAT**

| GN Range | MC Range (%) | 95th Percentile SEAT (Passed) | 5th Percentile SEAT (Failed) | Current SEAT | MnDOT Min. SEAT | MnDOT Max. SEAT | Tested Range | Recommended SEAT |
|---|---|---|---|---|---|---|---|---|
| 3.6–4.0 | <5 | 35 | 47 | 40 | 21 | 44 | 35-47 | 40 |
| | 5-8 | 62 | 38 | **45** | 29 | 56 | 38-62 | **50** |
| | >8 | 42 | - | 55 | 41 | 73 | 42-73 | 55 |
| 4.1–4.5 | <5 | 57 | 34 | 50 | 39 | 62 | 34-57 | 50 |
| | 5-8 | 57 | 46 | 60 | 47 | 75 | 46-75 | 60 |
| | >8 | 57 | 45 | 70 | 60 | 91 | 45-90 | 70 |

For materials with GN between 3.6 and 4.0 and MC less than 5%, the maximum allowable DPI is recommended to be increased from 10 to 13. In addition, for materials with GN between 3.6 and 4.0 and MC between 5% and 8%, the maximum allowable SEAT is recommended to be increased from 45 to 50. All other thresholds remain unchanged.

Table 14 presents the statistics of agreement between the relative density compaction criteria and both the current and modified DCP specifications for the 2023–2025 and 2019 databases. To evaluate the agreement between the DCP specification and the relative density compaction criteria, several performance metrics were calculated, as described below.

- TP (True Positive): Number of cases in which the DCP specification correctly predicts adequate compaction and the relative density also meets the required threshold.
- TN (True Negative): Number of cases in which the DCP specification correctly predicts inadequate compaction and the relative density fails to meet the required threshold.
- FP (False Positive): Number of cases in which the DCP specification predicts adequate compaction, but the relative density does not meet the required threshold.
- FN (False Negative): Number of cases in which the DCP specification predicts inadequate compaction while the relative density meets the required threshold.
- % Agreement (Percent Agreement): Percentage of cases in which the DCP specification and the relative density criteria provide the same compaction classification (either passing or failing).
- PPA (Positive Percent Agreement): Percentage of cases with adequate relative density that are correctly identified by the DCP specification. PPA is calculated as TP divided by the sum of TP and FN.
- NPA (Negative Percent Agreement): Percentage of cases with inadequate relative density that are correctly identified by the DCP specification. NPA is calculated as TN divided by the sum of TN and FP.

**Table 14. Statistics of Agreement Between Relative Density Compaction Criteria and DCP Specification**

| Database | Specification | % Agreement | PPA (%) | NPA (%) | TP | TN | FP | FN |
|---|---|---|---|---|---|---|---|---|
| 2023-2025 | Current | 87 | 91 | 50 | 39 | 2 | 2 | 4 |
| | Modified | 91 | 95 | 50 | 41 | 2 | 2 | 2 |
| 2019 | Current | 76 | 78 | 72 | 59 | 31 | 12 | 17 |
| | Modified | 79 | 83 | 72 | 63 | 31 | 12 | 13 |

It can be seen in Table 14 that the modified DCP specification improves the agreement with the relative density compaction criteria for both databases. For the 2023–2025 database, the overall agreement increases from 87% to 91%, primarily due to a reduction in FN instances from 4 to 2. This reduction results in an increase in PPA from 91% to 95%, while the NPA remains unchanged at 50%. Similarly, for the 2019 database, the modified specification increases the overall agreement from 76% to 79%, with PPA improving from 78% to 83% and NPA remaining unchanged at 72%. The improvement is mainly attributed to a reduction in FN instances from 17 to 13, indicating that the modified thresholds reduce the likelihood of incorrectly identifying adequately compacted materials as failing. Overall, these results demonstrate that the proposed modifications provide a modest but consistent improvement in the identification of compaction adequacy while maintaining the overall structure of the current DCP specification.

The optimization was intentionally constrained to preserve the overall structure of the specification and avoid excessive adjustments that could reduce its applicability across a broader range of GN values. As noted earlier, the number of datasets with failed relative density in the 2023–2025 database was very limited. To increase the number of failure cases available for analysis, the 2019 database was incorporated into the optimization. However, the 2019 dataset did not include one-point test results, which are currently used by SDDOT to determine MDUW and relative compaction at individual test locations. Therefore, although the inclusion of the 2019 database provided additional data for the analysis, the research team recognizes that the optimization results could potentially be further improved, particularly with respect to NPA, if additional datasets with failed relative density were available from recent projects or if one-point test results had been available for the 2019 database.

## 4.5 Conclusions

### 4.5.1 Development of the New SDDOT Moisture-Density Family of Curves

- A master database of 294 unique compaction curves was compiled and analyzed using a quadratic spline function to determine OMC and MDUW for each curve. The datasets were grouped into 2-pcf intervals, and a Gaussian model was fitted to each group, resulting in a new set of SDDOT Family of Curves.

- The redevelopment effort corrected the deficiencies of the earlier SDDOT curves by eliminating overlapping curves, expressing the family in terms of wet unit weight, centering curve peaks on a fitted line of optimums, and developing a universal model that permits interpolation at 1-pcf increments. Compared with the original SDDOT family, the new system provides direct determination of OMC and MDUW from the curves, smooth transitions across the wet unit weight range, 1-pcf spacing rather than 2-pcf spacing, and broader moisture-content coverage.

- The line of optimums for the OHD Family of Curves was plotted within a 95% prediction interval for South Dakota's granular materials. While the OHD curves closely followed the fitted regression line for MDUW values between approximately 117-131 pcf, deviations were noted outside this range.

- Statistical analysis revealed that the OHD Family of Curves tends to overestimate compaction compared to the SDDOT curves, with a mean difference of 2.01 pcf, which was statistically significant.

- Verification of the new SDDOT Family of Curves was conducted using 5% of randomly selected compaction curves (four-point datasets). The results showed that the SDDOT curves had lower mean absolute deviation (MAD) values for both OMC and MDUW compared to the OHD curves, confirming higher accuracy.

- Validation with 42 new compaction curves showed that the SDDOT Family of Curves performed better than the OHD curves. The 1-pcf SDDOT curves provided better accuracy for MDUW, while both the 1-pcf and 2-pcf SDDOT curves performed similarly for OMC and outperformed the OHD curves.

### 4.5.2 Excel Program for the Automated Calculation of OMC and MDUW

- The tool developed under the SD2023-02 project successfully automates moisture-density calculations for SDDOT granular materials by accurately matching one-point Proctor test results with the nearest curve from the newly developed 1-pcf SDDOT Family of Curves, enabling reliable estimation of OMC and MDUW.

- The optional checks for compliance with the MDUW tolerance relative to four-point curves per the SDDOT Materials Manual and for comparison with the OHD curves enhance the tool's reliability.

- This new tool meets the functional requirements outlined in the project scope and serves as an efficient alternative to traditional manual calculations.

### 4.5.3 Assessment of Agreement Between DCP Specification and the New SDDOT Moisture-Density Curves

- The MnDOT DCP-based compaction specification shows generally good agreement with compaction adequacy determined using the new SDDOT moisture–density curves.

- For the 2023–2025 non-recycled material database, the DCP specification agrees with the relative compaction assessment in 81% of cases when relative density is calculated using the new SDDOT curves.

- The DCP specification underestimates compaction adequacy in 17% of cases where the relative density meets or exceeds the required threshold, but the DCP specification indicates inadequate compaction.

- The DCP specification falsely predicts adequate compaction in 2% of cases, where the DCP criteria are satisfied but the relative density is below the required threshold.

- Compared with the OHD family of curves, the new SDDOT curves result in fewer cases where the DCP specification falsely predicts adequate compaction, indicating improved reliability of the DCP specification.

- Analysis of salvaged materials using the test strip target density method shows that the DCP specification agrees with the relative density assessment 80% of the time, with 10% underestimation and 10% overestimation of compaction adequacy.

- Overall, the results indicate that the DCP specification provides a reasonable assessment of compaction adequacy when used with the new SDDOT moisture–density curves, while still allowing room for further improvement in agreement.

### 4.5.4 Refinement of the MnDOT DCP Specification for SDDOT Granular Materials

- The available SDDOT database primarily included granular materials with GN values between 3.6 and 4.5. Accordingly, the refinement analysis focused on this GN range while maintaining the overall structure of the specification to ensure applicability to a broader range of GN values.

- Because the MnDOT regression equations represent the expected physical relationships among DPI, SEAT, GN, and MC, the MnDOT DPI and SEAT planes were used as a reference framework for refining allowable thresholds for SDDOT materials.

- An optimization analysis was conducted to determine DPI and SEAT thresholds that maximize the agreement between DCP-based compaction acceptance criteria and relative density requirements. The optimization evaluated candidate thresholds within percentile ranges derived from the datasets, while constraining the search space using the MnDOT DPI and SEAT planes and enforcing monotonic trends with respect to GN and MC.

- The results indicate that modifications to the current specification can improve performance, specifically:

  - Increasing the allowable DPI threshold from 10 to 13 for materials with GN between 3.6 and 4.0 and MC < 5%.

  - Increasing the allowable SEAT threshold from 45 to 50 for materials with GN between 3.6 and 4.0 and MC between 5% and 8%.

- Performance evaluation showed that the modified specification improves agreement with the relative density criteria, increasing overall agreement from 87% to 91% for the 2023–2025 database and from 76% to 79% for the 2019 database.

- Additional datasets containing more observations of inadequate compaction (failed relative density) would allow further refinement of the DCP specification and could potentially improve its predictive performance, especially with respect to Negative Percent Agreement (NPA).

# Chapter 5. Recommendations

The recommendations presented in this chapter are based on the findings and conclusions of this study regarding the development of the new SDDOT moisture–density family of curves and the evaluation of the DCP specification for compaction control of granular materials. These recommendations are intended to assist SDDOT in implementing the results of this research and improving current compaction evaluation practices. Each recommendation is derived from analyses presented in previous chapters and is accompanied by supporting explanation to facilitate practical application and future evaluation of its effectiveness.

## 5.1 Adoption of the Newly Developed SDDOT Moisture–Density Family of Curves for Determining Target Compaction Parameters

- It is recommended that SDDOT adopt the newly developed SDDOT moisture–density family of curves for determining OMC and MDUW of granular base and subbase materials.
- To ensure the ongoing reliability and accuracy of these curves, it is recommended that SDDOT periodically review and update the SDDOT family of curves as additional compaction data become available, preferably at five-year intervals. Periodic updates will ensure that the curves continue to reflect the characteristics of granular materials used in construction projects across the state.

The analysis presented in Chapter 4, Section 4.1 demonstrates that the SDDOT curves provide improved prediction accuracy compared with the OHD family of curves currently used by SDDOT. Verification and validation analyses showed lower mean absolute deviations in predicted OMC and MDUW values when using the SDDOT curves. Because the curves were developed using a comprehensive database of compaction tests from South Dakota construction projects, they better represent the characteristics of local granular materials. Adoption of these curves would improve the accuracy and consistency of target compaction parameters used in the field.

## 5.2 Implementation of the Automated Excel Tool for One-Point Proctor Analysis

- It is recommended that SDDOT implement the Excel-based tool developed in this study to automate the determination of OMC and MDUW from one-point Proctor test data.

The Excel program developed in this study allows users to input one-point Proctor test results and automatically determine the corresponding OMC and MDUW based on the SDDOT family of curves. The tool also includes automated plotting capabilities and built-in verification checks consistent with tolerances specified in the SDDOT Materials Manual. Implementation of this tool would reduce calculation errors, improve consistency in determining compaction parameters, and streamline the compaction evaluation process for field and laboratory personnel.

## 5.3 Evaluation of the DCP Specification Through a Three-Year Parallel Implementation Program

- It is recommended that SDDOT collect DCP data side by side with relative density data for a period of three years to support the validation and further refinement of the DCP specification.

- It is recommended that SDDOT continue using relative density, determined using the new SDDOT moisture–density family of curves, as the primary criterion for evaluating compaction adequacy of granular materials during the three-year parallel implementation program, and collect the DCP data as a supplemental for validation purposes.
- It is recommended that SDDOT implement the refined DPI and SEAT threshold values identified in this study when adopting the DCP specification during the three-year parallel implementation program.

The optimization analysis conducted in this study demonstrated that the current DCP specification performs reasonably well and that its performance can be further enhanced through targeted adjustments. Continued collection of relative density data alongside DCP test results during the three-year parallel implementation program will allow SDDOT to verify the correct implementation and integration of the refined DCP specification with the newly developed SDDOT moisture-density family of curves, and to validate the combined field performance of these two newly introduced components within the compaction process. Because this program represents the simultaneous incorporation of a new moisture–density reference system and a refined DCP-based compaction acceptance method, verification and validation are both essential to ensure procedural consistency, technical reliability, and performance under field conditions. The additional data collected during this period would also support further refinement of the DCP thresholds, particularly by improving the identification of inadequately compacted materials and strengthening the Negative Percent Agreement. This consideration is particularly important given the limited number of test locations exhibiting inadequate compaction and the relatively small number of datasets involving salvaged materials in the 2023–2025 database.

Upon completion of the evaluation period, SDDOT will have sufficient evidence to determine whether the DCP specification is suitable for broader implementation as a standalone acceptance method or should remain a supplemental quality control tool.

# Chapter 6. Research Benefit

The products of the proposed research effort will benefit SDDOT's pavement engineering practice in several ways:

- The modified OHD family of curves currently in use by SDDOT has shown a tendency to overestimate the target compaction density (Jones and Weber, 2019). The newly developed SDDOT moisture-density family of curves is expected to provide more accurate target compaction parameters for native granular materials in South Dakota. This improvement will help prevent over compaction in the field, resulting in direct cost savings through increased work efficiency as target densities are achieved in less time.

- Use of the refined SDDOT moisture-density family of curves will reduce the potential for early degradation of granular materials caused by over compaction (i.e., aggregate fracture, attrition, or abrasion). By preserving material integrity, this approach is expected to enhance the mechanical properties of granular layers and contribute to an extended pavement service life.

- The Excel-based tool developed to automatically calculate OMC and MDUW from one-point Proctor test data will improve the efficiency and effectiveness of SDDOT field and laboratory personnel. By simplifying calculations and improving accuracy, this tool will reduce time requirements and minimize costs associated with errors from manual computations.

- In the long term, implementation of DCP-based compaction quality control specifications has the potential to reduce safety risks associated with the operation of nuclear gauge density devices in the field, which is currently common practice in South Dakota.

- The DCP test provides a simple, reliable, and rapid alternative to the sand cone test for compaction quality control. When fully implemented, the DCP-based specification can reduce testing time relative to current practices, leading to improved work efficiency and additional cost savings.

- Implementation of the DCP specification will help bridge the gap between pavement design and construction by incorporating strength-based parameters, such as SEAT and DPI, into compaction control. DCP test results collected during construction can be more directly linked to pavement design in a more fundamental way through correlations with resilient modulus, which is a fundamental design input for unbound materials. The availability of such information can support improved pavement evaluation, performance analysis, and rehabilitation strategy development.

# References

AASHTO. (2022a). Standard method of test for family of curves—one-point method (AASHTO T 272-18). In Standard Specifications for Transportation Materials and Methods of Sampling and Testing. American Association of State Highway and Transportation Officials, Washington, DC.

AASHTO. (2022b). Standard method of test for moisture–density relations of soils using a 2.5-kg (5.5-lb) rammer and a 305-mm (12-in.) drop (AASHTO T 99). In Standard Specifications for Transportation Materials and Methods of Sampling and Testing. American Association of State Highway and Transportation Officials, Washington, DC.

Dai, S., & Kremer, C. (2006). Improvement and validation of Mn/DOT DCP specification for aggregate base materials and select granular. MN/RC-2005-32 Final Report. Minnesota Department of Transportation, Office of Materials and Road Research, Maplewood, MN.

Ghabchi, R. (2022). Evaluation of granular density and moisture testing. SD2019-05-F Final Report. South Dakota Department of Transportation, Office of Research, Pierre, SD.

Jones, A., & Weber, J. (2019). Compaction testing of granular material. SD2014-12-F Final Report. South Dakota Department of Transportation, Office of Research, Pierre, SD.

Minnesota Department of Transportation (MnDOT). (2025). Grading and base manual. MnDOT Geotechnical Section, Grading and Base Unit. https://www.dot.state.mn.us/materials/gbmanual.html

South Dakota Department of Transportation (SDDOT). (2015a). “Standard Specifications for Roads and Bridges.” SDDOT, Pierre, SD.

South Dakota Department of Transportation (SDDOT). (2015b). SD 104: Moisture–density relations of soils, aggregates, and specified mixtures. In South Dakota Department of Transportation Materials Manual. SDDOT, Pierre, SD.

South Dakota Department of Transportation (SDDOT). (2015c). SD 219: Determining target dry density and in-place density of salvaged/recycled materials using the nuclear gauge (test strip). In South Dakota Department of Transportation Materials Manual. SDDOT, Pierre, SD.

# Appendix A: Master Database for Developing SDDOT Family of Curves

# 4-point Data Along with OMC and MDUW Determined from Quadratic Spline Fit

| Sample ID | Project | Proctor Test Data: Percent Moisture (%) | | | | | | | Wet Density (pcf) | | | | | | | Dry Density (pcf) | | | | | | | Quadratic Spline Fit | |
|---|---|---|---|---|---|---|---|---|---|---|---|---|---|---|---|---|---|---|---|---|---|---|---|---|
| | | Specimen 1 | Specimen 2 | Specimen 3 | Specimen 4 | Specimen 5 | Specimen 6 | Specimen 7 | Specimen 1 | Specimen 2 | Specimen 3 | Specimen 4 | Specimen 5 | Specimen 6 | Specimen 7 | Specimen 1 | Specimen 2 | Specimen 3 | Specimen 4 | Specimen 5 | Specimen 6 | Specimen 7 | OMC | MDUW |
| 1466756 | IM 0901(135)14 | 3.7 | 6.5 | 8 | 7 | #N/A | #N/A | #N/A | 124.4 | 140.8 | 143.6 | 142.8 | #N/A | #N/A | #N/A | 120 | 132.2 | 133 | 133.5 | #N/A | #N/A | #N/A | 7.4 | 133.8 |
| 2131461 | P-PH 0073(48)177 | 5 | 6.6 | 9.7 | 10.7 | #N/A | #N/A | #N/A | 127.5 | 134.8 | 142.4 | 142.6 | #N/A | #N/A | #N/A | 121.4 | 126.5 | 129.8 | 128.8 | #N/A | #N/A | #N/A | 9.3 | 129.9 |
| 2157953 | EM 0385(15)0 | 3 | 5.7 | 7.3 | 8.2 | #N/A | #N/A | #N/A | 131.9 | 143.3 | 149.9 | 148.3 | #N/A | #N/A | #N/A | 128.1 | 135.6 | 139.7 | 137.1 | #N/A | #N/A | #N/A | 7.2 | 139.7 |
| 2173471 | EM 0385(15)0 | 3.7 | 5.8 | 8.4 | 10.8 | #N/A | #N/A | #N/A | 124.4 | 130.3 | 136.9 | 135.3 | #N/A | #N/A | #N/A | 120 | 123.2 | 126.3 | 122.1 | #N/A | #N/A | #N/A | 8.3 | 126.3 |
| 1414276 | POENH(G0) | 2.8 | 4.4 | 6.5 | 7.7 | #N/A | #N/A | #N/A | 128 | 136 | 147.7 | 148.9 | #N/A | #N/A | #N/A | 124.5 | 130.3 | 138.7 | 138.3 | #N/A | #N/A | #N/A | 7.0 | 139.1 |
| 1430197 | IM 0901(00)48 | 2.3 | 4.1 | 6.5 | 7.9 | #N/A | #N/A | #N/A | 130.5 | 138 | 146.7 | 147.3 | #N/A | #N/A | #N/A | 127.6 | 132.6 | 137.7 | 136.5 | #N/A | #N/A | #N/A | 6.7 | 137.8 |
| 2085782 | ES 3040(08)47 | 4.6 | 6.9 | 8.3 | 3.4 | #N/A | #N/A | #N/A | 134.7 | 140.1 | 142.8 | 127.1 | #N/A | #N/A | #N/A | 128.8 | 131.1 | 131.9 | 122.9 | #N/A | #N/A | #N/A | 8.3 | 131.9 |
| 2093486 | ES 3040(08)47 | 4.9 | 7.6 | 9.5 | 11.1 | #N/A | #N/A | #N/A | 136.3 | 143.6 | 142.8 | 140.1 | #N/A | #N/A | #N/A | 129.9 | 133.5 | 130.4 | 126.1 | #N/A | #N/A | #N/A | 7.2 | 133.6 |
| 2151550 | EM 0018(151)52 | 4 | 5.9 | 7.2 | 7.7 | #N/A | #N/A | #N/A | 136.9 | 143.8 | 148.8 | 148.2 | #N/A | #N/A | #N/A | 131.6 | 135.8 | 138.8 | 137.6 | #N/A | #N/A | #N/A | 7.1 | 138.8 |
| 2098574 | P 6106(06) | 4.2 | 6.1 | 7.7 | 10.2 | #N/A | #N/A | #N/A | 129.8 | 135.7 | 145.5 | 145.2 | #N/A | #N/A | #N/A | 124.6 | 127.9 | 135.1 | 131.8 | #N/A | #N/A | #N/A | 8.6 | 136.4 |
| 2237910 | P 6434(02) | 5.6 | 7.9 | 9.3 | 10.6 | #N/A | #N/A | #N/A | 130.4 | 139.7 | 142.3 | 140.9 | #N/A | #N/A | #N/A | 123.5 | 129.5 | 130.2 | 127.4 | #N/A | #N/A | #N/A | 8.9 | 130.3 |
| 1480874 | P 1014(45)28 | 5 | 6.1 | 8.6 | 9.5 | #N/A | #N/A | #N/A | 126.4 | 136.2 | 142.2 | 143.4 | #N/A | #N/A | #N/A | 120.4 | 128.4 | 130.9 | 131 | #N/A | #N/A | #N/A | 7.2 | 131.2 |
| 1414996 | IM 90-1(120)33 | 3.4 | 5.4 | 7.3 | 8.5 | #N/A | #N/A | #N/A | 132.4 | 139.9 | 145.9 | 147.5 | #N/A | #N/A | #N/A | 128 | 132.7 | 136 | 135.9 | #N/A | #N/A | #N/A | 7.8 | 136.2 |
| 2097623 | IM 0901(137)10 | 3.4 | 5.4 | 7.1 | 8.8 | 10.3 | #N/A | #N/A | 121.4 | 129.8 | 136.3 | 142.1 | 141.7 | #N/A | #N/A | 117.4 | 123.1 | 127.3 | 130.6 | 128.5 | #N/A | #N/A | 9.0 | 130.6 |
| 2184241 | BRF 6419(06) | 3 | 5.5 | 6.7 | 9.1 | #N/A | #N/A | #N/A | 132.8 | 137.1 | 143.1 | 146.1 | #N/A | #N/A | #N/A | 128.9 | 130 | 134.1 | 133.9 | #N/A | #N/A | #N/A | 7.9 | 135.7 |
| 2184259 | BRF 6419(06) | 3 | 5 | 7.5 | 10.6 | #N/A | #N/A | #N/A | 130.9 | 144.5 | 147.7 | 147.2 | #N/A | #N/A | #N/A | 127.1 | 137.6 | 137.4 | 133.1 | #N/A | #N/A | #N/A | 5.9 | 138.8 |
| 2080354 | ES 0016(68)61 | 2.2 | 4.3 | 5.8 | 9.6 | #N/A | #N/A | #N/A | 126.5 | 140.4 | 148.2 | 149.3 | #N/A | #N/A | #N/A | 123.8 | 134.6 | 140.1 | 136.2 | #N/A | #N/A | #N/A | 7.1 | 141.8 |
| 2087523 | P 0044(137)46 | 4.7 | 5.9 | 7.2 | 8.3 | #N/A | #N/A | #N/A | 138.2 | 146.3 | 150.1 | 150.3 | #N/A | #N/A | #N/A | 132 | 138.1 | 140 | 138.8 | #N/A | #N/A | #N/A | 7.2 | 140.0 |
| 2130660 | NH 014A(04)37 | 4.4 | 6.3 | 8 | 2.9 | #N/A | #N/A | #N/A | 137.8 | 149 | 150.9 | 126.1 | #N/A | #N/A | #N/A | 132 | 140.2 | 139.7 | 122.5 | #N/A | #N/A | #N/A | 7.0 | 141.0 |
| 2123815 | PH 1614(01) | 3.6 | 5.4 | 6.7 | 10.6 | 1.8 | #N/A | #N/A | 132.2 | 137.4 | 144.2 | 143.9 | 124.2 | #N/A | #N/A | 127.6 | 130.4 | 135.1 | 130.1 | 122 | #N/A | #N/A | 7.6 | 135.5 |
| 2243291 | BRO 8024(12) | 2.6 | 4.5 | 6.8 | 10.2 | #N/A | #N/A | #N/A | 131.2 | 136 | 147.5 | 150.1 | #N/A | #N/A | #N/A | 127.9 | 130.1 | 138.1 | 136.2 | #N/A | #N/A | #N/A | 8.2 | 139.8 |
| 2135201 | P 1608(04) | 5.3 | 6.9 | 8.2 | 3.8 | #N/A | #N/A | #N/A | 142 | 143.8 | 144 | 134.6 | #N/A | #N/A | #N/A | 134.9 | 134.5 | 133.1 | 129.7 | #N/A | #N/A | #N/A | 5.8 | 135.3 |
| 2067336 | BRO 8052(60) | 1.9 | 3.9 | 5.4 | 7.3 | #N/A | #N/A | #N/A | 132.2 | 138.1 | 147.4 | 149.3 | #N/A | #N/A | #N/A | 129.7 | 132.9 | 139.8 | 139.1 | #N/A | #N/A | #N/A | 6.3 | 141.1 |
| 2158483 | P-PH 0087(11)73 | 3.5 | 5.3 | 6.8 | 9.9 | #N/A | #N/A | #N/A | 131.7 | 139.6 | 148.3 | 148.9 | #N/A | #N/A | #N/A | 127.2 | 132.6 | 138.9 | 135.5 | #N/A | #N/A | #N/A | 8.0 | 140.6 |
| 2086285 | ES 0079(66)185 | 6.2 | 7.8 | 9.5 | 10.6 | #N/A | #N/A | #N/A | 128.8 | 134.6 | 142.7 | 145.8 | #N/A | #N/A | #N/A | 121.3 | 124.9 | 130.3 | 131.8 | #N/A | #N/A | #N/A | 10.6 | 131.8 |
| 2152663 | P 0034(133)34 | 5.5 | 6.8 | 8.8 | 9.7 | #N/A | #N/A | #N/A | 130.1 | 138 | 144.2 | 144 | #N/A | #N/A | #N/A | 123.3 | 129.2 | 132.5 | 131.3 | #N/A | #N/A | #N/A | 8.6 | 132.5 |
| 2209171 | NH 0016(78)67 | 4.3 | 5.6 | 7.1 | 8.3 | #N/A | #N/A | #N/A | 128.1 | 134.9 | 139.9 | 144.8 | #N/A | #N/A | #N/A | 122.8 | 127.7 | 130.6 | 133.7 | #N/A | #N/A | #N/A | 8.3 | 133.7 |
| 2100956 | P 7699(05) | 5.2 | 7.1 | 8.4 | 9.5 | 11.6 | #N/A | #N/A | 133.5 | 144.3 | 144 | 145.4 | 144.7 | #N/A | #N/A | 126.9 | 134.7 | 132.8 | 132.8 | 129.7 | #N/A | #N/A | 7.7 | 135.2 |
| 2224562 | IM 0901(162)14 | 2.1 | 3.8 | 5.5 | 8 | 10.2 | #N/A | #N/A | 125.5 | 129.3 | 136.3 | 145.5 | 150.6 | #N/A | #N/A | 122.9 | 124.6 | 129.2 | 134.7 | 136.7 | #N/A | #N/A | 10.2 | 136.7 |
| 2165374 | IM 0902(148)111 | 6 | 8 | 9.5 | 3.9 | #N/A | #N/A | #N/A | 138.9 | 142.4 | 139.1 | 128.1 | #N/A | #N/A | #N/A | 131 | 131.9 | 127 | 123.3 | #N/A | #N/A | #N/A | 7.3 | 132.5 |
| 2173242 | IM 0902(148)111 | 5.6 | 6.7 | 7.3 | 10.1 | #N/A | #N/A | #N/A | 141.2 | 146.4 | 147.3 | 142.5 | #N/A | #N/A | #N/A | 133.7 | 137.2 | 137.3 | 129.4 | #N/A | #N/A | #N/A | 7.0 | 137.4 |
| 2188570 | NH 0016(72)11 | 3.5 | 5.1 | 7.7 | 10.3 | #N/A | #N/A | #N/A | 117.1 | 124.5 | 133.2 | 136.7 | #N/A | #N/A | #N/A | 113.1 | 118.5 | 123.7 | 123.9 | #N/A | #N/A | #N/A | 9.1 | 124.4 |
| 2194424 | NH 0016(72)11 | 1.7 | 3.8 | 5.2 | 7.6 | #N/A | #N/A | #N/A | 128.7 | 135.3 | 141.9 | 150 | #N/A | #N/A | #N/A | 126.5 | 130.3 | 134.9 | 139.4 | #N/A | #N/A | #N/A | 7.6 | 139.4 |
| 2158018 | P 0073(52)177 | 5.4 | 7.3 | 8.9 | 9.9 | #N/A | #N/A | #N/A | 134.9 | 142.2 | 147.7 | 146 | #N/A | #N/A | #N/A | 128 | 132.5 | 135.6 | 132.8 | #N/A | #N/A | #N/A | 8.8 | 135.6 |
| 2160089 | NH 0018(175)12 | 2.9 | 5.1 | 7.2 | 9.8 | #N/A | #N/A | #N/A | 135.2 | 142.5 | 148.5 | 147.3 | #N/A | #N/A | #N/A | 131.4 | 135.6 | 138.5 | 134.2 | #N/A | #N/A | #N/A | 7.4 | 138.5 |
| 2313688 | NH 0044(167)44 | 2.9 | 5.6 | 6.9 | 10.1 | #N/A | #N/A | #N/A | 128.6 | 137.8 | 144.5 | 144.2 | #N/A | #N/A | #N/A | 125 | 130.5 | 135.2 | 131 | #N/A | #N/A | #N/A | 8.0 | 136.6 |
| 2321243 | NH 0044(167)44 | 10.1 | 14.4 | 15.4 | 16.4 | 9.2 | #N/A | #N/A | 114.1 | 123 | 128.1 | 129.4 | 114.1 | #N/A | #N/A | 103.6 | 107.5 | 111 | 111.2 | 104.5 | #N/A | #N/A | 16.0 | 111.6 |
| 2189750 | P 0085(72)23 | 3 | 5.3 | 6.4 | 8 | #N/A | #N/A | #N/A | 128.9 | 137.2 | 141.9 | 151.3 | #N/A | #N/A | #N/A | 125.1 | 130.3 | 133.4 | 140.1 | #N/A | #N/A | #N/A | 8.0 | 140.1 |
| 2146553 | BRF 0079(67)160 | 2.6 | 5 | 8.2 | 9.6 | #N/A | #N/A | #N/A | 129.1 | 137.1 | 144.5 | 143.5 | #N/A | #N/A | #N/A | 125.8 | 130.6 | 133.5 | 130.9 | #N/A | #N/A | #N/A | 7.5 | 133.8 |
| 2197078 | P 0034(143)44 | 4.2 | 5.9 | 7.9 | 9.8 | #N/A | #N/A | #N/A | 134 | 142.8 | 146.9 | 144.8 | #N/A | #N/A | #N/A | 128.6 | 134.8 | 136.1 | 131.9 | #N/A | #N/A | #N/A | 7.3 | 136.3 |
| 2139994 | P 6121(11) | 6.8 | 8.4 | 11.7 | 2.1 | #N/A | #N/A | #N/A | 135.3 | 140.8 | 141.9 | 122.5 | #N/A | #N/A | #N/A | 126.7 | 129.9 | 127 | 120 | #N/A | #N/A | #N/A | 9.4 | 130.5 |
| 2272425 | BRO 8041(00)01 | 4 | 5.6 | 7.2 | 8.2 | #N/A | #N/A | #N/A | 132.5 | 136.7 | 145.5 | 147.3 | #N/A | #N/A | #N/A | 127.4 | 129.5 | 135.7 | 136.1 | #N/A | #N/A | #N/A | 7.8 | 136.4 |
| 2369748 | BRO 8024(14) | 2.9 | 4.8 | 6.6 | 8.3 | 10.5 | #N/A | #N/A | 128.7 | 135.7 | 142.7 | 146.3 | 144.9 | #N/A | #N/A | 125.1 | 129.5 | 133.9 | 135.1 | 131.1 | #N/A | #N/A | 8.0 | 135.2 |
| 2378659 | BRO 8024(14) | 2.5 | 4.1 | 6.2 | 8.6 | #N/A | #N/A | #N/A | 122.9 | 130.5 | 137.6 | 139.6 | #N/A | #N/A | #N/A | 119.9 | 125.4 | 129.6 | 128.5 | #N/A | #N/A | #N/A | 7.0 | 130.0 |
| 2087317 | ES 0ENH(201) | 4.4 | 6.1 | 8.2 | 9.1 | #N/A | #N/A | #N/A | 133.9 | 143.2 | 148.6 | 149 | #N/A | #N/A | #N/A | 128.3 | 135 | 137.3 | 136.6 | #N/A | #N/A | #N/A | 8.0 | 137.3 |
| 2094340 | ES 0ENH(201) | 3.9 | 5.2 | 7 | 8.7 | #N/A | #N/A | #N/A | 131.9 | 143.2 | 150.3 | 149.9 | #N/A | #N/A | #N/A | 126.9 | 136.1 | 140.5 | 137.9 | #N/A | #N/A | #N/A | 7.1 | 140.5 |
| 2099125 | ES-NH-PH 0018(170) | 6.4 | 8.6 | 10.4 | 12.5 | #N/A | #N/A | #N/A | 119 | 127.5 | 131.4 | 131.5 | #N/A | #N/A | #N/A | 111.8 | 117.4 | 119 | 116.9 | #N/A | #N/A | #N/A | 10.5 | 119.0 |
| 2102524 | ES-NH-PH 0018(170) | 2.1 | 4 | 6.4 | 8.6 | #N/A | #N/A | #N/A | 133.5 | 137.6 | 145.1 | 146 | #N/A | #N/A | #N/A | 130.8 | 132.3 | 136.4 | 134.4 | #N/A | #N/A | #N/A | 6.8 | 136.5 |
| 2116953 | ES-NH-PH 0018(170) | 3.3 | 5.2 | 6.8 | 8.5 | #N/A | #N/A | #N/A | 136.6 | 141.9 | 146.2 | 146.9 | #N/A | #N/A | #N/A | 132.2 | 134.9 | 136.9 | 135.4 | #N/A | #N/A | #N/A | 7.0 | 136.9 |
| 2126809 | IM 0901(166)17 | 3.3 | 4.7 | 7.4 | 8.2 | 10.6 | #N/A | #N/A | 125.9 | 128.9 | 139.4 | 143.8 | 142.5 | #N/A | #N/A | 121.9 | 123.1 | 129.8 | 132.9 | 128.8 | #N/A | #N/A | 9.0 | 134.0 |
| 2271173 | PH 0012(168)80 | 4.4 | 7 | 8.5 | 11 | #N/A | #N/A | #N/A | 130.1 | 137.9 | 142.8 | 143.7 | #N/A | #N/A | #N/A | 124.6 | 128.9 | 131.6 | 129.5 | #N/A | #N/A | #N/A | 9.2 | 131.9 |
| 2277978 | PH 0012(168)80 | 2.9 | 4.8 | 7.4 | 10.5 | #N/A | #N/A | #N/A | 128.8 | 134.7 | 143.9 | 143.2 | #N/A | #N/A | #N/A | 125.2 | 128.5 | 134 | 129.6 | #N/A | #N/A | #N/A | 8.0 | 134.2 |
| 2244726 | NH-PH 0018(177)104 | 3.1 | 4.8 | 6.3 | 8.4 | #N/A | #N/A | #N/A | 133.1 | 137 | 147.2 | 147.6 | #N/A | #N/A | #N/A | 129.1 | 130.7 | 138.5 | 136.2 | #N/A | #N/A | #N/A | 7.1 | 139.9 |
| 2237835 | NH 0073(63)182 | 3.1 | 4.9 | 7.2 | 9.8 | 11.2 | #N/A | #N/A | 126 | 129.9 | 136.7 | 146 | 146.8 | #N/A | #N/A | 122.2 | 123.8 | 127.5 | 133 | 132 | #N/A | #N/A | 10.1 | 133.1 |
| 2166562 | P 1774(04) | 3.3 | 5 | 6.4 | 8.3 | #N/A | #N/A | #N/A | 129.9 | 137.6 | 144.1 | 148.1 | #N/A | #N/A | #N/A | 125.8 | 131 | 135.4 | 136.7 | #N/A | #N/A | #N/A | 7.7 | 137.0 |
| 2132472 | P 0034(152)69 | 2.5 | 4.2 | 6.4 | 9.4 | 10.6 | #N/A | #N/A | 126.8 | 130.2 | 138.7 | 145.1 | 146.2 | #N/A | #N/A | 123.7 | 125 | 130.4 | 132.6 | 132.2 | #N/A | #N/A | 9.2 | 132.6 |
| 2155333 | P 0034(152)69 | 6.2 | 7.6 | 8.6 | 10.5 | #N/A | #N/A | #N/A | 129.1 | 136.4 | 138.5 | 137.3 | #N/A | #N/A | #N/A | 121.6 | 126.8 | 127.5 | 124.3 | #N/A | #N/A | #N/A | 8.5 | 127.5 |
| 2189275 | IM 0901(173)10 | 2.4 | 4.4 | 6 | 7.2 | 9.2 | #N/A | #N/A | 129.7 | 134.5 | 146.7 | 149.7 | 149.1 | #N/A | #N/A | 126.7 | 128.8 | 138.4 | 139.6 | 136.5 | #N/A | #N/A | 6.9 | 139.6 |
| 2251193 | NH-PH 0034(159)39 | 4.5 | 5.4 | 7.5 | 9.6 | #N/A | #N/A | #N/A | 130.2 | 138 | 144.9 | 145.9 | #N/A | #N/A | #N/A | 124.6 | 130.9 | 134.8 | 133.1 | #N/A | #N/A | #N/A | 7.6 | 134.8 |
| 2206544 | P-PH 0240(12)128 | 3.7 | 4.9 | 7.4 | 8.8 | #N/A | #N/A | #N/A | 128.8 | 135.6 | 144.3 | 145.5 | #N/A | #N/A | #N/A | 124.2 | 129.3 | 134.4 | 133.7 | #N/A | #N/A | #N/A | 7.7 | 134.5 |
| 2226043 | P SRTS(18) | 2.9 | 4.4 | 5.9 | 7.8 | 10.9 | #N/A | #N/A | 126 | 135.3 | 143.1 | 148.3 | 148.8 | #N/A | #N/A | 122.4 | 129.6 | 135.1 | 137.6 | 134.2 | #N/A | #N/A | 8.2 | 137.6 |
| 2152515 | IM 0902(158)111 | 5 | 7.1 | 8.3 | 9.9 | #N/A | #N/A | #N/A | 133.8 | 145.1 | 149.3 | 145.3 | #N/A | #N/A | #N/A | 127.4 | 135.5 | 137.9 | 132.2 | #N/A | #N/A | #N/A | 8.3 | 137.9 |
| 2165977 | IM 0901(174)10 | 3 | 4.4 | 5.7 | 7.7 | #N/A | #N/A | #N/A | 124.4 | 133.8 | 141.4 | 145.1 | #N/A | #N/A | #N/A | 120.8 | 128.2 | 133.8 | 134.7 | #N/A | #N/A | #N/A | 6.9 | 135.6 |
| 2194320 | EM 8052(65) | 2.3 | 4.3 | 6.4 | 9.4 | #N/A | #N/A | #N/A | 129.9 | 133.7 | 147.1 | 146 | #N/A | #N/A | #N/A | 127 | 128.2 | 138.3 | 133.5 | #N/A | #N/A | #N/A | 7.4 | 139.8 |
| 2364526 | NH 0018(184)39 | 2.6 | 4.7 | 6.6 | 8.7 | #N/A | #N/A | #N/A | 126.9 | 132.4 | 141.6 | 148.4 | #N/A | #N/A | #N/A | 123.7 | 126.5 | 132.8 | 136.5 | #N/A | #N/A | #N/A | 8.7 | 136.5 |

# 4-point Data Along with OMC and MDUW Determined from Quadratic Spline Fit

| Sample ID | Project | Practor Test Data | | | | | | | | | | | | | | | | | | | | | Quadratic Spline Fit | |
|---|---|---|---|---|---|---|---|---|---|---|---|---|---|---|---|---|---|---|---|---|---|---|---|---|
| | | Percent Moisture (%) | | | | | | | Wet Density (pcf) | | | | | | | Dry Density (pcf) | | | | | | | | |
| | | Specimen 1 | Specimen 2 | Specimen 3 | Specimen 4 | Specimen 5 | Specimen 6 | Specimen 7 | Specimen 1 | Specimen 2 | Specimen 3 | Specimen 4 | Specimen 5 | Specimen 6 | Specimen 7 | Specimen 1 | Specimen 2 | Specimen 3 | Specimen 4 | Specimen 5 | Specimen 6 | Specimen 7 | OMC | MDUW |
| 2245289 | P 0040(22)65 | 3.4 | 5.1 | 7 | 10.1 | #N/A | #N/A | #N/A | 128.4 | 134.6 | 141.8 | 141.1 | #N/A | #N/A | #N/A | 124.2 | 128.1 | 132.5 | 128.2 | #N/A | #N/A | #N/A | 7.7 | 132.9 |
| 2257292 | P 0040(22)65 | 3.8 | 5.6 | 7 | 9.4 | #N/A | #N/A | #N/A | 130.2 | 136.7 | 144.7 | 145.2 | #N/A | #N/A | #N/A | 125.4 | 129.5 | 135.2 | 132.7 | #N/A | #N/A | #N/A | 7.9 | 136.4 |
| 2311204 | NH-P 0042(53) | 3.4 | 5.4 | 7.8 | 10.7 | #N/A | #N/A | #N/A | 130.4 | 137.4 | 147.4 | 144.9 | #N/A | #N/A | #N/A | 126.1 | 130.4 | 136.7 | 130.9 | #N/A | #N/A | #N/A | 8.3 | 136.9 |
| 2203766 | SB SD12(01) | 3.5 | 5.1 | 7.6 | 9.7 | #N/A | #N/A | #N/A | 127.7 | 138 | 143.9 | 142.1 | #N/A | #N/A | #N/A | 123.4 | 131.3 | 133.7 | 129.5 | #N/A | #N/A | #N/A | 6.9 | 134.0 |
| 2172989 | NH 0034(166)34 | 5.1 | 7 | 8.4 | 9.6 | #N/A | #N/A | #N/A | 135.2 | 145.1 | 148.3 | 146.7 | #N/A | #N/A | #N/A | 128.6 | 135.6 | 136.8 | 133.9 | #N/A | #N/A | #N/A | 8.1 | 136.9 |
| 2227768 | P 7668(05) | 2.2 | 4.1 | 6.4 | 8.7 | 10.2 | #N/A | #N/A | 128.8 | 133.2 | 141.6 | 145.2 | 143.7 | #N/A | #N/A | 126 | 128 | 133.1 | 133.6 | 130.4 | #N/A | #N/A | 7.8 | 134.2 |
| 2224599 | IM 0901(186)0 | 3.1 | 5.4 | 6.6 | 8.6 | #N/A | #N/A | #N/A | 132.9 | 145.6 | 150.5 | 146.9 | #N/A | #N/A | #N/A | 128.9 | 138.1 | 141.2 | 135.3 | #N/A | #N/A | #N/A | 6.8 | 141.3 |
| 2224917 | IM 0901(186)0 | 2.2 | 3.7 | 5.5 | 7 | #N/A | #N/A | #N/A | 128.7 | 134.8 | 143.9 | 146 | #N/A | #N/A | #N/A | 125.9 | 130 | 136.4 | 136.4 | #N/A | #N/A | #N/A | 6.3 | 137.1 |
| 2225092 | IM 0901(186)0 | 2.4 | 4.2 | 5.8 | 8.8 | #N/A | #N/A | #N/A | 129.1 | 134.3 | 145.2 | 146.7 | #N/A | #N/A | #N/A | 126.1 | 128.9 | 137.2 | 134.8 | #N/A | #N/A | #N/A | 7.1 | 139.6 |
| 2308517 | NH 014A(15)41 | 2.4 | 3.8 | 5.8 | 9.1 | #N/A | #N/A | #N/A | 127.9 | 132.4 | 143.9 | 147.1 | #N/A | #N/A | #N/A | 124.9 | 127.6 | 136 | 134.8 | #N/A | #N/A | #N/A | 7.3 | 138.3 |
| 2359529 | P 016A(08)59 | 1.2 | 3.5 | 6.3 | 9.8 | #N/A | #N/A | #N/A | 118.5 | 128.8 | 146.1 | 144.3 | #N/A | #N/A | #N/A | 117.1 | 124.4 | 137.4 | 131.4 | #N/A | #N/A | #N/A | 7.4 | 138.7 |
| 2290469 | P 0071(03)06 | 2.9 | 5.1 | 7.2 | 8.4 | #N/A | #N/A | #N/A | 127.3 | 135.9 | 141.9 | 142.6 | #N/A | #N/A | #N/A | 123.7 | 129.3 | 132.4 | 131.5 | #N/A | #N/A | #N/A | 7.3 | 132.4 |
| 2364625 | P 0040(343)32 | 2 | 3.8 | 5.9 | 7.3 | 8.9 | #N/A | #N/A | 129.3 | 133.1 | 148.3 | 151.6 | 147.6 | #N/A | #N/A | 126.8 | 128.2 | 140 | 141.3 | 135.5 | #N/A | #N/A | 6.9 | 141.6 |
| 2364988 | P 0040(343)32 | 2.9 | 4.5 | 6.9 | 9.7 | #N/A | #N/A | #N/A | 129.1 | 135.1 | 147.6 | 146.1 | #N/A | #N/A | #N/A | 125.5 | 129.3 | 138.1 | 133.2 | #N/A | #N/A | #N/A | 7.6 | 138.7 |
| 2281413 | P TAPU(05) | 2.6 | 4.4 | 6.3 | 8.6 | #N/A | #N/A | #N/A | 126.3 | 134.4 | 142.5 | 145.7 | #N/A | #N/A | #N/A | 123.1 | 128.7 | 134.1 | 134.2 | #N/A | #N/A | #N/A | 7.5 | 135.1 |
| 2378501 | P TAPU(09) | 3.6 | 5 | 7 | 9.2 | #N/A | #N/A | #N/A | 131.3 | 135.7 | 145.2 | 146 | #N/A | #N/A | #N/A | 126.7 | 129.2 | 135.7 | 133.7 | #N/A | #N/A | #N/A | 7.7 | 136.3 |
| 2328530 | NH 014A(20)29 | 4.6 | 5.8 | 3.1 | 7.9 | #N/A | #N/A | #N/A | 138.1 | 145.2 | 128.9 | 151 | #N/A | #N/A | #N/A | 132 | 137.2 | 125 | 139.9 | #N/A | #N/A | #N/A | 7.5 | 140.1 |
| 2290575 | NH 0018(201)62 | 6.5 | 7.5 | 9.1 | 5.7 | #N/A | #N/A | #N/A | 142.4 | 148.4 | 147.6 | 139.6 | #N/A | #N/A | #N/A | 133.7 | 138 | 135.3 | 132.1 | #N/A | #N/A | #N/A | 8.0 | 138.7 |
| 2337149 | NH 0018(205)52 | 2.3 | 4.1 | 6.7 | 9.2 | #N/A | #N/A | #N/A | 130.5 | 135.7 | 147.1 | 150.4 | #N/A | #N/A | #N/A | 127.6 | 130.4 | 137.9 | 137.7 | #N/A | #N/A | #N/A | 7.9 | 139.0 |
| 2341966 | NH 0018(205)52 | 2.3 | 4.3 | 6.9 | 9 | #N/A | #N/A | #N/A | 131.8 | 139.3 | 147.1 | 145.9 | #N/A | #N/A | #N/A | 128.8 | 133.6 | 137.6 | 133.9 | #N/A | #N/A | #N/A | 6.8 | 137.6 |
| 2214781 | P 00SW(16) | 5.4 | 7.5 | 9.2 | 11.3 | #N/A | #N/A | #N/A | 131.6 | 139.9 | 145.9 | 144.8 | #N/A | #N/A | #N/A | 124.9 | 130.1 | 133.6 | 130.1 | #N/A | #N/A | #N/A | 9.5 | 133.7 |
| 2203662 | NH-PH 0085(20)26 | 2 | 3.6 | 5.6 | 8.4 | 9.7 | #N/A | #N/A | 129.7 | 131.1 | 142.9 | 150 | 149.5 | #N/A | #N/A | 127.2 | 126.5 | 135.3 | 138.4 | 136.3 | #N/A | #N/A | 7.9 | 138.6 |
| 1077254 | P-BRF 0385(14)115 | 5.6 | 7.6 | 9.6 | 11 | #N/A | #N/A | #N/A | 123 | 130.6 | 134.3 | 122.9 | #N/A | #N/A | #N/A | 116.5 | 121.4 | 122.5 | 110.7 | #N/A | #N/A | #N/A | 8.9 | 123.9 |
| 2316518 | P 0020(166)41 | 4.6 | 6.5 | 8.3 | 9.7 | #N/A | #N/A | #N/A | 132.5 | 141.6 | 144.1 | 144 | #N/A | #N/A | #N/A | 126.7 | 133 | 133.1 | 131.3 | #N/A | #N/A | #N/A | 7.3 | 133.6 |
| 2258776 | P 1614(00)1 | 4 | 5.7 | 7.6 | 9.3 | #N/A | #N/A | #N/A | 135 | 143.2 | 146.9 | 146.1 | #N/A | #N/A | #N/A | 129.8 | 135.5 | 136.5 | 133.7 | #N/A | #N/A | #N/A | 7.0 | 136.7 |
| 2363722 | IM 0901(192)0 | 3.1 | 4.9 | 6.5 | 9 | #N/A | #N/A | #N/A | 127.8 | 137.2 | 148.3 | 146.7 | #N/A | #N/A | #N/A | 124 | 130.8 | 139.2 | 134.6 | #N/A | #N/A | #N/A | 7.3 | 140.4 |
| 2223821 | P 0040(00)68 | 2.9 | 4.9 | 6.4 | 9.4 | #N/A | #N/A | #N/A | 128.3 | 134.5 | 142 | 145.1 | #N/A | #N/A | #N/A | 124.7 | 128.2 | 133.5 | 132.6 | #N/A | #N/A | #N/A | 7.8 | 135.3 |
| 2246755 | P 0079(77)150 | 4.9 | 7 | 8.2 | 10 | #N/A | #N/A | #N/A | 133.9 | 142.6 | 147.5 | 143.6 | #N/A | #N/A | #N/A | 127.6 | 133.3 | 136.3 | 130.5 | #N/A | #N/A | #N/A | 8.4 | 136.3 |
| 2308988 | BRO 8052(00)16-1 | 3.7 | 5.3 | 6.9 | 2.7 | #N/A | #N/A | #N/A | 135.1 | 147.7 | 149.1 | 128.9 | #N/A | #N/A | #N/A | 130.3 | 140.3 | 139.5 | 125.5 | #N/A | #N/A | #N/A | 6.0 | 141.6 |
| 2275037 | NH 0018(207)15 | 2.3 | 4.6 | 7 | 8.5 | #N/A | #N/A | #N/A | 128.9 | 133.9 | 146.1 | 147.7 | #N/A | #N/A | #N/A | 126 | 128 | 136.5 | 136.1 | #N/A | #N/A | #N/A | 7.6 | 137.0 |
| 2337168 | NH 0034(189)35 | 2.7 | 4.7 | 7.2 | 9.2 | #N/A | #N/A | #N/A | 125.3 | 135.6 | 146.5 | 147.9 | #N/A | #N/A | #N/A | 122 | 129.5 | 136.7 | 135.4 | #N/A | #N/A | #N/A | 7.8 | 137.1 |
| 2338094 | NH 0014(226)113 | 3.9 | 5.3 | 8.2 | 9.8 | #N/A | #N/A | #N/A | 130.2 | 140.3 | 143.7 | 140.9 | #N/A | #N/A | #N/A | 125.3 | 133.2 | 132.8 | 128.3 | #N/A | #N/A | #N/A | 6.5 | 135.2 |
| 2303374 | P TAPU(20) | 2.5 | 4.6 | 6 | 8.3 | #N/A | #N/A | #N/A | 126.4 | 124.8 | 144.7 | 148 | #N/A | #N/A | #N/A | 123.3 | 119.3 | 136.5 | 136.7 | #N/A | #N/A | #N/A | 7.2 | 137.4 |
| 2367775 | NH 0050(135)354 | 11.2 | 13 | 15.5 | 17.3 | #N/A | #N/A | #N/A | 116.1 | 123.4 | 129.4 | 128.8 | #N/A | #N/A | #N/A | 104.4 | 109.2 | 112 | 109.8 | #N/A | #N/A | #N/A | 15.3 | 112.0 |
| 2353610 | NH 0040(331) | 2.6 | 4.8 | 7.5 | 9.8 | #N/A | #N/A | #N/A | 123.9 | 132.6 | 143 | 146.2 | #N/A | #N/A | #N/A | 120.8 | 126.5 | 133 | 133.2 | #N/A | #N/A | #N/A | 8.7 | 133.8 |
| 2329075 | NH 0018(00)101 | 3.5 | 5.1 | 7.1 | 8.4 | #N/A | #N/A | #N/A | 136.1 | 141.8 | 146.1 | 144.2 | #N/A | #N/A | #N/A | 131.5 | 134.9 | 136.4 | 133 | #N/A | #N/A | #N/A | 6.6 | 136.7 |
| 2317839 | NH 0041(173) | 1.8 | 3.6 | 5.5 | 9.3 | #N/A | #N/A | #N/A | 127.6 | 131 | 137.3 | 142 | #N/A | #N/A | #N/A | 125.3 | 126.4 | 130.1 | 129.9 | #N/A | #N/A | #N/A | 7.3 | 131.5 |
| 2372590 | P TAPU(24) | 3 | 4.7 | 7.5 | 9.7 | #N/A | #N/A | #N/A | 129.2 | 134.5 | 144.1 | 144.3 | #N/A | #N/A | #N/A | 125.4 | 128.5 | 134 | 131.5 | #N/A | #N/A | #N/A | 7.9 | 134.1 |
| 2353472 | ER 0079(85)160 | 3.7 | 5.1 | 7.4 | 10.8 | #N/A | #N/A | #N/A | 123.3 | 131.8 | 140.3 | 141.5 | #N/A | #N/A | #N/A | 118.9 | 125.4 | 130.6 | 127.7 | #N/A | #N/A | #N/A | 8.3 | 131.0 |
| 2366884 | P TAPU(28) | 1.8 | 4.5 | 7 | 10.9 | #N/A | #N/A | #N/A | 129.9 | 135.1 | 148.8 | 145.7 | #N/A | #N/A | #N/A | 127.6 | 129.3 | 139.1 | 131.4 | #N/A | #N/A | #N/A | 8.1 | 140.4 |
| 2369853 | P TAPU(29) | 2.4 | 4.4 | 6.2 | 9 | #N/A | #N/A | #N/A | 127.9 | 134.3 | 143.6 | 146.1 | #N/A | #N/A | #N/A | 124.9 | 128.6 | 135.2 | 134 | #N/A | #N/A | #N/A | 7.4 | 136.7 |
| 1083366 | IM 90-2( | 1.4 | 3 | 4.6 | 7.2 | 9.7 | #N/A | #N/A | 130.4 | 133.1 | 142.6 | 148.9 | 148.4 | #N/A | #N/A | 128.6 | 129.2 | 136.3 | 138.9 | 135.3 | #N/A | #N/A | 7.1 | 138.9 |
| 2222983 | IM 1902(61)0 | 2.1 | 4 | 5.9 | 8.8 | #N/A | #N/A | #N/A | 127.7 | 136.5 | 145.5 | 149.1 | #N/A | #N/A | #N/A | 125.1 | 131.3 | 137.4 | 137 | #N/A | #N/A | #N/A | 7.2 | 138.9 |
| 1127153 | IM-BRF 90-1(85)30 | 15.5 | 11 | 12.5 | 14.1 | #N/A | #N/A | #N/A | 132.8 | 119.9 | 124.7 | 131.5 | #N/A | #N/A | #N/A | 115 | 108 | 110.8 | 115.2 | #N/A | #N/A | #N/A | 14.7 | 115.7 |
| 1414190 | EM 0902(39)61 | 2.1 | 4.1 | 5.5 | 7.2 | #N/A | #N/A | #N/A | 129.3 | 138.8 | 148.1 | 150.8 | #N/A | #N/A | #N/A | 126.6 | 133.3 | 140.4 | 140.7 | #N/A | #N/A | #N/A | 6.4 | 141.9 |
| 1071758 | P 3071(7)28 | 2.3 | 4.6 | 6.3 | 8.7 | #N/A | #N/A | #N/A | 119.9 | 127.8 | 131.9 | 133.9 | #N/A | #N/A | #N/A | 117.2 | 122.2 | 124.1 | 123.2 | #N/A | #N/A | #N/A | 7.0 | 124.3 |
| 1088757 | P 3071(7)28 | 2.8 | 5.2 | 6.8 | 8.4 | 10.1 | #N/A | #N/A | 124.7 | 136.8 | 145.9 | 149.2 | 146.9 | #N/A | #N/A | 121.3 | 130 | 136.6 | 137.6 | 133.4 | #N/A | #N/A | 7.8 | 137.9 |
| 1466032 | BRF 3071(05)3 | 1.5 | 5.4 | 7.5 | 8.2 | #N/A | #N/A | #N/A | 130.9 | 142.6 | 146.3 | 147.5 | #N/A | #N/A | #N/A | 129 | 135.3 | 136.1 | 136.3 | #N/A | #N/A | #N/A | 8.2 | 136.3 |
| 1077471 | NH 0235(01)0 | 6.7 | 8.7 | 10.7 | 12.4 | 13 | #N/A | #N/A | 120.6 | 126.3 | 131.1 | 136.3 | 135.5 | #N/A | #N/A | 113 | 116.2 | 118.4 | 121.3 | 119.9 | #N/A | #N/A | 12.4 | 121.3 |
| 1256497 | NH 0235(01)0 | 6 | 7.8 | 9.7 | 7 | #N/A | #N/A | #N/A | 140.3 | 144.8 | 143.1 | 142.8 | #N/A | #N/A | #N/A | 132.4 | 134.3 | 130.4 | 133.5 | #N/A | #N/A | #N/A | 7.9 | 134.3 |
| 2204159 | IM 0901(108)44 | 3.3 | 5.3 | 7.1 | 10 | #N/A | #N/A | #N/A | 131.6 | 136.8 | 145.3 | 147.7 | #N/A | #N/A | #N/A | 127.4 | 129.9 | 135.7 | 134.3 | #N/A | #N/A | #N/A | 8.3 | 137.1 |
| 1092095 | P 0016(57)69 | 2.4 | 4.4 | 5.9 | 7.4 | 9.9 | #N/A | #N/A | 125.1 | 131.2 | 139.2 | 146.5 | 145.7 | #N/A | #N/A | 122.2 | 125.7 | 131.4 | 136.4 | 132.6 | #N/A | #N/A | 8.1 | 137.0 |
| 1030404 | P 0020(60)80 | 3.6 | 7.1 | 9.7 | 11.9 | #N/A | #N/A | #N/A | 131.1 | 141.1 | 144.3 | 142.2 | #N/A | #N/A | #N/A | 126.5 | 131.7 | 131.5 | 127.1 | #N/A | #N/A | #N/A | 8.5 | 132.2 |
| 1049793 | P 0020(60)80 | 2.9 | 4.9 | 7.1 | 9.6 | 11.6 | #N/A | #N/A | 125.9 | 130.2 | 136.4 | 143.1 | 144.8 | #N/A | #N/A | 122.4 | 124.1 | 127.4 | 130.6 | 129.7 | #N/A | #N/A | 10.1 | 130.7 |
| 1294082 | IM-P 90-2(134)59 | 2.6 | 4.6 | 6.2 | 1.8 | 9 | #N/A | #N/A | 132 | 142.7 | 149.6 | 129.1 | 150.1 | #N/A | #N/A | 128.7 | 136.4 | 140.9 | 126.8 | 137.7 | #N/A | #N/A | 7.0 | 141.5 |
| 1444575 | BRF 90-2(92)64 | 4.3 | 5.9 | 9.2 | 9.9 | #N/A | #N/A | #N/A | 132.2 | 140.7 | 143.6 | 145.1 | #N/A | #N/A | #N/A | 126.7 | 132.9 | 131.5 | 132 | #N/A | #N/A | #N/A | 6.7 | 133.7 |
| 1476917 | P 0020(73)66 | 6.3 | 7.5 | 10.3 | 12.4 | #N/A | #N/A | #N/A | 127 | 131.7 | 138.8 | 140.4 | #N/A | #N/A | #N/A | 119.5 | 122.5 | 125.8 | 124.9 | #N/A | #N/A | #N/A | 10.7 | 125.9 |
| 1478797 | P 0020(73)66 | 4.8 | 9.1 | 10.8 | 12.9 | #N/A | #N/A | #N/A | 121.3 | 134.1 | 140.7 | 139.7 | #N/A | #N/A | #N/A | 115.7 | 122.9 | 127 | 123.7 | #N/A | #N/A | #N/A | 11.2 | 127.2 |
| 1480106 | P 0020(73)66 | 6.4 | 7.9 | 9.8 | 11.7 | #N/A | #N/A | #N/A | 130.7 | 133.4 | 140.7 | 144.7 | #N/A | #N/A | #N/A | 122.8 | 123.6 | 128.1 | 129.5 | #N/A | #N/A | #N/A | 11.4 | 129.6 |
| 2252694 | IM 0901(38)40 | 3.4 | 5.2 | 7 | 9.7 | #N/A | #N/A | #N/A | 130.7 | 139.6 | 148.4 | 148 | #N/A | #N/A | #N/A | 126.4 | 132.7 | 138.7 | 134.9 | #N/A | #N/A | #N/A | 7.7 | 139.4 |
| 1467177 | IM-PH 0901(61)49 | 0.9 | 3 | 5.1 | 7.2 | #N/A | #N/A | #N/A | 123.9 | 127.4 | 134 | 136.7 | #N/A | #N/A | #N/A | 122.8 | 123.7 | 127.5 | 127.5 | #N/A | #N/A | #N/A | 6.1 | 128.1 |
| 1467520 | IM-PH 0901(61)49 | 3.2 | 4.9 | 6.7 | 8.6 | #N/A | #N/A | #N/A | 134.6 | 144.7 | 148.8 | 149 | #N/A | #N/A | #N/A | 130.4 | 137.9 | 139.5 | 137.2 | #N/A | #N/A | #N/A | 6.4 | 139.5 |
| 1261746 | BRF 0087(6)63 | 2.3 | 4 | 5.5 | 7.9 | #N/A | #N/A | #N/A | 121.8 | 131.6 | 141.5 | 148.3 | #N/A | #N/A | #N/A | 119.1 | 126.5 | 134.1 | 137.4 | #N/A | #N/A | #N/A | 7.3 | 137.8 |
| 1128196 | P 3471(00)21 | 3.9 | 5.8 | 7.9 | 9.6 | #N/A | #N/A | #N/A | 131.1 | 138.6 | 141.8 | 143.7 | #N/A | #N/A | #N/A | 126.2 | 131 | 131.4 | 131.1 | #N/A | #N/A | #N/A | 6.7 | 131.6 |
| 1039193 | NH-PH 0079(11)47 | 5.2 | 6.2 | 7.6 | 8.7 | 7.9 | #N/A | #N/A | 136.8 | 139.6 | 143.2 | 143.2 | 141.9 | #N/A | #N/A | 130 | 131.5 | 133.1 | 131.7 | 131.5 | #N/A | #N/A | 7.6 | 133.1 |

# 4-point Data Along with OMC and MDUW Determined from Quadratic Spline Fit

| Sample ID | Project | Practor Test Data | | | | | | | | | | | | | | | | | | | | | Quadratic Spline Fit | |
|---|---|---|---|---|---|---|---|---|---|---|---|---|---|---|---|---|---|---|---|---|---|---|---|---|
| | | Percent Moisture (%) | | | | | | | Wet Density (pcf) | | | | | | | Dry Density (pcf) | | | | | | | | |
| | | Specimen 1 | Specimen 2 | Specimen 3 | Specimen 4 | Specimen 5 | Specimen 6 | Specimen 7 | Specimen 1 | Specimen 2 | Specimen 3 | Specimen 4 | Specimen 5 | Specimen 6 | Specimen 7 | Specimen 1 | Specimen 2 | Specimen 3 | Specimen 4 | Specimen 5 | Specimen 6 | Specimen 7 | OMC | MDUW |
| 2327549 | P 6480(04) | 2.2 | 3.9 | 5.7 | 8.6 | #N/A | #N/A | #N/A | 129.3 | 134.2 | 147.2 | 149.2 | #N/A | #N/A | #N/A | 126.5 | 129.2 | 139.3 | 137.4 | #N/A | #N/A | #N/A | 6.9 | 141.9 |
| 1274800 | NH 0079(26)33 | 4.7 | 5.8 | 7.5 | 9.2 | #N/A | #N/A | #N/A | 141.4 | 142.9 | 148.3 | 145.6 | #N/A | #N/A | #N/A | 135.1 | 135.1 | 138 | 133.3 | #N/A | #N/A | #N/A | 7.5 | 138.0 |
| 2084659 | ES 0085(51)55 | 2.9 | 4.7 | 6.8 | 8.9 | 11.1 | #N/A | #N/A | 120.3 | 124.8 | 132.9 | 138 | 139.8 | #N/A | #N/A | 116.9 | 119.2 | 124.4 | 126.7 | 125.8 | #N/A | #N/A | 9.4 | 126.8 |
| 2108201 | BRF-NH 0018(66)43 | 3.8 | 5.6 | 7.6 | 10 | #N/A | #N/A | #N/A | 136.4 | 142.3 | 145.8 | 145.7 | #N/A | #N/A | #N/A | 131.4 | 134.8 | 135.5 | 132.5 | #N/A | #N/A | #N/A | 7.1 | 135.6 |
| 1035175 | BRF 1014(1)24 | 6.4 | 8.2 | 4.8 | 9.9 | 11.5 | #N/A | #N/A | 130.8 | 136.4 | 125 | 141 | 142.2 | #N/A | #N/A | 122.9 | 126.1 | 119.3 | 128.3 | 127.5 | #N/A | #N/A | 10.3 | 128.4 |
| 1271152 | BRF 0212(64)36 | 4.5 | 6.3 | 8.4 | 10.1 | #N/A | #N/A | #N/A | 132.8 | 139.8 | 146.4 | 144.5 | #N/A | #N/A | #N/A | 127.1 | 131.5 | 135.1 | 131.2 | #N/A | #N/A | #N/A | 8.3 | 135.1 |
| 1404236 | NH 0079(02)26 | 6 | 3.5 | 8.7 | 9.2 | #N/A | #N/A | #N/A | 139.1 | 129 | 142.8 | 140.7 | #N/A | #N/A | #N/A | 131.2 | 124.6 | 131.4 | 128.8 | #N/A | #N/A | #N/A | 7.6 | 133.6 |
| 1430212 | NH 0079(48)26 | 4.4 | 5.9 | 7.7 | 3.8 | #N/A | #N/A | #N/A | 136.7 | 143.9 | 146.5 | 132.9 | #N/A | #N/A | #N/A | 130.9 | 135.9 | 136 | 128 | #N/A | #N/A | #N/A | 6.8 | 136.8 |
| 1434633 | NH 0079(48)26 | 2 | 4.1 | 6.2 | 7.2 | #N/A | #N/A | #N/A | 132.3 | 138.8 | 147.1 | 146.9 | #N/A | #N/A | #N/A | 129.7 | 133.3 | 138.5 | 137 | #N/A | #N/A | #N/A | 6.3 | 138.5 |
| 1467173 | IM 0901(120)33 | 5 | 7.4 | 9.4 | 11.6 | #N/A | #N/A | #N/A | 116.6 | 124.3 | 128.9 | 133.4 | #N/A | #N/A | #N/A | 111 | 115.7 | 117.8 | 119.5 | #N/A | #N/A | #N/A | 11.6 | 119.5 |
| 1028708 | NH 0018(91)22 | 4.6 | 6.1 | 7.6 | 8.9 | 9.8 | #N/A | #N/A | 132.7 | 138.8 | 143.5 | 146.8 | 144.5 | #N/A | #N/A | 126.9 | 130.8 | 133.4 | 134.8 | 131.6 | #N/A | #N/A | 8.6 | 135.0 |
| 1314477 | BRO 8041(13) | 5.6 | 7.8 | 9.5 | 11.2 | #N/A | #N/A | #N/A | 129.5 | 137.1 | 143.2 | 142 | #N/A | #N/A | #N/A | 122.6 | 127.2 | 130.8 | 127.7 | #N/A | #N/A | #N/A | 9.7 | 130.8 |
| 1464795 | P 0044(52)50 | 2.6 | 6.3 | 8.4 | 10.3 | #N/A | #N/A | #N/A | 128.4 | 143.2 | 144.6 | 141.4 | #N/A | #N/A | #N/A | 125.1 | 134.7 | 133.4 | 128.2 | #N/A | #N/A | #N/A | 6.8 | 134.8 |
| 2067613 | P 0087(07)56 | 2.4 | 4.4 | 6.8 | 8.5 | #N/A | #N/A | #N/A | 126.9 | 136.8 | 141.1 | 140.5 | #N/A | #N/A | #N/A | 123.9 | 131 | 132.1 | 129.5 | #N/A | #N/A | #N/A | 5.9 | 132.4 |
| 1804140 | IM 0901(110)46 | 5.3 | 7.7 | 9.2 | 3.4 | #N/A | #N/A | #N/A | 138.9 | 147.8 | 149 | 129.7 | #N/A | #N/A | #N/A | 131.9 | 137.2 | 136.4 | 125.4 | #N/A | #N/A | #N/A | 8.1 | 137.3 |
| 2337633 | IM 0902(112)59 | 2.6 | 5.1 | 7.3 | 9.7 | #N/A | #N/A | #N/A | 125.9 | 141.8 | 150.6 | 147.8 | #N/A | #N/A | #N/A | 122.7 | 134.9 | 140.4 | 134.7 | #N/A | #N/A | #N/A | 7.5 | 140.4 |
| 1256991 | P 3079(12)203 | 5.8 | 7.9 | 9.8 | 11.9 | #N/A | #N/A | #N/A | 120.1 | 128.2 | 134.6 | 137.8 | #N/A | #N/A | #N/A | 113.5 | 118.8 | 122.6 | 123.1 | #N/A | #N/A | #N/A | 11.1 | 123.4 |
| 1259765 | P 3079(12)203 | 5.1 | 7 | 8.9 | 9.9 | #N/A | #N/A | #N/A | 132.3 | 141.8 | 145.7 | 144.5 | #N/A | #N/A | #N/A | 125.9 | 132.5 | 133.8 | 131.5 | #N/A | #N/A | #N/A | 8.3 | 134.1 |
| 1449921 | PH 0016(40)11 | 2 | 4.1 | 5.5 | 8.1 | #N/A | #N/A | #N/A | 129.1 | 129.8 | 137.8 | 137.5 | #N/A | #N/A | #N/A | 126.6 | 124.7 | 130.6 | 127.2 | #N/A | #N/A | #N/A | 6.4 | 132.0 |
| 1439391 | PH 1014(12)27 | 2.5 | 4.3 | 6.4 | 8.5 | #N/A | #N/A | #N/A | 127 | 130.7 | 141.6 | 139.5 | #N/A | #N/A | #N/A | 123.9 | 125.3 | 133.1 | 128.6 | #N/A | #N/A | #N/A | 6.9 | 133.4 |
| 2108501 | P 8301(01) | 7.5 | 9.6 | 10.8 | 4.8 | #N/A | #N/A | #N/A | 134.5 | 140 | 141.8 | 120.4 | #N/A | #N/A | #N/A | 125.1 | 127.7 | 128 | 114.9 | #N/A | #N/A | #N/A | 10.7 | 128.0 |
| 2336844 | BRO 8052(49) | 0.5 | 3 | 4.9 | 7.1 | 9.5 | #N/A | #N/A | 127.8 | 128.6 | 137 | 146.2 | 147.7 | #N/A | #N/A | 127.2 | 124.9 | 130.6 | 136.5 | 134.9 | #N/A | #N/A | 7.9 | 137.0 |
| 2203731 | P 0044(149)40 | 3.6 | 4.9 | 6.8 | 8.9 | #N/A | #N/A | #N/A | 134.1 | 139.1 | 146.5 | 146.1 | #N/A | #N/A | #N/A | 129.4 | 132.6 | 137.2 | 134.2 | #N/A | #N/A | #N/A | 7.2 | 137.4 |
| 2126475 | P 1648(03) | 2.4 | 4.1 | 6.1 | 6.9 | #N/A | #N/A | #N/A | 129.2 | 138.8 | 147.6 | 149.2 | #N/A | #N/A | #N/A | 126.2 | 133.3 | 139.1 | 139.6 | #N/A | #N/A | #N/A | 6.9 | 139.6 |
| 2158306 | BRO 8052(53) | 3.1 | 5.2 | 6.3 | 7 | #N/A | #N/A | #N/A | 134.6 | 144.2 | 149.7 | 149.7 | #N/A | #N/A | #N/A | 130.6 | 137.1 | 140.8 | 139.9 | #N/A | #N/A | #N/A | 6.4 | 140.9 |
| 2204583 | BRO 8052(56) | 2.5 | 5 | 7.1 | 10.1 | #N/A | #N/A | #N/A | 122.7 | 139.3 | 147.2 | 148.8 | #N/A | #N/A | #N/A | 119.7 | 132.7 | 137.4 | 135.1 | #N/A | #N/A | #N/A | 8.0 | 137.8 |
| 2092808 | 000I-452 | 3 | 4.5 | 6.3 | 8.4 | #N/A | #N/A | #N/A | 128.4 | 140.4 | 146.6 | 149.5 | #N/A | #N/A | #N/A | 124.7 | 134.4 | 137.9 | 137.9 | #N/A | #N/A | #N/A | 7.4 | 138.3 |
| 2182106 | 079 N-492 | 5.2 | 7.9 | 8.7 | 3.5 | #N/A | #N/A | #N/A | 138.7 | 146.4 | 146.1 | 130.9 | #N/A | #N/A | #N/A | 131.8 | 135.7 | 134.4 | 126.5 | #N/A | #N/A | #N/A | 7.5 | 135.9 |
| 2213132 | 085-471 | 2.4 | 4.3 | 6.3 | 8.2 | 9.4 | #N/A | #N/A | 125.2 | 131.5 | 136 | 143.5 | 144.8 | #N/A | #N/A | 122.3 | 126.1 | 127.9 | 132.6 | 132.4 | #N/A | #N/A | 8.7 | 132.9 |
| 2277070 | 4 10D392( | 2 | 3.8 | 5.2 | 7.9 | #N/A | #N/A | #N/A | 134 | 135.9 | 144.4 | 148.5 | #N/A | #N/A | #N/A | 131.4 | 130.9 | 137.3 | 137.6 | #N/A | #N/A | #N/A | 6.8 | 138.0 |
| 2279762 | 014A-451 | 5.8 | 7.3 | 9.9 | 12.1 | 13.7 | #N/A | #N/A | 117.5 | 123.5 | 132 | 136.1 | 134.1 | #N/A | #N/A | 111.1 | 115.1 | 120.1 | 121.4 | 117.9 | #N/A | #N/A | 11.5 | 121.6 |
| 2312027 | 18B-492 | 2.7 | 4.8 | 6.7 | 9.9 | #N/A | #N/A | #N/A | 127 | 136.2 | 144.9 | 146.2 | #N/A | #N/A | #N/A | 123.7 | 130 | 135.8 | 133 | #N/A | #N/A | #N/A | 7.8 | 136.8 |
| 2308477 | 079-471 | 2.3 | 4.3 | 6.6 | 10.2 | #N/A | #N/A | #N/A | 127.2 | 132.9 | 140 | 142.1 | #N/A | #N/A | #N/A | 124.3 | 127.4 | 131.3 | 128.9 | #N/A | #N/A | #N/A | 7.6 | 131.8 |
| 2310959 | 087-491 | 0.4 | 3.3 | 6 | 8.4 | #N/A | #N/A | #N/A | 124.6 | 130.9 | 140 | 142.6 | #N/A | #N/A | #N/A | 124.1 | 126.7 | 132.1 | 131.5 | #N/A | #N/A | #N/A | 6.9 | 132.6 |
| 2329173 | 000I-469 | 2 | 3.6 | 6.4 | 8.7 | #N/A | #N/A | #N/A | 127.2 | 135.2 | 141.2 | 146.5 | #N/A | #N/A | #N/A | 124.7 | 130.5 | 132.7 | 134.8 | #N/A | #N/A | #N/A | 8.7 | 134.8 |
| 2354399 | 212-471 | 2.1 | 4.3 | 6.3 | 8.7 | #N/A | #N/A | #N/A | 123.2 | 132.8 | 143.9 | 143.5 | #N/A | #N/A | #N/A | 120.7 | 127.3 | 135.4 | 132 | #N/A | #N/A | #N/A | 7.0 | 136.1 |
| 1070477 | CP-1-2003 | 3.5 | 5.4 | 7.3 | 9 | 10.6 | #N/A | #N/A | 123.1 | 131 | 139.5 | 141.9 | 141.8 | #N/A | #N/A | 118.9 | 124.3 | 130 | 130.2 | 128.2 | #N/A | #N/A | 8.1 | 130.6 |
| 2085979 | ES 3040(08)47 | 2.7 | 3.4 | 4.3 | 6 | #N/A | #N/A | #N/A | 122.2 | 128 | 133.7 | 138.2 | #N/A | #N/A | #N/A | 119 | 123.8 | 128.2 | 130.4 | #N/A | #N/A | #N/A | 5.6 | 130.6 |
| 2080343 | P 1612(01) | 4.5 | 5.8 | 7 | 7.9 | #N/A | #N/A | #N/A | 143.6 | 148.4 | 147.2 | 145.7 | #N/A | #N/A | #N/A | 137.4 | 140.3 | 137.6 | 135 | #N/A | #N/A | #N/A | 5.7 | 140.3 |
| 2173247 | IM 0902(148)111 | 4.5 | 5.9 | 7.9 | 12.2 | #N/A | #N/A | #N/A | 130.9 | 137.8 | 144 | 139.3 | #N/A | #N/A | #N/A | 125.3 | 130.1 | 133.5 | 124.2 | #N/A | #N/A | #N/A | 8.3 | 133.6 |
| 2166515 | IM 0901(174)10 | 4.5 | 5.9 | 7.1 | 8.1 | 3.7 | #N/A | #N/A | 142 | 144.9 | 148.8 | 148.3 | 136.2 | #N/A | #N/A | 135.9 | 136.8 | 138.9 | 137.2 | 131.3 | #N/A | #N/A | 6.2 | 139.4 |
| 2347287 | NH 0034(189)35 | 3.2 | 5.2 | 7.1 | 8.2 | #N/A | #N/A | #N/A | 126.5 | 141.9 | 147.5 | 146.7 | #N/A | #N/A | #N/A | 122.6 | 134.9 | 137.7 | 135.6 | #N/A | #N/A | #N/A | 6.8 | 137.8 |
| 1352940 | P 3040(00)65 | 4.5 | 5.8 | 7.5 | 8.6 | #N/A | #N/A | #N/A | 135.5 | 139.5 | 147.5 | 147.1 | #N/A | #N/A | #N/A | 129.7 | 131.9 | 137.2 | 135.5 | #N/A | #N/A | #N/A | 7.7 | 137.3 |
| 2411921 | P 0047(111)203 | 5.3 | 6.3 | 7.8 | 9.9 | 12.7 | #N/A | #N/A | 123.6 | 127.7 | 133.2 | 138.7 | 136.7 | #N/A | #N/A | 117.4 | 120.1 | 123.6 | 126.2 | 121.3 | #N/A | #N/A | 9.9 | 126.2 |
| 2306193 | NH-EM 0083(74)55 | 3.4 | 6.4 | 8.4 | 9.6 | #N/A | #N/A | #N/A | 132.7 | 134.5 | 140.5 | 138.9 | #N/A | #N/A | #N/A | 128.3 | 126.4 | 129.6 | 126.7 | #N/A | #N/A | #N/A | 8.2 | 129.6 |
| 2348212 | P 1806(12)149 | 3.9 | 5.4 | 6.9 | 7.6 | 9.6 | #N/A | #N/A | 131.6 | 137.7 | 142.8 | 146.4 | 144.8 | #N/A | #N/A | 126.7 | 130.6 | 133.6 | 136.1 | 132.1 | #N/A | #N/A | 7.8 | 136.2 |
| 2365416 | P 1806(12)149 | 6.1 | 7.9 | 10.1 | 13.5 | #N/A | #N/A | #N/A | 125.6 | 130.8 | 137.5 | 137.3 | #N/A | #N/A | #N/A | 118.4 | 121.2 | 124.9 | 121 | #N/A | #N/A | #N/A | 10.8 | 125.2 |
| 2343745 | NH 0212(165)224 | 8.3 | 11 | 12.6 | 14.6 | #N/A | #N/A | #N/A | 123.6 | 131.2 | 136.1 | 135.1 | #N/A | #N/A | #N/A | 114.1 | 118.2 | 120.9 | 117.9 | #N/A | #N/A | #N/A | 12.9 | 121.0 |
| 2363085 | NH 0212(165)224 | 7.2 | 9.5 | 11.3 | 11.8 | 14.9 | #N/A | #N/A | 124.1 | 128.1 | 133.6 | 134.9 | 133.2 | #N/A | #N/A | 115.8 | 117 | 120 | 120.7 | 115.9 | #N/A | #N/A | 12.4 | 121.0 |
| 2318819 | NH 0083(82)25 | 5.8 | 8.4 | 10.1 | 12 | #N/A | #N/A | #N/A | 135.3 | 139.1 | 138.5 | 138.1 | #N/A | #N/A | #N/A | 127.9 | 128.3 | 125.8 | 123.3 | #N/A | #N/A | #N/A | 7.3 | 128.8 |
| 2290377 | P 0044(192)254 | 4.5 | 6.9 | 8.3 | 9.3 | 10.4 | #N/A | #N/A | 126.8 | 133.3 | 141.2 | 143.2 | 140.7 | #N/A | #N/A | 121.3 | 124.7 | 130.4 | 131 | 127.4 | #N/A | #N/A | 9.0 | 131.2 |
| 2289247 | P 0020(145)240 | 4.8 | 7 | 8.5 | 11.5 | 13 | 14.6 | #N/A | 117.1 | 125.5 | 128.3 | 137.1 | 139.6 | 136.8 | #N/A | 111.7 | 117.3 | 118.2 | 123 | 123.5 | 119.4 | #N/A | 12.5 | 123.7 |
| 2335859 | NH-P 0031(29) | 3.9 | 5.6 | 7.5 | 9.4 | 10.2 | 12.4 | #N/A | 125.7 | 129.1 | 134.8 | 138.7 | 141.1 | 140 | #N/A | 121 | 122.3 | 125.4 | 126.8 | 128 | 124.6 | #N/A | 10.6 | 128.2 |
| 2349271 | BRF 6302(00)19-1 | 6 | 6.9 | 7.9 | 8.4 | 11.5 | #N/A | #N/A | 133.1 | 136.1 | 137.9 | 140.4 | 140.5 | #N/A | #N/A | 125.6 | 127.3 | 127.8 | 129.5 | 126 | #N/A | #N/A | 8.4 | 129.5 |
| 2318769 | IM-FP 0903(106)15 | 6.3 | 7.6 | 8.8 | 10.1 | #N/A | #N/A | #N/A | 138.5 | 142.8 | 141.2 | 143.2 | #N/A | #N/A | #N/A | 130.3 | 132.7 | 129.8 | 130.1 | #N/A | #N/A | #N/A | 7.4 | 132.8 |
| 2389623 | IM 0904(60)204 | 5.9 | 7.2 | 8.6 | 9.5 | 10 | #N/A | #N/A | 137.6 | 138.9 | 144.3 | 144.9 | 144 | #N/A | #N/A | 129.9 | 129.6 | 132.9 | 132.3 | 130.9 | #N/A | #N/A | 8.8 | 133.0 |
| 2392045 | IM 0904(60)204 | 6 | 7.3 | 8.1 | 9.5 | #N/A | #N/A | #N/A | 137.7 | 143.1 | 143.9 | 143.1 | #N/A | #N/A | #N/A | 129.9 | 133.4 | 133.1 | 130.7 | #N/A | #N/A | #N/A | 7.5 | 133.5 |
| 2395497 | IM 0904(60)204 | 6.3 | 7.3 | 8.2 | 8.7 | #N/A | #N/A | #N/A | 139.9 | 143.9 | 144.9 | 142.8 | #N/A | #N/A | #N/A | 131.6 | 134.1 | 133.9 | 131.4 | #N/A | #N/A | #N/A | 7.8 | 134.5 |
| 2364407 | NH-EM 0083(74)55 | 8.2 | 9.3 | 10.1 | 12.9 | #N/A | #N/A | #N/A | 133.1 | 137.3 | 140 | 138.7 | #N/A | #N/A | #N/A | 123 | 125.6 | 127.2 | 122.9 | #N/A | #N/A | #N/A | 10.8 | 127.6 |
| 2411925 | P 0044(211)200 | 6.7 | 7.9 | 9 | 11 | #N/A | #N/A | #N/A | 139.1 | 142.8 | 145.1 | 142.9 | #N/A | #N/A | #N/A | 130.4 | 132.3 | 133.1 | 128.7 | #N/A | #N/A | #N/A | 8.9 | 133.1 |
| 2370514 | P 0049(05)27 | 5.7 | 6.6 | 8 | 8.8 | 11 | #N/A | #N/A | 133.5 | 135.9 | 140.5 | 142.8 | 140.7 | #N/A | #N/A | 126.3 | 127.5 | 130.1 | 131.3 | 126.8 | #N/A | #N/A | 9.1 | 131.4 |
| 2388597 | I-PS 0012(187)10 COU | 6.3 | 8.2 | 8.4 | 10.8 | #N/A | #N/A | #N/A | 137.1 | 142.4 | 144.7 | 142.7 | #N/A | #N/A | #N/A | 129 | 131.6 | 133.5 | 128.8 | #N/A | #N/A | #N/A | 8.5 | 133.5 |
| 2388276 | I-PS 0012(187)10 COU | 6.2 | 7.1 | 8 | 10.3 | #N/A | #N/A | #N/A | 135.7 | 137.9 | 142.9 | 143.3 | #N/A | #N/A | #N/A | 127.8 | 128.8 | 132.3 | 129.9 | #N/A | #N/A | #N/A | 8.9 | 133.6 |
| 2388787 | I-PS 0012(187)10 COU | 6.1 | 7.3 | 8.2 | 9.1 | 12.1 | #N/A | #N/A | 133.3 | 134.3 | 138.4 | 140.9 | 140 | #N/A | #N/A | 125.6 | 125.2 | 127.9 | 129.1 | 124.9 | #N/A | #N/A | 9.6 | 129.3 |
| 2308328 | NH 0014(209)190 | 6.6 | 8.4 | 10.9 | 13.2 | 15.6 | 16.7 | #N/A | 118.3 | 121.9 | 126.1 | 130.4 | 131.9 | 129.6 | #N/A | 111 | 112.5 | 113.7 | 115.2 | 114.1 | 111.1 | #N/A | 14.0 | 115.3 |

# 4-point Data Along with OMC and MDUW Determined from Quadratic Spline Fit

| Sample ID | Project | Proctor Test Data | | | | | | | | | | | | | | | | | | | | | Quadratic Spline Fit | |
|---|---|---|---|---|---|---|---|---|---|---|---|---|---|---|---|---|---|---|---|---|---|---|---|---|
| | | Percent Moisture (%) | | | | | | | Wet Density (pcf) | | | | | | | Dry Density (pcf) | | | | | | | | |
| | | Specimen 1 | Specimen 2 | Specimen 3 | Specimen 4 | Specimen 5 | Specimen 6 | Specimen 7 | Specimen 1 | Specimen 2 | Specimen 3 | Specimen 4 | Specimen 5 | Specimen 6 | Specimen 7 | Specimen 1 | Specimen 2 | Specimen 3 | Specimen 4 | Specimen 5 | Specimen 6 | Specimen 7 | OMC | MDUW |
| 2389310 | -B 0212(184)143 COUN | 5.2 | 6.1 | 6.9 | 8.7 | 10.9 | #N/A | #N/A | 131.9 | 133.5 | 136.5 | 143.7 | 142 | #N/A | #N/A | 125.4 | 125.8 | 127.7 | 132.2 | 128 | #N/A | #N/A | 9.1 | 132.4 |
| 2411836 | -B 0212(184)143 COUN | 6.7 | 7.5 | 9.3 | 9.6 | #N/A | #N/A | #N/A | 137.7 | 139.3 | 144.8 | 144.3 | #N/A | #N/A | #N/A | 129.1 | 129.6 | 132.5 | 131.7 | #N/A | #N/A | #N/A | 9.0 | 132.8 |
| 2336130 | -PH 0018(198)17 COUN | 6.3 | 8.8 | 9.7 | 12.5 | #N/A | #N/A | #N/A | 134.9 | 142.7 | 142 | 140.4 | #N/A | #N/A | #N/A | 126.9 | 131.2 | 129.4 | 124.8 | #N/A | #N/A | #N/A | 8.3 | 131.5 |
| 2390441 | P 1806(16)138 | 4.7 | 5.1 | 6.4 | 7.4 | 9.9 | 12.8 | #N/A | 120.1 | 122.5 | 127.2 | 132.3 | 139.7 | 138.1 | #N/A | 114.7 | 116.6 | 119.5 | 123.2 | 127.1 | 122.4 | #N/A | 9.9 | 127.1 |
| 2372005 | NH 0212(182)187 | 5.6 | 6.4 | 9.3 | 10.7 | 13.3 | #N/A | #N/A | 126.8 | 129.5 | 136.3 | 138.4 | 136.7 | #N/A | #N/A | 120.1 | 121.7 | 124.7 | 125 | 120.7 | #N/A | #N/A | 10.3 | 125.1 |
| 2318779 | NH 0012(213)159 | 5.1 | 7.6 | 9 | 11.2 | #N/A | #N/A | #N/A | 134.4 | 142.8 | 142.1 | 143.3 | #N/A | #N/A | #N/A | 127.9 | 132.7 | 130.4 | 128.9 | #N/A | #N/A | #N/A | 7.3 | 132.8 |
| 2333666 | P 0248(11)145 | 6.1 | 8.1 | 9.6 | 10.7 | #N/A | #N/A | #N/A | 136.1 | 142.9 | 141.5 | 139.3 | #N/A | #N/A | #N/A | 128.3 | 132.2 | 129.1 | 125.8 | #N/A | #N/A | #N/A | 7.9 | 132.3 |
| 2382116 | NH 0012(226)190 | 4.8 | 6 | 6.3 | 7.9 | 11.5 | #N/A | #N/A | 129.6 | 130.9 | 133.7 | 138.9 | 140 | #N/A | #N/A | 123.7 | 123.5 | 125.8 | 128.7 | 125.6 | #N/A | #N/A | 8.9 | 129.3 |
| 2382259 | P 0053(09)10 | 5.5 | 6.1 | 6.8 | 7.6 | 10 | #N/A | #N/A | 132.1 | 135.5 | 138.5 | 139.2 | 142.3 | #N/A | #N/A | 125.2 | 127.7 | 129.7 | 129.4 | 129.4 | #N/A | #N/A | 7.0 | 129.8 |
| 2370031 | P 0010(148)182 | 6 | 7 | 7.9 | 9.5 | #N/A | #N/A | #N/A | 137.5 | 141.6 | 143.3 | 143.9 | #N/A | #N/A | #N/A | 129.7 | 132.3 | 132.8 | 131.4 | #N/A | #N/A | #N/A | 7.8 | 132.8 |
| 2401332 | NH 0300(31) | 6.3 | 7.6 | 8.9 | 10.5 | 12 | #N/A | #N/A | 130.3 | 133.6 | 137.5 | 140.8 | 138.8 | #N/A | #N/A | 122.6 | 124.2 | 126.3 | 127.4 | 123.9 | #N/A | #N/A | 10.2 | 127.5 |
| 2389220 | NH 0014(237)245 | 4.4 | 4.9 | 6.1 | 10.1 | #N/A | #N/A | #N/A | 133.2 | 136 | 140.8 | 144 | #N/A | #N/A | #N/A | 127.6 | 129.6 | 132.7 | 130.8 | #N/A | #N/A | #N/A | 7.7 | 134.1 |
| 2278243 | IM-FP 0903(104)15 | 5.6 | 8.3 | 10.4 | 11.8 | #N/A | #N/A | #N/A | 127.1 | 136.4 | 139.5 | 137.7 | #N/A | #N/A | #N/A | 120.4 | 125.9 | 126.4 | 123.2 | #N/A | #N/A | #N/A | 9.7 | 126.8 |
| 2346605 | NH-EM 0083(74)55 | 5.1 | 6.4 | 9.5 | 15.2 | #N/A | #N/A | #N/A | 119.5 | 124.3 | 133.7 | 134.5 | #N/A | #N/A | #N/A | 113.7 | 116.8 | 122.1 | 116.8 | #N/A | #N/A | #N/A | 10.9 | 122.7 |
| 2369578 | IM 0905(109)226 | 5.6 | 7.5 | 8.8 | 13.2 | #N/A | #N/A | #N/A | 126.8 | 132.5 | 137.2 | 138.7 | #N/A | #N/A | #N/A | 120.1 | 123.3 | 126.1 | 122.5 | #N/A | #N/A | #N/A | 10.3 | 127.3 |
| 2271357 | IM 0909(75)402 | 5.3 | 7.2 | 8.7 | 10.1 | #N/A | #N/A | #N/A | 134.7 | 143.4 | 144.3 | 140.8 | #N/A | #N/A | #N/A | 127.9 | 133.8 | 132.8 | 127.9 | #N/A | #N/A | #N/A | 7.6 | 134.0 |
| 2310444 | BRF 6358(04) | 4.8 | 6.5 | 8.2 | 9.6 | #N/A | #N/A | #N/A | 131.3 | 140.7 | 145.5 | 143.5 | #N/A | #N/A | #N/A | 125.3 | 132.1 | 134.5 | 130.9 | #N/A | #N/A | #N/A | 8.0 | 134.6 |
| 2247796 | NH 0050(97)411 | 5.7 | 8.1 | 10.2 | 11 | #N/A | #N/A | #N/A | 125.1 | 134.8 | 138.8 | 138.3 | #N/A | #N/A | #N/A | 118.4 | 124.7 | 126 | 124.6 | #N/A | #N/A | #N/A | 9.7 | 126.3 |
| 2313409 | P-PH 0046(47)356 | 5.5 | 7.2 | 8.6 | 9.3 | 10.5 | #N/A | #N/A | 130.8 | 136.7 | 142.6 | 143.5 | 142.6 | #N/A | #N/A | 124 | 127.5 | 131.3 | 131.3 | 129 | #N/A | #N/A | 8.9 | 131.5 |
| 2334188 | BRF 6304(00) | 5.1 | 7.1 | 8.7 | 10.1 | #N/A | #N/A | #N/A | 126.3 | 137.9 | 142.2 | 141.6 | #N/A | #N/A | #N/A | 120.2 | 128.8 | 130.8 | 128.6 | #N/A | #N/A | #N/A | 8.6 | 130.8 |
| 2369138 | IM 0293(106)76 | 3 | 4.6 | 6.4 | 7.4 | 9.5 | #N/A | #N/A | 133.5 | 137.5 | 145.2 | 149.1 | 149.9 | #N/A | #N/A | 129.6 | 131.5 | 136.5 | 138.8 | 136.9 | #N/A | #N/A | 8.1 | 139.3 |
| 2313304 | P 0034(181)313 | 6.1 | 8 | 9.5 | 11 | #N/A | #N/A | #N/A | 136.3 | 141.1 | 142.7 | 142.6 | #N/A | #N/A | #N/A | 128.5 | 130.6 | 130.3 | 128.5 | #N/A | #N/A | #N/A | 8.5 | 130.7 |
| 2267862 | P 0044(202)312 | 7.2 | 9 | 11.1 | 12.2 | #N/A | #N/A | #N/A | 133.4 | 140.7 | 143.1 | 141.9 | #N/A | #N/A | #N/A | 124.4 | 129.1 | 128.8 | 126.5 | #N/A | #N/A | #N/A | 9.9 | 129.7 |
| 2300705 | IM-NH-P 0021(151) | 5.7 | 7.6 | 8.9 | 10.9 | 13.1 | #N/A | #N/A | 127.7 | 135.6 | 140.8 | 141.6 | 139.2 | #N/A | #N/A | 120.8 | 126 | 129.3 | 127.7 | 123.1 | #N/A | #N/A | 9.4 | 129.6 |
| 2309515 | IM-NH-P 0022(44) | 4.2 | 6 | 8 | 9.8 | #N/A | #N/A | #N/A | 125 | 135.5 | 142.7 | 142.7 | #N/A | #N/A | #N/A | 120 | 127.8 | 132.1 | 130 | #N/A | #N/A | #N/A | 8.3 | 132.2 |
| 2348361 | NH-P 0023(37) | 5.5 | 7.9 | 9.3 | 11 | #N/A | #N/A | #N/A | 130.8 | 138.6 | 141.8 | 139.8 | #N/A | #N/A | #N/A | 124 | 128.5 | 129.7 | 125.9 | #N/A | #N/A | #N/A | 9.1 | 129.7 |
| 2366036 | ER 0081(104)112 | 5.6 | 6.9 | 9 | 10.8 | #N/A | #N/A | #N/A | 129.6 | 134.4 | 142 | 142 | #N/A | #N/A | #N/A | 122.7 | 125.7 | 130.3 | 128.2 | #N/A | #N/A | #N/A | 9.3 | 130.4 |
| 2311842 | P 0011(88)81 | 2.9 | 4.9 | 6.3 | 8.1 | #N/A | #N/A | #N/A | 129.1 | 134.4 | 140.8 | 145.8 | #N/A | #N/A | #N/A | 125.5 | 128.1 | 132.5 | 134.9 | #N/A | #N/A | #N/A | 8.1 | 134.9 |
| 2370514 | P 0049(05)27 | 5.7 | 6.6 | 8 | 8.8 | 11 | #N/A | #N/A | 133.5 | 135.9 | 140.5 | 142.8 | 140.7 | #N/A | #N/A | 126.3 | 127.5 | 130.1 | 131.3 | 126.8 | #N/A | #N/A | 9.1 | 131.4 |
| 2349573 | P-PH 0052(05)315 | 6.2 | 6.7 | 8.9 | 9.7 | #N/A | #N/A | #N/A | 133 | 135 | 142.4 | 142.4 | #N/A | #N/A | #N/A | 125.2 | 126.5 | 130.8 | 129.8 | #N/A | #N/A | #N/A | 8.8 | 130.8 |
| 2352261 | P-PH 0052(05)315 | 3.9 | 5.6 | 7 | 8.3 | 9.1 | #N/A | #N/A | 128.4 | 136 | 141.4 | 144.6 | 144.6 | #N/A | #N/A | 123.6 | 128.8 | 132.1 | 133.5 | 132.5 | #N/A | #N/A | 8.2 | 133.5 |
| 2314099 | NH-PH 0050(114)324 | 7.5 | 8.8 | 11.4 | 13 | #N/A | #N/A | #N/A | 138.8 | 144.2 | 144.7 | 143 | #N/A | #N/A | #N/A | 129.1 | 132.5 | 129.9 | 126.5 | #N/A | #N/A | #N/A | 9.3 | 132.8 |
| 2371373 | PH 0018(192)390 | 5 | 6.5 | 8.5 | 9.9 | #N/A | #N/A | #N/A | 131.2 | 136.5 | 141.2 | 142.2 | #N/A | #N/A | #N/A | 125 | 128.2 | 130.1 | 129.4 | #N/A | #N/A | #N/A | 8.7 | 130.1 |
| 2380266 | PH 0018(192)390 | 5.7 | 7.8 | 8.4 | 11.7 | #N/A | #N/A | #N/A | 131.5 | 138.7 | 142.6 | 142.6 | #N/A | #N/A | #N/A | 124.4 | 128.7 | 131.5 | 127.7 | #N/A | #N/A | #N/A | 9.7 | 134.2 |
| 2385490 | IM 0906(75)263 | 5 | 6.9 | 8.7 | 9.3 | #N/A | #N/A | #N/A | 128.3 | 136.8 | 141.9 | 141.7 | #N/A | #N/A | #N/A | 122.2 | 128 | 130.5 | 129.6 | #N/A | #N/A | #N/A | 8.5 | 130.6 |
| 2267577 | P 0045(54)27 | 5.1 | 7 | 9.1 | 11 | 12.5 | #N/A | #N/A | 118.8 | 130.6 | 139.1 | 140.7 | 139.2 | #N/A | #N/A | 113 | 122.1 | 127.5 | 126.8 | 123.7 | #N/A | #N/A | 9.7 | 127.8 |
| 2354899 | NH 0050(117)406 | 4 | 6.3 | 8.4 | 10.3 | #N/A | #N/A | #N/A | 133 | 136.8 | 141.9 | 141.2 | #N/A | #N/A | #N/A | 127.9 | 128.7 | 130.9 | 128 | #N/A | #N/A | #N/A | 8.4 | 130.9 |
| 2343168 | P 0048(12)371 | 2.5 | 4.6 | 6.4 | 7.4 | #N/A | #N/A | #N/A | 130.7 | 134.8 | 141.8 | 147.3 | #N/A | #N/A | #N/A | 127.5 | 128.9 | 133.3 | 137.2 | #N/A | #N/A | #N/A | 7.4 | 137.2 |
| 2309026 | P 1358(05) | 4 | 6 | 7.5 | 9.5 | #N/A | #N/A | #N/A | 133.2 | 140.3 | 146.3 | 143.9 | #N/A | #N/A | #N/A | 128.1 | 132.4 | 136.1 | 131.4 | #N/A | #N/A | #N/A | 7.8 | 136.2 |
| 2293419 | PH 0037(147)067 | 7.1 | 8.4 | 11.4 | 12.8 | #N/A | #N/A | #N/A | 132.4 | 138.7 | 140.4 | 138.5 | #N/A | #N/A | #N/A | 123.6 | 128 | 126 | 122.8 | #N/A | #N/A | #N/A | 9.3 | 128.9 |
| 2333033 | BRF 6332(02) | 7.3 | 9.4 | 11.1 | 12.1 | #N/A | #N/A | #N/A | 127.2 | 135.1 | 140.8 | 138.6 | #N/A | #N/A | #N/A | 118.5 | 123.5 | 126.7 | 123.6 | #N/A | #N/A | #N/A | 10.9 | 126.8 |
| 2259347 | P 0042(69)333 | 6 | 8.8 | 10.7 | 12 | #N/A | #N/A | #N/A | 134.3 | 143.1 | 145.5 | 143.4 | #N/A | #N/A | #N/A | 126.7 | 131.5 | 131.4 | 128 | #N/A | #N/A | #N/A | 9.9 | 132.0 |
| 2344200 | P 0045(58)66 | 5.5 | 7.4 | 10.1 | 10.8 | #N/A | #N/A | #N/A | 131.6 | 142 | 144.7 | 142.3 | #N/A | #N/A | #N/A | 124.7 | 132.2 | 131.4 | 128.4 | #N/A | #N/A | #N/A | 8.7 | 133.7 |
| 2299987 | NH 0018(218)339 | 4.8 | 6.6 | 9.4 | 9.9 | #N/A | #N/A | #N/A | 133.3 | 144.3 | 146.7 | 144.8 | #N/A | #N/A | #N/A | 127.2 | 135.4 | 134.1 | 131.8 | #N/A | #N/A | #N/A | 7.8 | 137.1 |
| 2305981 | IM 0908(96)334 | 7 | 9.1 | 10.9 | 12.4 | #N/A | #N/A | #N/A | 125.2 | 137.2 | 141.1 | 139.5 | #N/A | #N/A | #N/A | 117 | 125.8 | 127.2 | 124.1 | #N/A | #N/A | #N/A | 10.4 | 127.4 |
| 2306255 | IM 0908(96)334 | 5.2 | 7.7 | 9.7 | 10.9 | #N/A | #N/A | #N/A | 128.7 | 137.9 | 143.6 | 142.8 | #N/A | #N/A | #N/A | 122.3 | 128 | 130.9 | 128.8 | #N/A | #N/A | #N/A | 9.6 | 130.9 |
| 2307966 | IM 0908(96)334 | 5.5 | 8.6 | 10.2 | 11.9 | #N/A | #N/A | #N/A | 130.4 | 136.8 | 142.6 | 145 | #N/A | #N/A | #N/A | 123.6 | 126 | 129.4 | 129.6 | #N/A | #N/A | #N/A | 11.1 | 130.0 |
| 2325848 | PH 0044(213)312 | 5.8 | 7.9 | 9.8 | 11.9 | #N/A | #N/A | #N/A | 134.4 | 142 | 143.4 | 143 | #N/A | #N/A | #N/A | 127 | 131.6 | 130.6 | 127.8 | #N/A | #N/A | #N/A | 8.3 | 131.7 |
| 2321741 | P TAPU(23) | 3 | 5.1 | 6.9 | 8.5 | #N/A | #N/A | #N/A | 133.6 | 140.8 | 147.8 | 149.8 | #N/A | #N/A | #N/A | 129.7 | 134 | 138.3 | 138.1 | #N/A | #N/A | #N/A | 7.6 | 138.8 |
| 2378617 | NH 2042(29) | 3.3 | 4.8 | 6.6 | 8 | 9 | #N/A | #N/A | 128.5 | 133.6 | 142 | 144.2 | 144.4 | #N/A | #N/A | 124.4 | 127.5 | 133.2 | 133.5 | 132.5 | #N/A | #N/A | 7.3 | 133.8 |
| 2317882 | PH 0020(198) | 6.7 | 8.4 | 9.5 | 10.9 | #N/A | #N/A | #N/A | 135.2 | 142.3 | 143.6 | 143.5 | #N/A | #N/A | #N/A | 126.7 | 131.3 | 131.1 | 129.4 | #N/A | #N/A | #N/A | 8.8 | 131.5 |
| 2366750 | BRF 6102(00)19-1 | 7.4 | 8.9 | 10.6 | 11.5 | #N/A | #N/A | #N/A | 133.6 | 139.5 | 142.6 | 142.6 | #N/A | #N/A | #N/A | 124.4 | 128.1 | 128.9 | 127.9 | #N/A | #N/A | #N/A | 10.1 | 129.0 |
| 2384162 | BRF 6337(00)19-1 | 3.3 | 4.9 | 6.6 | 8.1 | #N/A | #N/A | #N/A | 131.7 | 140.1 | 146.4 | 146.2 | #N/A | #N/A | #N/A | 127.5 | 133.6 | 137.3 | 135.2 | #N/A | #N/A | #N/A | 6.8 | 137.3 |
| 2357943 | ER-P 0038(52)330 | 6.7 | 8.1 | 10 | 12.2 | #N/A | #N/A | #N/A | 133.9 | 143 | 144.3 | 142.4 | #N/A | #N/A | #N/A | 125.5 | 132.3 | 131.2 | 126.9 | #N/A | #N/A | #N/A | 8.7 | 132.9 |
| 2369667 | NH 0050(135)354 | 5.8 | 7.8 | 10 | 11.3 | #N/A | #N/A | #N/A | 131.5 | 140.7 | 145 | 141.5 | #N/A | #N/A | #N/A | 124.3 | 130.5 | 131.8 | 127.1 | #N/A | #N/A | #N/A | 9.3 | 132.5 |
| 2358326 | P 0050(111)231 | 4.2 | 5.9 | 8.3 | 9.1 | #N/A | #N/A | #N/A | 120.2 | 129.2 | 135.4 | 139.1 | #N/A | #N/A | #N/A | 115.4 | 122 | 125 | 127.5 | #N/A | #N/A | #N/A | 9.1 | 127.5 |
| 2251657 | 044-251 | 5.4 | 7.4 | 10.1 | 11 | #N/A | #N/A | #N/A | 128.2 | 136 | 140.7 | 140.3 | #N/A | #N/A | #N/A | 121.6 | 126.6 | 127.8 | 126.4 | #N/A | #N/A | #N/A | 9.2 | 128.2 |
| 2324964 | 090 E-271 | 6.1 | 7.5 | 9 | 10.1 | #N/A | #N/A | #N/A | 131.9 | 137.8 | 141 | 140.7 | #N/A | #N/A | #N/A | 124.3 | 128.2 | 129.4 | 127.8 | #N/A | #N/A | #N/A | 8.7 | 129.5 |
| 2365142 | EM 0295(45)130 | 5.1 | 7 | 8.7 | 10.9 | #N/A | #N/A | #N/A | 131.1 | 138.6 | 143.9 | 141.2 | #N/A | #N/A | #N/A | 124.7 | 129.5 | 132.4 | 127.3 | #N/A | #N/A | #N/A | 8.8 | 132.4 |
| 2385404 | EM 0295(45)130 | 5 | 5.9 | 8.9 | 11.2 | #N/A | #N/A | #N/A | 128.7 | 136.3 | 143 | 140.3 | #N/A | #N/A | #N/A | 122.6 | 128.7 | 131.3 | 126.2 | #N/A | #N/A | #N/A | 7.3 | 132.4 |
| 2288054 | NH-P 0037(128)125 | 5.5 | 6.8 | 8.9 | 10.3 | #N/A | #N/A | #N/A | 131.1 | 140.7 | 142.7 | 141 | #N/A | #N/A | #N/A | 124.3 | 131.7 | 131 | 127.8 | #N/A | #N/A | #N/A | 7.5 | 132.8 |
| 2370586 | NH 0212(174)377 | 3.7 | 6.2 | 7.6 | 9.8 | #N/A | #N/A | #N/A | 131.1 | 141.5 | 146.2 | 143.8 | #N/A | #N/A | #N/A | 126.4 | 133.2 | 135.9 | 131 | #N/A | #N/A | #N/A | 7.8 | 136.0 |
| 2372441 | NH 0212(174)377 | 6.7 | 8.7 | 9.1 | 10.6 | 12.5 | #N/A | #N/A | 123 | 131.5 | 133.1 | 135.8 | 135.5 | #N/A | #N/A | 115.3 | 121 | 122 | 122.8 | 120.4 | #N/A | #N/A | 10.1 | 122.9 |
| 2295345 | PH 0212(167)245 | 6.6 | 7.9 | 9.7 | 11.8 | #N/A | #N/A | #N/A | 125.8 | 133.4 | 138.3 | 137 | #N/A | #N/A | #N/A | 118 | 123.6 | 126.1 | 122.5 | #N/A | #N/A | #N/A | 9.6 | 126.1 |
| 2302137 | PH 0212(167)245 | 4.3 | 6 | 7.4 | 9.4 | 11.8 | #N/A | #N/A | 117.2 | 124.7 | 131.6 | 139.5 | 139.1 | #N/A | #N/A | 112.4 | 117.6 | 122.5 | 127.5 | 124.4 | #N/A | #N/A | 9.9 | 127.7 |

# 4-point Data Along with OMC and MDUW Determined from Quadratic Spline Fit

| Sample ID | Project | Practor Test Data | | | | | | | | | | | | | | | | | | | | | Quadratic Spline Fit | |
|---|---|---|---|---|---|---|---|---|---|---|---|---|---|---|---|---|---|---|---|---|---|---|---|---|
| | | Percent Moisture (%) | | | | | | | Wet Density (pcf) | | | | | | | Dry Density (pcf) | | | | | | | | |
| | | Specimen 1 | Specimen 2 | Specimen 3 | Specimen 4 | Specimen 5 | Specimen 6 | Specimen 7 | Specimen 1 | Specimen 2 | Specimen 3 | Specimen 4 | Specimen 5 | Specimen 6 | Specimen 7 | Specimen 1 | Specimen 2 | Specimen 3 | Specimen 4 | Specimen 5 | Specimen 6 | Specimen 7 | OMC | MDUW |
| 2303664 | PH 0212(167)245 | 5.1 | 7.8 | 8.6 | 11.3 | #N/A | #N/A | #N/A | 127.8 | 134.8 | 140 | 138.4 | #N/A | #N/A | #N/A | 121.6 | 125 | 128.9 | 124.3 | #N/A | #N/A | #N/A | 9.5 | 130.7 |
| 2305160 | PH 0212(167)245 | 5.7 | 7.5 | 8.9 | 11.8 | #N/A | #N/A | #N/A | 126.6 | 134 | 140.3 | 139.6 | #N/A | #N/A | #N/A | 119.8 | 124.7 | 128.8 | 124.9 | #N/A | #N/A | #N/A | 9.8 | 129.6 |
| 2326735 | PH 0212(167)245 | 5.5 | 7.2 | 9.1 | 10.9 | 13.8 | #N/A | #N/A | 114.4 | 122.3 | 130.3 | 136.2 | 135.6 | #N/A | #N/A | 108.4 | 114.1 | 119.4 | 122.8 | 119.2 | #N/A | #N/A | 11.5 | 123.0 |
| 2332011 | PH 0212(167)245 | 5.3 | 7.8 | 9 | 11.7 | 12.9 | 14.8 | #N/A | 112.8 | 118.7 | 127.4 | 133.4 | 134.2 | 133.6 | #N/A | 107.1 | 110.1 | 116.9 | 119.4 | 118.9 | 116.4 | #N/A | 10.3 | 119.8 |
| 2333479 | PH 0212(167)245 | 7.5 | 9.8 | 11.1 | 13.5 | 15.5 | #N/A | #N/A | 118.3 | 124.4 | 131.5 | 133.8 | 132 | #N/A | #N/A | 110 | 113.3 | 118.4 | 117.9 | 114.3 | #N/A | #N/A | 11.9 | 119.6 |
| 2295810 | P 0037(140)140 | 5.8 | 7.1 | 8.9 | 11.3 | #N/A | #N/A | #N/A | 126.8 | 132.8 | 137.5 | 138.2 | #N/A | #N/A | #N/A | 119.8 | 124 | 126.3 | 124.2 | #N/A | #N/A | #N/A | 9.2 | 126.3 |
| 2305960 | P 0037(140)140 | 6.6 | 9.1 | 11 | 13 | #N/A | #N/A | #N/A | 133.1 | 138.2 | 141.8 | 138.6 | #N/A | #N/A | #N/A | 124.9 | 126.7 | 127.7 | 122.7 | #N/A | #N/A | #N/A | 10.6 | 127.8 |
| 2301402 | P 0026(03)250 | 4 | 6 | 7.3 | 9.9 | 10.8 | #N/A | #N/A | 126.2 | 133.4 | 140.3 | 141 | 140.8 | #N/A | #N/A | 121.3 | 125.8 | 130.8 | 128.3 | 127.1 | #N/A | #N/A | 8.0 | 131.6 |
| 2341287 | P-PH 0015(77)155 | 4.8 | 6.5 | 8.1 | 9.8 | #N/A | #N/A | #N/A | 133.8 | 140.6 | 144.3 | 141.9 | #N/A | #N/A | #N/A | 127.7 | 132 | 133.5 | 129.2 | #N/A | #N/A | #N/A | 7.8 | 133.6 |
| 2374240 | P 0026(04)230 | 5.5 | 8 | 9.8 | 11.7 | 12.1 | #N/A | #N/A | 125.2 | 132 | 138.8 | 138.8 | 137 | #N/A | #N/A | 118.7 | 122.2 | 126.4 | 124.3 | 122.2 | #N/A | #N/A | 10.4 | 126.8 |
| 2338546 | P 0015(83)199 | 4.8 | 6.9 | 8.9 | 9.5 | #N/A | #N/A | #N/A | 132.2 | 143.6 | 143.1 | 132.2 | #N/A | #N/A | #N/A | 126.1 | 134.3 | 131.4 | 120.7 | #N/A | #N/A | #N/A | 8.0 | 137.1 |
| 2380414 | P-PH-B 0015(82)167 | 4.6 | 6.6 | 8.5 | 9.7 | #N/A | #N/A | #N/A | 132 | 138.2 | 142.8 | 142.2 | #N/A | #N/A | #N/A | 126.2 | 129.6 | 131.6 | 129.6 | #N/A | #N/A | #N/A | 8.3 | 131.6 |
| 2380656 | P-PH-B 0015(82)167 | 4.1 | 5.9 | 8 | 10 | #N/A | #N/A | #N/A | 136.7 | 144.2 | 143.6 | 142.6 | #N/A | #N/A | #N/A | 131.3 | 136.2 | 133 | 129.6 | #N/A | #N/A | #N/A | 6.1 | 136.2 |
| 2341455 | NH 0012(218)387 | 4.1 | 5.8 | 8.1 | 10.1 | 11.3 | #N/A | #N/A | 124.6 | 134 | 141.5 | 141.9 | 139.2 | #N/A | #N/A | 119.7 | 126.7 | 130.9 | 128.9 | 125.1 | #N/A | #N/A | 8.4 | 130.9 |
| 2342091 | NH 0012(218)387 | 3.4 | 4.9 | 7.2 | 9.4 | 10.4 | #N/A | #N/A | 126.3 | 133.5 | 142 | 143.6 | 142.3 | #N/A | #N/A | 122.1 | 127.3 | 132.5 | 131.3 | 128.9 | #N/A | #N/A | 7.9 | 132.8 |
| 2372598 | P 0022(74)333 | 5.8 | 7 | 9.3 | 11.4 | #N/A | #N/A | #N/A | 135 | 143.5 | 144.4 | 144.2 | #N/A | #N/A | #N/A | 127.6 | 134.1 | 132.1 | 129.4 | #N/A | #N/A | #N/A | 7.6 | 135.0 |
| 2311401 | NH-P 0013(46) | 9.2 | 11.1 | 13.3 | 13.5 | 15.5 | #N/A | #N/A | 122.8 | 129.4 | 133.6 | 133 | 131.8 | #N/A | #N/A | 112.5 | 116.5 | 117.9 | 117.2 | 114.1 | #N/A | #N/A | 12.6 | 119.0 |
| 2325685 | NH-P 0013(46) | 5 | 7.1 | 8.5 | 10.8 | #N/A | #N/A | #N/A | 121.9 | 129.6 | 137.4 | 135.8 | #N/A | #N/A | #N/A | 116.1 | 121 | 126.6 | 122.6 | #N/A | #N/A | #N/A | 9.2 | 127.4 |
| 2366855 | NH-PH 0012(229)264 | 4.2 | 6 | 7.7 | 8.9 | #N/A | #N/A | #N/A | 138.6 | 146.2 | 146.4 | 144.8 | #N/A | #N/A | #N/A | 133 | 137.9 | 135.9 | 133 | #N/A | #N/A | #N/A | 6.2 | 138.0 |
| 2369810 | NH-PH 0012(229)264 | 4.6 | 6.9 | 8.9 | 9.9 | #N/A | #N/A | #N/A | 138.3 | 143.8 | 145.4 | 143.1 | #N/A | #N/A | #N/A | 132.2 | 134.5 | 133.5 | 130.2 | #N/A | #N/A | #N/A | 7.7 | 134.7 |
| 2370324 | BRF 6312(00)18-1 | 5.1 | 6.9 | 8.9 | 10.3 | #N/A | #N/A | #N/A | 134.8 | 142.6 | 143.2 | 142.3 | #N/A | #N/A | #N/A | 128.3 | 133.4 | 131.5 | 129 | #N/A | #N/A | #N/A | 7.3 | 133.5 |
| 2344093 | NH 0012(280)298 | 8.9 | 9.5 | 11.4 | 13.2 | #N/A | #N/A | #N/A | 128.3 | 132.2 | 134.3 | 133.5 | #N/A | #N/A | #N/A | 117.8 | 120.7 | 120.6 | 117.9 | #N/A | #N/A | #N/A | 10.2 | 121.9 |
| 2336937 | NH 0212(201)377 | 5 | 7.1 | 8.7 | 10.1 | #N/A | #N/A | #N/A | 140.2 | 146.6 | 144.6 | 143.9 | #N/A | #N/A | #N/A | 133.5 | 136.9 | 133 | 130.7 | #N/A | #N/A | #N/A | 6.7 | 137.1 |
| 2338279 | NH 0212(201)377 | 4.5 | 6.8 | 8.3 | 9.8 | #N/A | #N/A | #N/A | 134.8 | 142.3 | 143.4 | 140.4 | #N/A | #N/A | #N/A | 129 | 133.2 | 132.4 | 127.9 | #N/A | #N/A | #N/A | 7.2 | 133.3 |
| 1 | 2019 SDSU Research | 6.9 | 8.5 | 9.9 | 11.7 | 13.7 | 16.9 | #N/A | 116.4 | 122.4 | 126.4 | 130.9 | 131.2 | 128.8 | #N/A | 108.9 | 112.9 | 115 | 117.2 | 115.4 | 110.2 | #N/A | 11.8 | 117.2 |
| 2 | 2019 SDSU Research | 3.1 | 4 | 5.1 | 7.4 | 10.7 | 14.2 | #N/A | 117 | 117.6 | 120.8 | 127.3 | 134 | 136.3 | #N/A | 113.5 | 113.1 | 115 | 118.5 | 121.1 | 119.4 | #N/A | 11.2 | 121.2 |
| 3 | 2019 SDSU Research | 4.9 | 6.1 | 6.9 | 7.6 | 7.5 | #N/A | #N/A | 137.4 | 141.5 | 144.8 | 145.3 | 145.2 | #N/A | #N/A | 131 | 133.3 | 135.5 | 135.1 | 135.1 | #N/A | #N/A | 7.0 | 135.5 |
| 4 | 2019 SDSU Research | 5.8 | 7.6 | 9.2 | 10.6 | #N/A | #N/A | #N/A | 132.8 | 140.1 | 144.4 | 142.5 | #N/A | #N/A | #N/A | 125.5 | 130.2 | 132.3 | 128.9 | #N/A | #N/A | #N/A | 9.0 | 132.3 |
| 5 | 2019 SDSU Research | 2.4 | 4.5 | 6.7 | 8.8 | 10.7 | 12.4 | #N/A | 121.9 | 125 | 132 | 139.7 | 141 | 139.6 | #N/A | 119.1 | 119.7 | 123.8 | 128.4 | 127.4 | 124.2 | #N/A | 9.3 | 128.6 |
| 6 | 2019 SDSU Research | 3.9 | 5 | 7.1 | 9.3 | 11.8 | 14.3 | 15.7 | 109.1 | 108.9 | 109.7 | 111.3 | 118 | 116.4 | 114.9 | 109.1 | 108.9 | 109.7 | 111.3 | 118 | 116.4 | 114.9 | 12.4 | 118.4 |
| 7 | 2019 SDSU Research | 2.5 | 3.5 | 4.8 | 6.5 | 8.6 | 11.4 | #N/A | 118.1 | 124.4 | 127.5 | 132.3 | 137.4 | 132.4 | #N/A | 115.2 | 120.2 | 121.7 | 124.2 | 126.5 | 118.8 | #N/A | 8.4 | 126.5 |
| 8 | 2019 SDSU Research | 2.9 | 4.9 | 7.1 | 8.9 | 10.2 | 11.6 | #N/A | 121.4 | 132.6 | 140.7 | 141.2 | 139.2 | 137.7 | #N/A | 118 | 126.4 | 131.3 | 129.6 | 126.4 | 123.4 | #N/A | 7.4 | 131.4 |
| 9 | 2019 SDSU Research | 4.1 | 5.8 | 8 | 9.8 | 10.7 | 12 | #N/A | 120.1 | 123.7 | 130.5 | 137 | 140.3 | 139.5 | #N/A | 115.3 | 116.9 | 120.9 | 124.8 | 126.8 | 124.6 | #N/A | 11.0 | 126.9 |
| 10 | 2019 SDSU Research | 3.4 | 5.3 | 7.3 | 8.9 | 9.9 | 10.7 | #N/A | 124 | 131.5 | 138.7 | 143.5 | 144.5 | 143.6 | #N/A | 120 | 124.9 | 129.2 | 131.8 | 131.4 | 129.7 | #N/A | 9.2 | 131.9 |

# Appendix B: Validation Database for the New SDDOT Family of Curves

# 4-point Data Along with OMC and MDUW Determined from Quadratic Spline Fit for Validation DataSets

| Sample ID | Project | Practor Test Data | | | | | | | | | | | | | | | | | | | | | Quadratic Spline Fit | |
|---|---|---|---|---|---|---|---|---|---|---|---|---|---|---|---|---|---|---|---|---|---|---|---|---|
| | | Percent Moisture (%) | | | | | | | Wet Density (pcf) | | | | | | | Dry Density (pcf) | | | | | | | | |
| | | Specimen 1 | Specimen 2 | Specimen 3 | Specimen 4 | Specimen 5 | Specimen 6 | Specimen 7 | Specimen 1 | Specimen 2 | Specimen 3 | Specimen 4 | Specimen 5 | Specimen 6 | Specimen 7 | Specimen 1 | Specimen 2 | Specimen 3 | Specimen 4 | Specimen 5 | Specimen 6 | Specimen 7 | OMC | MDUW |
| 2390119 | P-PH 0034(170)350 | 7.2 | 9.1 | 11.3 | 13.4 | #N/A | #N/A | #N/A | 134.2 | 141.9 | 142.6 | 142 | #N/A | #N/A | #N/A | 125.2 | 130.1 | 128.1 | 125.2 | #N/A | #N/A | #N/A | 9.5 | 130.2 |
| 2400445 | NH 0018(203)333 | 8.7 | 10.7 | 12.2 | 13.2 | #N/A | #N/A | #N/A | 132.6 | 140.4 | 141.9 | 140.3 | #N/A | #N/A | #N/A | 122 | 126.8 | 126.5 | 123.9 | #N/A | #N/A | #N/A | 11.4 | 127.1 |
| 2402606 | P-PH-EM 0046(60)34 | 5 | 7.3 | 9.2 | 10.4 | #N/A | #N/A | #N/A | 128.3 | 141 | 144.7 | 143.6 | #N/A | #N/A | #N/A | 122.2 | 131.4 | 132.5 | 130.1 | #N/A | #N/A | #N/A | 8.6 | 132.8 |
| 2395185 | IM 2292(98)9 | 6.8 | 9.6 | 11 | 12.1 | #N/A | #N/A | #N/A | 129.6 | 138 | 143.4 | 141.6 | #N/A | #N/A | #N/A | 121.3 | 125.9 | 129.2 | 126.3 | #N/A | #N/A | #N/A | 11.0 | 129.2 |
| 2416173 | IM 2292(98)9 | 2.9 | 4.3 | 5.9 | 7.3 | 9 | #N/A | #N/A | 128.4 | 131.5 | 139.6 | 143.2 | 143 | #N/A | #N/A | 124.8 | 126.1 | 131.8 | 133.5 | 131.2 | #N/A | #N/A | 7.3 | 133.5 |
| 2391744 | 1 | 1.9 | 3.7 | 6.4 | 9.3 | #N/A | #N/A | #N/A | 128.6 | 133.1 | 137.4 | 143.8 | #N/A | #N/A | #N/A | 126.2 | 128.4 | 129.1 | 131.6 | #N/A | #N/A | #N/A | 9.3 | 131.6 |
| 2413907 | IM 0906(73)272 | 5 | 7 | 9.4 | 11.8 | #N/A | #N/A | #N/A | 123.8 | 130.6 | 137.5 | 135.5 | #N/A | #N/A | #N/A | 117.9 | 122.1 | 125.7 | 121.2 | #N/A | #N/A | #N/A | 9.4 | 125.7 |
| 2400552 | IM 2292(103)2 | 4.1 | 5.4 | 7 | 9.5 | 11.1 | #N/A | #N/A | 128.2 | 133.5 | 140.4 | 142.3 | 143.6 | #N/A | #N/A | 123.2 | 126.7 | 131.2 | 130 | 129.3 | #N/A | #N/A | 7.6 | 131.7 |
| 2390640 | PH 0020(201) | 3.2 | 4.9 | 6.9 | 8.4 | 9.5 | #N/A | #N/A | 121.2 | 128 | 137.1 | 142.8 | 142.6 | #N/A | #N/A | 117.4 | 122 | 128.3 | 131.7 | 130.2 | #N/A | #N/A | 8.5 | 131.7 |
| 2395860 | PH 0020(201) | 6.8 | 8.8 | 12 | 12.4 | #N/A | #N/A | #N/A | 132.3 | 142 | 144.3 | 143.1 | #N/A | #N/A | #N/A | 123.9 | 130.5 | 128.8 | 127.3 | #N/A | #N/A | #N/A | 10.1 | 131.8 |
| 2410583 | PH 0020(199) | 4.5 | 5.8 | 7.9 | 9.2 | #N/A | #N/A | #N/A | 123.2 | 131 | 138.7 | 140.8 | #N/A | #N/A | #N/A | 117.9 | 123.8 | 128.5 | 128.9 | #N/A | #N/A | #N/A | 8.8 | 129.0 |
| 2409672 | P TAPU(22) | 5.7 | 7 | 9.5 | 10.5 | #N/A | #N/A | #N/A | 130.4 | 139.5 | 143.9 | 141.5 | #N/A | #N/A | #N/A | 123.4 | 130.4 | 131.4 | 128.1 | #N/A | #N/A | #N/A | 8.3 | 132.8 |
| 2392228 | IM 0905(118)260 | 5.8 | 8.7 | 10.2 | 11.3 | #N/A | #N/A | #N/A | 127 | 135.5 | 139.9 | 139.8 | #N/A | #N/A | #N/A | 120 | 124.7 | 127 | 125.6 | #N/A | #N/A | #N/A | 10.2 | 127.0 |
| 2404911 | P TAPR(41) | 6.3 | 8.6 | 10.1 | 11.9 | #N/A | #N/A | #N/A | 131.5 | 140.6 | 142.3 | 140.2 | #N/A | #N/A | #N/A | 123.7 | 129.5 | 129.2 | 125.3 | #N/A | #N/A | #N/A | 9.2 | 129.7 |
| 2419984 | P TAPR(31) | 8.3 | 9 | 11 | 13.3 | #N/A | #N/A | #N/A | 130 | 136.2 | 141.2 | 139.9 | #N/A | #N/A | #N/A | 120 | 125 | 127.2 | 123.5 | #N/A | #N/A | #N/A | 10.0 | 127.6 |
| 2413595 | BRO-B 8005(14) | 3.7 | 5.5 | 7.1 | 9.5 | #N/A | #N/A | #N/A | 121.2 | 131 | 142.6 | 138.3 | #N/A | #N/A | #N/A | 116.9 | 124.2 | 133.1 | 126.3 | #N/A | #N/A | #N/A | 7.7 | 134.0 |
| 2419324 | BRO-B 8005(14) | 4.8 | 6.6 | 7.7 | 10.3 | #N/A | #N/A | #N/A | 123.1 | 133 | 138.7 | 141 | #N/A | #N/A | #N/A | 117.5 | 124.8 | 128.8 | 127.8 | #N/A | #N/A | #N/A | 8.9 | 130.3 |
| 2410531 | BRF-B 6516(05) | 5.4 | 7.3 | 8.8 | 11.3 | #N/A | #N/A | #N/A | 123.8 | 132.6 | 139.6 | 141.9 | #N/A | #N/A | #N/A | 117.5 | 123.6 | 128.3 | 127.5 | #N/A | #N/A | #N/A | 9.9 | 129.4 |
| 2403728 | IM 0909(97)404 | 1.6 | 2.5 | 4.5 | 6.4 | #N/A | #N/A | #N/A | 129.8 | 131.1 | 136 | 135.2 | #N/A | #N/A | #N/A | 127.8 | 127.9 | 130.1 | 127.1 | #N/A | #N/A | #N/A | 4.6 | 130.1 |
| 2420067 | P-PH 0015(76)128 | 3.7 | 5.9 | 8 | 9.6 | 10.8 | #N/A | #N/A | 125.6 | 134.8 | 142.3 | 142.7 | 139.9 | #N/A | #N/A | 121.1 | 127.3 | 131.8 | 130.2 | 126.3 | #N/A | #N/A | 8.3 | 131.9 |
| 2414295 | NH 0014(230)145 | 3.8 | 5.9 | 7.9 | 9.6 | #N/A | #N/A | #N/A | 126.4 | 135.6 | 143.1 | 141.2 | #N/A | #N/A | #N/A | 121.8 | 128 | 132.6 | 128.8 | #N/A | #N/A | #N/A | 8.0 | 132.6 |
| 2416366 | P0044(212)172 | 4.1 | 5.8 | 7.1 | 9.4 | #N/A | #N/A | #N/A | 132 | 132 | 145.9 | 146.8 | #N/A | #N/A | #N/A | 126.8 | 124.8 | 136.2 | 134.2 | #N/A | #N/A | #N/A | 8.1 | 139.7 |
| 2391011 | PH 8041(20) | 4.1 | 6.2 | 7.5 | 9.1 | #N/A | #N/A | #N/A | 136.4 | 146.7 | 150.1 | 147.9 | #N/A | #N/A | #N/A | 131 | 138.1 | 139.6 | 135.6 | #N/A | #N/A | #N/A | 7.4 | 139.6 |
| 2406521 | IM-NH-P 0041(163) | 2.3 | 3.4 | 6.9 | 9.4 | #N/A | #N/A | #N/A | 127.2 | 129.7 | 146.5 | 147.3 | #N/A | #N/A | #N/A | 124.3 | 125.4 | 137 | 134.6 | #N/A | #N/A | #N/A | 7.7 | 137.6 |
| 2389811 | P 0044(217)88 | 3.3 | 5 | 7.5 | 9.7 | #N/A | #N/A | #N/A | 131.2 | 137.7 | 143.9 | 143.3 | #N/A | #N/A | #N/A | 127 | 131.1 | 133.9 | 130.6 | #N/A | #N/A | #N/A | 7.4 | 133.9 |
| 2387741 | PH 0034(202)12 | 3.8 | 5.5 | 7.7 | 10.4 | 11.6 | #N/A | #N/A | 129.2 | 135.5 | 141.1 | 143.9 | 145.6 | #N/A | #N/A | 124.5 | 128.4 | 131 | 130.3 | 130.5 | #N/A | #N/A | 8.2 | 131.1 |
| 2413313 | NH-P 0041(169) | 2.6 | 5.6 | 9.7 | 11.2 | #N/A | #N/A | #N/A | 129 | 134 | 144.7 | 143.5 | #N/A | #N/A | #N/A | 125.7 | 126.9 | 131.9 | 129 | #N/A | #N/A | #N/A | 9.1 | 132.1 |
| 2405743 | BR CSBP(01) | 3 | 5 | 7.6 | 9.6 | #N/A | #N/A | #N/A | 130 | 135.1 | 148.5 | 148.3 | #N/A | #N/A | #N/A | 126.2 | 128.7 | 138 | 135.3 | #N/A | #N/A | #N/A | 8.1 | 138.4 |
| 2414351 | NH 0085(112)146 | 2.7 | 5.1 | 7.1 | 9.3 | 9.6 | #N/A | #N/A | 127.4 | 137.6 | 144 | 146.3 | 144.8 | #N/A | #N/A | 124.1 | 130.9 | 134.5 | 133.9 | 132.1 | #N/A | #N/A | 8.4 | 136.2 |
| 2403726 | IM 0901(203)45 | 2.7 | 5.4 | 9.2 | 10.6 | #N/A | #N/A | #N/A | 128.9 | 136.8 | 145.6 | 144.1 | #N/A | #N/A | #N/A | 125.5 | 129.8 | 133.3 | 130.3 | #N/A | #N/A | #N/A | 8.4 | 133.7 |
| 2409289 | P 6403(10) | 4.9 | 7.4 | 11.1 | 13.2 | #N/A | #N/A | #N/A | 116.8 | 122.3 | 132.9 | 134.8 | #N/A | #N/A | #N/A | 111.3 | 113.9 | 119.6 | 119.1 | #N/A | #N/A | #N/A | 11.9 | 119.8 |
| 2409599 | P 6403(10) | 4.7 | 7.7 | 10.7 | 9.6 | #N/A | #N/A | #N/A | 114.8 | 126 | 134.7 | 133.9 | #N/A | #N/A | #N/A | 109.6 | 117 | 121.7 | 122.2 | #N/A | #N/A | #N/A | 10.0 | 122.4 |
| 2418452 | P 016A(00)24 | 1.8 | 4.3 | 7.1 | 8.3 | #N/A | #N/A | #N/A | 127.6 | 139 | 150.7 | 149.1 | #N/A | #N/A | #N/A | 125.3 | 133.3 | 140.7 | 137.7 | #N/A | #N/A | #N/A | 6.9 | 140.8 |
| 2388175 | I-FP-PP-B 0901(195 COUN | 2.6 | 3.8 | 5.5 | 7.6 | 9.5 | #N/A | #N/A | 126.7 | 133.3 | 142.1 | 146.4 | 146 | #N/A | #N/A | 123.5 | 128.4 | 134.7 | 136.1 | 133.3 | #N/A | #N/A | 7.0 | 136.3 |
| 2391204 | I-FP-PP-B 0901(195 COUN | 4.4 | 5.8 | 7.5 | 10.5 | #N/A | #N/A | #N/A | 132.1 | 137.5 | 146.1 | 144.1 | #N/A | #N/A | #N/A | 126.5 | 130 | 135.9 | 130.4 | #N/A | #N/A | #N/A | 8.3 | 136.7 |
| 2418113 | IM-B-TA 1902(67)0 | 1.3 | 2.6 | 6.8 | 10.6 | #N/A | #N/A | #N/A | 127.4 | 132.2 | 145.7 | 146.5 | #N/A | #N/A | #N/A | 125.8 | 128.8 | 136.4 | 132.5 | #N/A | #N/A | #N/A | 7.4 | 136.6 |
| 2401134 | NH 0016(95)50 | 1.3 | 4.1 | 6.1 | 7.3 | #N/A | #N/A | #N/A | 123.7 | 127.6 | 131.5 | 130.4 | #N/A | #N/A | #N/A | 122.1 | 122.6 | 123.9 | 121.5 | #N/A | #N/A | #N/A | 5.7 | 124.0 |
| 2406238 | NH 0016(95)50 | 2.2 | 3.9 | 4.8 | 7.5 | 8.7 | #N/A | #N/A | 125.9 | 132.8 | 138.8 | 143.5 | 149.3 | #N/A | #N/A | 123.2 | 127.8 | 132.4 | 133.5 | 137.4 | #N/A | #N/A | 8.7 | 137.4 |
| 2404487 | 018-492 | 1.8 | 4.5 | 7 | 10.3 | #N/A | #N/A | #N/A | 129.1 | 134.9 | 145.9 | 148 | #N/A | #N/A | #N/A | 126.8 | 129.1 | 136.4 | 134.2 | #N/A | #N/A | #N/A | 8.2 | 137.5 |
| 2417722 | P-PT 0020(208)296 | 6 | 8.7 | 9.8 | 12.2 | 14.8 | #N/A | #N/A | 117.9 | 124.6 | 128.4 | 135 | 132.8 | #N/A | #N/A | 111.2 | 114.6 | 116.9 | 120.3 | 115.7 | #N/A | #N/A | 12.2 | 120.3 |
| 2413634 | P 0026(06)253 | 6.5 | 8.1 | 9.8 | 11.6 | 13 | 14 | #N/A | 117.6 | 122.2 | 127.8 | 131.2 | 133.6 | 132.8 | #N/A | 110.4 | 113 | 116.4 | 117.6 | 118.2 | 116.5 | #N/A | 12.7 | 118.3 |
| 2414460 | NH-CR 0081(127)119 | 5.6 | 8 | 9 | 9.8 | #N/A | #N/A | #N/A | 139.6 | 144.8 | 145.8 | 144.4 | #N/A | #N/A | #N/A | 132.2 | 134.1 | 133.8 | 131.5 | #N/A | #N/A | #N/A | 8.5 | 134.2 |

# Appendix C: Validation Analysis for the New SDDOT Family of Curves

## Absolute Deviation Values based on SDDOT 2-pcf Curves

| Sample ID | Proctor Parameter | | 4-point density test | | | SDDOT 2-pcf Curves Predicted Values | | | | |
|---|---|---|---|---|---|---|---|---|---|---|
| | OMC | MDUW | Moisture Content | Density | Wet Density | One point OMC | One Point MDUW | Curve | Absolute Deviation OMC | Absolute Deviation MDUW |
| 2390119 | 9.5 | 130.2 | 9.1 | 130.1 | 141.9 | 8.6 | 131.1 | 130-132 | 0.84 | 0.87 |
| 2400445 | 11.4 | 127.1 | 8.7 | 122 | 132.6 | 10.6 | 123.3 | 122-124 | 0.83 | 3.86 |
| 2402606 | 8.6 | 132.8 | 7.3 | 131.4 | 141.0 | 8.2 | 133.1 | 132-134 | 0.37 | 0.26 |
| 2402606 | 8.6 | 132.8 | 9.2 | 132.5 | 144.7 | 8.2 | 133.1 | 132-134 | 0.37 | 0.26 |
| 2395185 | 11.0 | 129.2 | 9.6 | 125.9 | 138.0 | 10.1 | 125.0 | 124-126 | 0.91 | 4.23 |
| 2416173 | 7.3 | 133.5 | 5.9 | 131.8 | 139.6 | 7.9 | 134.9 | 134-136 | 0.62 | 1.42 |
| 2416173 | 7.3 | 133.5 | 7.3 | 133.5 | 143.2 | 8.2 | 133.1 | 132-134 | 0.96 | 0.45 |
| 2416173 | 7.3 | 133.5 | 9 | 131.2 | 143.0 | 8.6 | 131.1 | 130-132 | 1.34 | 2.40 |
| 2413907 | 9.4 | 125.7 | 9.4 | 125.7 | 137.5 | 10.1 | 125.0 | 124-126 | 0.67 | 0.73 |
| 2413907 | 9.4 | 125.7 | 11.8 | 121.2 | 135.5 | 11.2 | 121.3 | 120-122 | 1.77 | 4.37 |
| 2400552 | 7.6 | 131.7 | 7 | 131.2 | 140.4 | 8.2 | 133.1 | 132-134 | 0.59 | 1.34 |
| 2400552 | 7.6 | 131.7 | 9.5 | 130 | 142.4 | 8.6 | 131.1 | 130-132 | 0.98 | 0.61 |
| 2390640 | 8.5 | 131.7 | 6.9 | 128.3 | 137.2 | 8.6 | 131.1 | 130-132 | 0.07 | 0.63 |
| 2390640 | 8.5 | 131.7 | 8.4 | 131.7 | 142.8 | 8.6 | 131.1 | 130-132 | 0.07 | 0.63 |
| 2390640 | 8.5 | 131.7 | 9.5 | 130.2 | 142.6 | 8.6 | 131.1 | 130-132 | 0.07 | 0.63 |
| 2395860 | 10.1 | 131.8 | 8.8 | 130.5 | 142.0 | 8.6 | 131.1 | 130-132 | 1.53 | 0.70 |
| 2410583 | 8.8 | 129.0 | 7.9 | 128.5 | 138.7 | 9.0 | 129.2 | 128-130 | 0.21 | 0.18 |
| 2410583 | 8.8 | 129.0 | 9.2 | 128.9 | 140.8 | 9.0 | 129.2 | 128-130 | 0.21 | 0.18 |
| 2409672 | 8.3 | 132.8 | 7 | 130.4 | 139.5 | 8.6 | 131.1 | 130-132 | 0.29 | 1.65 |
| 2392228 | 10.2 | 127.0 | 8.7 | 124.7 | 135.5 | 10.1 | 125.0 | 124-126 | 0.18 | 2.04 |
| 2392228 | 10.2 | 127.0 | 10.2 | 127 | 140.0 | 9.5 | 127.0 | 126-128 | 0.72 | 0.03 |
| 2404911 | 9.2 | 129.7 | 8.6 | 129.5 | 140.6 | 9.0 | 129.2 | 128-130 | 0.16 | 0.59 |
| 2419984 | 10.0 | 127.6 | 9 | 125 | 136.3 | 10.1 | 125.0 | 124-126 | 0.05 | 2.65 |
| 2413595 | 7.7 | 134.0 | 7.1 | 133.1 | 142.6 | 8.2 | 133.1 | 132-134 | 0.49 | 0.96 |
| 2413595 | 7.7 | 134.0 | 9.5 | 126.3 | 138.3 | 9.5 | 127.0 | 126-128 | 1.78 | 6.98 |
| 2419324 | 8.9 | 130.3 | 7.7 | 128.8 | 138.7 | 9.0 | 129.2 | 128-130 | 0.17 | 1.16 |
| 2410531 | 9.9 | 129.4 | 8.8 | 128.3 | 139.6 | 9.0 | 129.2 | 128-130 | 0.84 | 0.28 |
| 2420067 | 8.3 | 131.9 | 8 | 131.8 | 142.3 | 8.6 | 131.1 | 130-132 | 0.32 | 0.77 |
| 2420067 | 8.3 | 131.9 | 9.6 | 130.2 | 142.7 | 8.6 | 131.1 | 130-132 | 0.32 | 0.77 |
| 2414295 | 8.0 | 132.6 | 7.9 | 132.6 | 143.1 | 8.2 | 133.1 | 132-134 | 0.27 | 0.45 |
| 2414295 | 8.0 | 132.6 | 9.6 | 128.8 | 141.2 | 9.0 | 129.2 | 128-130 | 1.07 | 3.45 |
| 2416366 | 8.1 | 139.7 | 7.1 | 136.2 | 145.9 | 7.6 | 137.0 | 136-138 | 0.56 | 2.70 |
| 2391011 | 7.4 | 139.6 | 6.2 | 138.1 | 146.7 | 7.2 | 139.1 | 138-140 | 0.14 | 0.54 |
| 2391011 | 7.4 | 139.6 | 7.5 | 139.6 | 150.1 | 7.2 | 139.1 | 138-140 | 0.14 | 0.54 |
| 2406521 | 7.7 | 137.6 | 6.9 | 137 | 146.5 | 7.6 | 137.0 | 136-138 | 0.12 | 0.57 |
| 2389811 | 7.4 | 133.9 | 7.5 | 133.9 | 143.9 | 7.9 | 134.9 | 134-136 | 0.52 | 1.01 |
| 2387741 | 8.2 | 131.1 | 7.7 | 131 | 141.1 | 8.6 | 131.1 | 130-132 | 0.40 | 0.00 |
| 2405743 | 8.1 | 138.4 | 7.6 | 138 | 148.5 | 7.2 | 139.1 | 138-140 | 0.89 | 0.73 |
| 2414351 | 8.4 | 136.2 | 7.1 | 134.5 | 144.0 | 7.9 | 134.9 | 134-136 | 0.52 | 1.24 |

**Absolute Deviation Values based on SDDOT 2-pcf Curves**

| Sample ID | Proctor Parameter | | 4-point density test | | | SDDOT 2-pcf Curves Predicted Values | | | | |
|---|---|---|---|---|---|---|---|---|---|---|
| | OMC | MDUW | Moisture Content | Density | Wet Density | One point OMC | One Point MDUW | Curve | Absolute Deviation OMC | Absolute Deviation MDUW |
| 2409289 | 11.9 | 119.8 | 11.1 | 119.6 | 132.9 | 11.9 | 119.2 | 118-120 | 0.06 | 0.62 |
| 2409599 | 10.0 | 122.4 | 10.7 | 121.7 | 134.7 | 11.2 | 121.3 | 120-122 | 1.19 | 1.05 |
| 2409599 | 10.0 | 122.4 | 9.6 | 122.2 | 133.9 | 10.6 | 123.3 | 122-124 | 0.58 | 0.90 |
| 2418452 | 6.9 | 140.8 | 7.1 | 140.7 | 150.7 | 7.0 | 141.0 | 140- 142 | 0.06 | 0.20 |
| 2388175 | 7.0 | 136.3 | 7.6 | 136.1 | 146.4 | 7.6 | 137.0 | 136-138 | 0.57 | 0.71 |
| 2391204 | 8.3 | 136.7 | 7.5 | 135.9 | 146.1 | 7.6 | 137.0 | 136-138 | 0.73 | 0.27 |
| 2418113 | 7.4 | 136.6 | 6.8 | 136.4 | 145.7 | 7.6 | 137.0 | 136-138 | 0.15 | 0.43 |
| 2406238 | 8.7 | 137.4 | 7.5 | 133.5 | 143.5 | 8.2 | 133.1 | 132-134 | 0.47 | 4.35 |
| 2404487 | 8.2 | 137.5 | 7 | 136.4 | 145.9 | 7.6 | 137.0 | 136-138 | 0.68 | 0.52 |
| 2420069 | 8.3 | 131.9 | 8 | 131.8 | 142.3 | 8.6 | 131.1 | 130-132 | 0.32 | 0.77 |
| 2420070 | 8.3 | 131.9 | 9.6 | 130.2 | 142.7 | 8.6 | 131.1 | 130-132 | 0.32 | 0.77 |
| 2413637 | 12.7 | 118.3 | 11.6 | 117.6 | 131.2 | 12.7 | 117.2 | 116 -118 | 0.00 | 1.07 |
| 2414461 | 8.5 | 134.2 | 8 | 134.1 | 144.8 | 7.9 | 134.9 | 134-136 | 0.63 | 0.74 |

**Absolute Deviation Values based on SDDOT 1-pcf Curves**

| Sample ID | Proctor Parameter | | 4-point density test | | | SDDOT 1-pcf Curves Predicted Values | | | | |
|---|---|---|---|---|---|---|---|---|---|---|
| | OMC | MDUW | Moisture Content | Density | Wet Density | One point OMC | One Point MDUW | Curve | Absolute Deviation OMC | Absolute Deviation MDUW |
| 2390119 | 9.5 | 130.2 | 9.1 | 130.1 | 141.9 | 8.8 | 130.0 | 130 | 0.61 | 0.23 |
| 2400445 | 11.4 | 127.1 | 8.7 | 122 | 132.6 | 10.3 | 124.0 | 124 | 1.04 | 3.14 |
| 2402606 | 8.6 | 132.8 | 7.3 | 131.4 | 141.0 | 8.4 | 132.0 | 132 | 0.17 | 0.80 |
| 2402606 | 8.6 | 132.8 | 9.2 | 132.5 | 144.7 | 8.2 | 133.0 | 133 | 0.36 | 0.20 |
| 2395185 | 11.0 | 129.2 | 9.6 | 125.9 | 138.0 | 9.8 | 126.0 | 126 | 1.19 | 3.20 |
| 2416173 | 7.3 | 133.5 | 5.9 | 131.8 | 139.6 | 7.9 | 135.0 | 135 | 0.61 | 1.50 |
| 2416173 | 7.3 | 133.5 | 7.3 | 133.5 | 143.2 | 8.1 | 134.0 | 134 | 0.78 | 0.50 |
| 2416173 | 7.3 | 133.5 | 9 | 131.2 | 143.0 | 8.6 | 131.0 | 131 | 1.36 | 2.50 |
| 2413907 | 9.4 | 125.7 | 9.4 | 125.7 | 137.5 | 9.8 | 126.0 | 126 | 0.39 | 0.30 |
| 2413907 | 9.4 | 125.7 | 11.8 | 121.2 | 135.5 | 11.3 | 121.0 | 121 | 1.88 | 4.70 |
| 2400552 | 7.6 | 131.7 | 7 | 131.2 | 140.4 | 8.4 | 132.0 | 132 | 0.80 | 0.29 |
| 2400552 | 7.6 | 131.7 | 9.5 | 130 | 142.4 | 8.8 | 130.0 | 130 | 1.21 | 1.71 |
| 2390640 | 8.5 | 131.7 | 6.9 | 128.3 | 137.2 | 8.8 | 130.0 | 130 | 0.30 | 1.72 |
| 2390640 | 8.5 | 131.7 | 8.4 | 131.7 | 142.8 | 8.4 | 132.0 | 132 | 0.11 | 0.28 |
| 2390640 | 8.5 | 131.7 | 9.5 | 130.2 | 142.6 | 8.6 | 131.0 | 131 | 0.09 | 0.72 |
| 2395860 | 10.1 | 131.8 | 8.8 | 130.5 | 142.0 | 8.6 | 131.0 | 131 | 1.51 | 0.80 |
| 2410583 | 8.8 | 129.0 | 7.9 | 128.5 | 138.7 | 9.1 | 129.0 | 129 | 0.24 | 0.03 |
| 2410583 | 8.8 | 129.0 | 9.2 | 128.9 | 140.8 | 9.1 | 129.0 | 129 | 0.24 | 0.03 |
| 2409672 | 8.3 | 132.8 | 7 | 130.4 | 139.5 | 8.4 | 132.0 | 132 | 0.11 | 0.75 |
| 2392228 | 10.2 | 127.0 | 8.7 | 124.7 | 135.5 | 9.8 | 126.0 | 126 | 0.46 | 1.00 |
| 2392228 | 10.2 | 127.0 | 10.2 | 127 | 140.0 | 9.5 | 127.0 | 127 | 0.71 | 0.00 |
| 2404911 | 9.2 | 129.7 | 8.6 | 129.5 | 140.6 | 8.8 | 130.0 | 130 | 0.34 | 0.26 |
| 2419984 | 10.0 | 127.6 | 9 | 125 | 136.3 | 10.1 | 125.0 | 125 | 0.04 | 2.61 |
| 2413595 | 7.7 | 134.0 | 7.1 | 133.1 | 142.6 | 8.1 | 134.0 | 134 | 0.31 | 0.02 |
| 2413595 | 7.7 | 134.0 | 9.5 | 126.3 | 138.3 | 9.8 | 126.0 | 126 | 2.05 | 8.02 |
| 2419324 | 8.9 | 130.3 | 7.7 | 128.8 | 138.7 | 8.8 | 130.0 | 130 | 0.01 | 0.31 |
| 2410531 | 9.9 | 129.4 | 8.8 | 128.3 | 139.6 | 9.3 | 128.0 | 128 | 0.58 | 1.43 |
| 2420067 | 8.3 | 131.9 | 8 | 131.8 | 142.3 | 8.4 | 132.0 | 132 | 0.14 | 0.13 |
| 2420067 | 8.3 | 131.9 | 9.6 | 130.2 | 142.7 | 8.6 | 131.0 | 131 | 0.34 | 0.87 |
| 2414295 | 8.0 | 132.6 | 7.9 | 132.6 | 143.1 | 8.2 | 133.0 | 133 | 0.28 | 0.39 |
| 2414295 | 8.0 | 132.6 | 9.6 | 128.8 | 141.2 | 9.1 | 129.0 | 129 | 1.10 | 3.61 |
| 2416366 | 8.1 | 139.7 | 7.1 | 136.2 | 145.9 | 7.7 | 136.0 | 136 | 0.40 | 3.69 |
| 2391011 | 7.4 | 139.6 | 6.2 | 138.1 | 146.7 | 7.3 | 139.0 | 139 | 0.13 | 0.62 |
| 2391011 | 7.4 | 139.6 | 7.5 | 139.6 | 150.1 | 7.1 | 140.0 | 140 | 0.27 | 0.38 |
| 2406521 | 7.7 | 137.6 | 6.9 | 137 | 146.5 | 7.6 | 137.0 | 137 | 0.12 | 0.57 |
| 2389811 | 7.4 | 133.9 | 7.5 | 133.9 | 143.9 | 8.1 | 134.0 | 134 | 0.68 | 0.09 |
| 2387741 | 8.2 | 131.1 | 7.7 | 131 | 141.1 | 8.6 | 131.0 | 131 | 0.42 | 0.10 |
| 2405743 | 8.1 | 138.4 | 7.6 | 138 | 148.5 | 7.4 | 138.0 | 138 | 0.73 | 0.36 |
| 2414351 | 8.4 | 136.2 | 7.1 | 134.5 | 144.0 | 7.9 | 135.0 | 135 | 0.53 | 1.16 |
| 2409289 | 11.9 | 119.8 | 11.1 | 119.6 | 132.9 | 11.6 | 120.0 | 120 | 0.23 | 0.18 |

**Absolute Deviation Values based on SDDOT 1-pcf Curves**

| Sample ID | Proctor Parameter | | 4-point density test | | | SDDOT 1-pcf Curves Predicted Values | | | | |
|---|---|---|---|---|---|---|---|---|---|---|
| | OMC | MDUW | Moisture Content | Density | Wet Density | One point OMC | One Point MDUW | Curve | Absolute Deviation OMC | Absolute Deviation MDUW |
| 2409599 | 10.0 | 122.4 | 10.7 | 121.7 | 134.7 | 10.9 | 122.0 | 122 | 0.98 | 0.38 |
| 2409599 | 10.0 | 122.4 | 9.6 | 122.2 | 133.9 | 10.6 | 123.0 | 123 | 0.66 | 0.62 |
| 2418452 | 6.9 | 140.8 | 7.1 | 140.7 | 150.7 | 7.0 | 141.0 | 141 | 0.06 | 0.24 |
| 2388175 | 7.0 | 136.3 | 7.6 | 136.1 | 146.4 | 7.7 | 136.0 | 136 | 0.72 | 0.28 |
| 2391204 | 8.3 | 136.7 | 7.5 | 135.9 | 146.1 | 7.7 | 136.0 | 136 | 0.57 | 0.72 |
| 2418113 | 7.4 | 136.6 | 6.8 | 136.4 | 145.7 | 7.6 | 137.0 | 137 | 0.15 | 0.44 |
| 2406238 | 8.7 | 137.4 | 7.5 | 133.5 | 143.5 | 8.1 | 134.0 | 134 | 0.64 | 3.40 |
| 2404487 | 8.2 | 137.5 | 7 | 136.4 | 145.9 | 7.6 | 137.0 | 137 | 0.68 | 0.52 |
| 2420069 | 8.3 | 131.9 | 8 | 131.8 | 142.3 | 8.4 | 132.0 | 132 | 0.14 | 0.13 |
| 2420070 | 8.3 | 131.9 | 9.6 | 130.2 | 142.7 | 8.6 | 131.0 | 131 | 0.34 | 0.87 |
| 2413637 | 12.7 | 118.3 | 11.6 | 117.6 | 131.2 | 12.4 | 118.0 | 118 | 0.32 | 0.29 |
| 2414461 | 8.5 | 134.2 | 8 | 134.1 | 144.8 | 8.1 | 134.0 | 134 | 0.47 | 0.18 |

**Absolute Deviation Values based on OHD Curves**

| Sample ID | Proctor Parameter | | 4-point density test | | | OHD Curves Predicted Values | | | | |
|---|---|---|---|---|---|---|---|---|---|---|
| | OMC | MDUW | Moisture Content | Density | Wet Density | One point OMC | One Point MDUW | Curve | Absolute Deviation OMC | Absolute Deviation MDUW |
| 2390119 | 9.5 | 130.2 | 9.1 | 130.1 | 141.9 | 9.3 | 130.7 | e | 0.15 | 0.47 |
| 2400445 | 11.4 | 127.1 | 8.7 | 122 | 132.6 | 10.5 | 126.6 | G | 0.88 | 0.54 |
| 2402606 | 8.6 | 132.8 | 7.3 | 131.4 | 141.0 | 8.5 | 134.1 | D | 0.10 | 1.30 |
| 2402606 | 8.6 | 132.8 | 9.2 | 132.5 | 144.7 | 8.5 | 134.1 | D | 0.10 | 1.30 |
| 2395185 | 11.0 | 129.2 | 9.6 | 125.9 | 138.0 | 10.1 | 128.0 | f | 0.88 | 1.20 |
| 2416173 | 7.3 | 133.5 | 5.9 | 131.8 | 139.6 | 7.9 | 136.3 | C | 0.63 | 2.80 |
| 2416173 | 7.3 | 133.5 | 7.3 | 133.5 | 143.2 | 8.2 | 135.2 | c | 0.93 | 1.70 |
| 2416173 | 7.3 | 133.5 | 9 | 131.2 | 143.0 | 9.0 | 132.0 | E | 1.73 | 1.50 |
| 2413907 | 9.4 | 125.7 | 9.4 | 125.7 | 137.5 | 10.1 | 128.0 | f | 0.70 | 2.30 |
| 2413907 | 9.4 | 125.7 | 11.8 | 121.2 | 135.5 | 11.9 | 121.7 | I | 2.50 | 4.00 |
| 2400552 | 7.6 | 131.7 | 7 | 131.2 | 140.4 | 8.5 | 134.1 | D | 0.86 | 2.39 |
| 2400552 | 7.6 | 131.7 | 9.5 | 130 | 142.4 | 9.3 | 130.7 | e | 1.66 | 1.01 |
| 2390640 | 8.5 | 131.7 | 6.9 | 128.3 | 137.2 | 8.7 | 133.0 | d | 0.15 | 1.28 |
| 2390640 | 8.5 | 131.7 | 8.4 | 131.7 | 142.8 | 8.7 | 133.0 | d | 0.15 | 1.28 |
| 2390640 | 8.5 | 131.7 | 9.5 | 130.2 | 142.6 | 9.3 | 130.7 | e | 0.75 | 1.02 |
| 2395860 | 10.1 | 131.8 | 8.8 | 130.5 | 142.0 | 9.0 | 132.0 | E | 1.14 | 0.20 |
| 2410583 | 8.8 | 129.0 | 7.9 | 128.5 | 138.7 | 9.0 | 132.0 | E | 0.18 | 3.03 |
| 2410583 | 8.8 | 129.0 | 9.2 | 128.9 | 140.8 | 9.7 | 129.3 | F | 0.88 | 0.33 |
| 2409672 | 8.3 | 132.8 | 7 | 130.4 | 139.5 | 8.5 | 134.1 | D | 0.18 | 1.35 |
| 2392228 | 10.2 | 127.0 | 8.7 | 124.7 | 135.5 | 10.1 | 128.0 | f | 0.14 | 1.00 |
| 2392228 | 10.2 | 127.0 | 10.2 | 127 | 140.0 | 10.1 | 128.0 | f | 0.14 | 1.00 |
| 2404911 | 9.2 | 129.7 | 8.6 | 129.5 | 140.6 | 9.3 | 130.7 | e | 0.12 | 0.96 |
| 2419984 | 10.0 | 127.6 | 9 | 125 | 136.3 | 10.1 | 128.0 | f | 0.08 | 0.39 |
| 2413595 | 7.7 | 134.0 | 7.1 | 133.1 | 142.6 | 8.2 | 135.2 | c | 0.46 | 1.18 |
| 2413595 | 7.7 | 134.0 | 9.5 | 126.3 | 138.3 | 10.1 | 128.0 | f | 2.36 | 6.02 |
| 2419324 | 8.9 | 130.3 | 7.7 | 128.8 | 138.7 | 9.0 | 132.0 | E | 0.14 | 1.69 |
| 2410531 | 9.9 | 129.4 | 8.8 | 128.3 | 139.6 | 9.3 | 130.7 | e | 0.57 | 1.27 |
| 2420067 | 8.3 | 131.9 | 8 | 131.8 | 142.3 | 8.7 | 133.0 | d | 0.41 | 1.13 |
| 2420067 | 8.3 | 131.9 | 9.6 | 130.2 | 142.7 | 9.3 | 130.7 | e | 1.01 | 1.17 |
| 2414295 | 8.0 | 132.6 | 7.9 | 132.6 | 143.1 | 8.5 | 134.1 | D | 0.54 | 1.49 |
| 2414295 | 8.0 | 132.6 | 9.6 | 128.8 | 141.2 | 9.7 | 129.3 | F | 1.74 | 3.31 |
| 2416366 | 8.1 | 139.7 | 7.1 | 136.2 | 145.9 | 7.6 | 137.7 | b | 0.52 | 1.99 |
| 2391011 | 7.4 | 139.6 | 6.2 | 138.1 | 146.7 | 6.9 | 140.5 | a | 0.48 | 0.88 |
| 2391011 | 7.4 | 139.6 | 7.5 | 139.6 | 150.1 | 6.6 | 141.8 | A | 0.78 | 2.18 |
| 2406521 | 7.7 | 137.6 | 6.9 | 137 | 146.5 | 7.6 | 137.7 | b | 0.08 | 0.13 |
| 2389811 | 7.4 | 133.9 | 7.5 | 133.9 | 143.9 | 8.2 | 135.2 | c | 0.83 | 1.29 |
| 2387741 | 8.2 | 131.1 | 7.7 | 131 | 141.1 | 8.7 | 133.0 | d | 0.49 | 1.90 |
| 2405743 | 8.1 | 138.4 | 7.6 | 138 | 148.5 | 7.2 | 139.1 | B | 0.93 | 0.74 |
| 2414351 | 8.4 | 136.2 | 7.1 | 134.5 | 144.0 | 7.9 | 136.3 | C | 0.52 | 0.14 |
| 2409289 | 11.9 | 119.8 | 11.1 | 119.6 | 132.9 | 12.3 | 120.5 | i | 0.44 | 0.68 |

## Absolute Deviation Values based on OHD Curves

| Sample ID | Proctor Parameter | | 4-point density test | | | OHD Curves Predicted Values | | | | |
|---|---|---|---|---|---|---|---|---|---|---|
| | OMC | MDUW | Moisture Content | Density | Wet Density | One point OMC | One Point MDUW | Curve | Absolute Deviation OMC | Absolute Deviation MDUW |
| 2409599 | 10.0 | 122.4 | 10.7 | 121.7 | 134.7 | 11.5 | 123.0 | h | 1.53 | 0.62 |
| 2409599 | 10.0 | 122.4 | 9.6 | 122.2 | 133.9 | 11.2 | 124.2 | H | 1.23 | 1.82 |
| 2418452 | 6.9 | 140.8 | 7.1 | 140.7 | 150.7 | 6.6 | 141.8 | A | 0.32 | 1.04 |
| 2388175 | 7.0 | 136.3 | 7.6 | 136.1 | 146.4 | 7.9 | 136.3 | C | 0.91 | 0.02 |
| 2391204 | 8.3 | 136.7 | 7.5 | 135.9 | 146.1 | 7.9 | 136.3 | C | 0.38 | 0.42 |
| 2418113 | 7.4 | 136.6 | 6.8 | 136.4 | 145.7 | 7.6 | 137.7 | b | 0.19 | 1.14 |
| 2406238 | 8.7 | 137.4 | 7.5 | 133.5 | 143.5 | 8.2 | 135.2 | c | 0.50 | 2.20 |
| 2404487 | 8.2 | 137.5 | 7 | 136.4 | 145.9 | 7.6 | 137.7 | b | 0.64 | 0.18 |
| 2420069 | 8.3 | 131.9 | 8 | 131.8 | 142.3 | 8.7 | 133.0 | d | 0.41 | 1.13 |
| 2420070 | 8.3 | 131.9 | 9.6 | 130.2 | 142.7 | 9.3 | 130.7 | e | 1.01 | 1.17 |
| 2413637 | 12.7 | 118.3 | 11.6 | 117.6 | 131.2 | 12.7 | 119.3 | J | 0.01 | 1.01 |
| 2414461 | 8.5 | 134.2 | 8 | 134.1 | 144.8 | 8.2 | 135.2 | c | 0.33 | 1.02 |

# Appendix D: Analysis of Agreement between Density-based and DCP-based Compaction Acceptance

# 2023-2025 SDDOT DCP Database - MDUW Based on SDDOT Curves

| Material ID (PCN) | Sample ID | In-Situ Density (pcf) | MDUW based on SDDOT Curve (pcf) | Relative Density | MC% | GN | SEAT (mm) | DPI (mm/blow) | Max Allowable SEAT | Max Allowable DPI | Adequate Compaction based on DCP Specification |
|---|---|---|---|---|---|---|---|---|---|---|---|
| 06P3 | 2456487 | 128 | 132 | 0.97 | 6.9 | 3.1 | 60 | 18 | 40 | 12 | No |
| 06P3 | 2456487 | 128 | 132 | 0.97 | 6.9 | 3.1 | 60 | 18 | 40 | 12 | No |
| 04HM | 2464078 | 132 | 136 | 0.97 | 7.7 | 4.3 | 9 | 10 | 60 | 17 | Yes |
| 04HM | 2464078 | 132 | 136 | 0.97 | 7.7 | 4.3 | 44 | 9 | 60 | 17 | Yes |
| 04HM | 2464268 | 139 | 135 | 1.03 | 7.1 | 4.5 | 20 | 9 | 60 | 17 | Yes |
| 04HM | 2464268 | 139 | 135 | 1.03 | 7.1 | 4.5 | 32 | 11 | 60 | 17 | Yes |
| 04HM | 2464268 | 139 | 135 | 1.03 | 7.1 | 4.5 | 17 | 5 | 60 | 17 | Yes |
| 04XC | 2405958 | 129 | 125 | 1.03 | 8.8 | 4.3 | 20 | 8 | 70 | 21 | Yes |
| 05HN | 2454260 | 147 | 140 | 1.05 | 4.9 | 3.9 | 34 | 12 | 40 | 10 | No |
| 07M9 | 2460463 | 133 | 131 | 1.02 | 5 | 4 | 28 | 10 | 45 | 15 | Yes |
| 05HN | 2461251 | 133 | 140 | 0.95 | 5.5 | 3.9 | 32 | 12 | 45 | 15 | Yes |
| 05HN | 2461252 | 133 | 140 | 0.95 | 5 | 3.9 | 39 | 17 | 45 | 15 | No |
| 01V7 | 2462696 | 143 | 135 | 1.06 | 4.4 | 3.9 | 19 | 8 | 40 | 10 | Yes |
| 05UW | 2463201 | 130 | 132 | 0.99 | 6.2 | 3.7 | 23 | 8 | 45 | 15 | Yes |
| 609 | 2463622 | 134 | 134 | 1.00 | 3.6 | 4.2 | 33 | 10 | 50 | 13 | Yes |
| 04JF | 2466702 | 135 | 132 | 1.02 | 5.4 | 4.1 | 25 | 10 | 60 | 17 | Yes |
| 04KR | 2397936 | 124 | 130 | 0.95 | 7.7 | 4.4 | 62 | 18 | 45 | 15 | No |
| 04X4 | 2411655 | 132 | 132 | 1.00 | 5.8 | 3.1 | 71 | 9 | 40 | 12 | No |
| 05ET | 2403896 | 129 | 132 | 0.97 | 6 | 4.1 | 47 | 12 | 60 | 17 | Yes |
| 06JF | 2397145 | 129 | 129 | 1.00 | 7.6 | 4 | 62 | 18 | 45 | 15 | No |
| 069Q | 2451448 | 130 | 132 | 0.99 | 6.1 | 4 | 35 | 12 | 45 | 15 | Yes |
| 06K7 | 2398137 | 142 | 132 | 1.08 | 5 | 4.2 | 22 | 7 | 60 | 17 | Yes |
| 05HW | 2456655 | 133 | 128 | 1.04 | 5.8 | 4 | 18 | 7 | 45 | 15 | Yes |
| 092U | 2459175 | 137 | 137 | 1.00 | 5.4 | 3.9 | 31 | 11 | 45 | 15 | Yes |
| 092U | 2459175 | 137 | 137 | 1.00 | 5.4 | 3.9 | 25 | 10 | 45 | 15 | Yes |
| 092U | 2459175 | 137 | 137 | 1.00 | 5.4 | 3.9 | 31 | 10 | 45 | 15 | Yes |
| 04FC | 2462110 | 118 | 118 | 1.00 | 12.1 | 3.9 | 25 | 7 | 55 | 19 | Yes |
| 035F | 2464060 | 132 | 134 | 0.98 | 3.4 | 4 | 19 | 6 | 40 | 10 | Yes |
| 06TD | 2465833 | 127 | 128 | 0.99 | 7.1 | 4.1 | 35 | 13 | 60 | 17 | Yes |
| 05F8 | 2395515 | 131 | 129 | 1.02 | 7.1 | 4 | 30 | 17 | 45 | 15 | No |
| 05F8 | 2396567 | 140 | 135 | 1.04 | 5.9 | 4 | 2 | 3 | 45 | 15 | Yes |

# 2023-2025 SDDOT DCP Database - MDUW Based on SDDOT Curves

| Material ID (PCN) | Sample ID | In-Situ Density (pcf) | MDUW based on SDDOT Curve (pcf) | Relative Density | MC% | GN | SEAT (mm) | DPI (mm/blow) | Max Allowable SEAT | Max Allowable DPI | Adequate Compaction based on DCP Specification |
|---|---|---|---|---|---|---|---|---|---|---|---|
| 06UM | 2397634 | 12.9.9 | 132 | 0.98 | 6.1 | 3.8 | 40 | 15 | 45 | 15 | Yes |
| 021G | 2398830 | 139 | 135 | 1.03 | 5.7 | 3.9 | 26 | 7 | 45 | 15 | Yes |
| 021G | 2399132 | 138 | 135 | 1.03 | 5.3 | 3.9 | 35 | 8 | 45 | 15 | Yes |
| 06UM | 2402461 | 133 | 133 | 1.00 | 5 | 3.8 | 34 | 13 | 45 | 15 | Yes |
| 081J | 2404363 | 149 | 136 | 1.10 | 5.6 | 3.8 | 18 | 10 | 45 | 15 | Yes |
| 06R3 | 2405409 | 143 | 134 | 1.06 | 4.3 | 4 | 22 | 9 | 40 | 10 | Yes |
| 021G | 2406495 | 138 | 135 | 1.03 | 4.9 | 3.8 | 35 | 13 | 40 | 10 | No |
| 08LD | 2406755 | 137 | 132 | 1.04 | 4.2 | 4.2 | 31 | 8 | 50 | 13 | Yes |
| 06FK | 2406749 | 138 | 142 | 0.97 | 3.6 | 4.2 | 12 | 5 | 50 | 13 | Yes |
| 08P3 | 2409196 | 134 | 123 | 1.09 | 11.4 | 3.5 | 25 | 7 | 40 | 16 | Yes |
| 07ME | 2409511 | 137 | 141 | 0.97 | 3.9 | 3.5 | 22 | 8 | 40 | 10 | Yes |

# 2023-2025 SDDOT DCP Database - MDUW Based on OHD Curves

| Material ID (PCN) | Sample ID | In-Situ Density (pcf) | MDUW based on OHD Curve (pcf) | Relative Density | MC% | GN | SEAT (mm) | DPI (mm/blow) | Max Allowable SEAT | Max Allowable DPI | Adequate Compaction based on DCP |
|---|---|---|---|---|---|---|---|---|---|---|---|
| 05EX | 2447755 | 130 | 132 | 0.99 | 9.3 | 4.3 | 51 | 17 | 70 | 21 | Yes |
| 05EX | 2447893 | 121 | 132 | 0.92 | 9.3 | 4.3 | 54 | 13 | 70 | 21 | Yes |
| 05EX | 2447895 | 121 | 132 | 0.92 | 9.3 | 4.3 | 42 | 11 | 70 | 21 | Yes |
| 05EX | 2449849 | 132 | 132 | 1.00 | 8.5 | 4.2 | 25 | 15 | 70 | 21 | Yes |
| 05EX | 2449862 | 132 | 132 | 1.00 | 8.5 | 4.2 | 40 | 12 | 70 | 21 | Yes |
| 05EX | 2449863 | 132 | 132 | 1.00 | 8.5 | 4.2 | 28 | 15 | 70 | 21 | Yes |
| 06P3 | 2456487 | 128 | 133 | 0.96 | 6.9 | 3.1 | 60 | 18 | 40 | 12 | No |
| 06P3 | 2456487 | 128 | 133 | 0.96 | 6.9 | 3.1 | 60 | 18 | 40 | 12 | No |
| 04HM | 2464078 | 132 | 136 | 0.97 | 7.7 | 4.3 | 9 | 10 | 60 | 17 | Yes |
| 04HM | 2464078 | 132 | 136 | 0.97 | 7.7 | 4.3 | 44 | 9 | 60 | 17 | Yes |
| 04HM | 2464268 | 139 | 136 | 1.02 | 7.1 | 4.5 | 20 | 9 | 60 | 17 | Yes |
| 04HM | 2464268 | 139 | 136 | 1.02 | 7.1 | 4.5 | 32 | 11 | 60 | 17 | Yes |
| 04HM | 2464268 | 139 | 136 | 1.02 | 7.1 | 4.5 | 17 | 5 | 60 | 17 | Yes |
| 04XC | 2401780 | 123 | 123 | 1.00 | 8.7 | 4.3 | 36 | 9 | 70 | 21 | Yes |
| 04XC | 2401984 | 124 | 125 | 0.99 | 7.9 | 4.3 | 25 | 9 | 60 | 17 | Yes |
| 04XC | 2405958 | 129 | 125 | 1.03 | 8.8 | 4.3 | 20 | 8 | 70 | 21 | Yes |
| 05HN | 2454260 | 147 | 142 | 1.04 | 4.9 | 3.9 | 34 | 12 | 40 | 10 | No |
| 07M9 | 2460463 | 133 | 132 | 1.01 | 5 | 4 | 28 | 10 | 45 | 15 | Yes |
| 05HN | 2461251 | 133 | 141 | 0.95 | 5.5 | 3.9 | 32 | 12 | 45 | 15 | Yes |
| 05HN | 2461252 | 133 | 141 | 0.95 | 5 | 3.9 | 39 | 17 | 45 | 15 | No |
| 01V7 | 2462696 | 143 | 136 | 1.05 | 4.4 | 3.9 | 19 | 8 | 40 | 10 | Yes |
| 05UW | 2463201 | 130 | 134 | 0.97 | 6.2 | 3.7 | 23 | 8 | 45 | 15 | Yes |
| 609 | 2463622 | 134 | 135 | 0.99 | 3.6 | 4.2 | 33 | 10 | 50 | 13 | Yes |
| 04JF | 2466702 | 135 | 134 | 1.01 | 5.4 | 4.1 | 25 | 10 | 60 | 17 | Yes |
| 04KR | 2397936 | 124 | 132 | 0.94 | 7.7 | 4.4 | 62 | 18 | 45 | 15 | No |
| 04X4 | 2411655 | 132 | 134 | 0.98 | 5.8 | 3.1 | 71 | 9 | 40 | 12 | No |
| 05ET | 2403896 | 129 | 133 | 0.97 | 6 | 4.1 | 47 | 12 | 60 | 17 | Yes |
| 06JF | 2397145 | 129 | 132 | 0.97 | 7.6 | 4 | 62 | 18 | 45 | 15 | No |
| 06K4 | 2403587 | 127 | 132 | 0.96 | 5.1 | 4.4 | 53 | 16 | 60 | 17 | Yes |
| 069Q | 2451448 | 130 | 133 | 0.98 | 6.1 | 4 | 35 | 12 | 45 | 15 | Yes |
| 06K7 | 2398137 | 142 | 133 | 1.07 | 5 | 4.2 | 22 | 7 | 60 | 17 | Yes |
| 05HW | 2456655 | 133 | 129 | 1.03 | 5.8 | 4 | 18 | 7 | 45 | 15 | Yes |
| 092U | 2459175 | 137 | 138 | 0.99 | 5.4 | 3.9 | 31 | 11 | 45 | 15 | Yes |

# 2023-2025 SDDOT DCP Database - MDUW Based on OHD Curves

| Material ID (PCN) | Sample ID | In-Situ Density (pcf) | MDUW based on OHD Curve (pcf) | Relative Density | MC% | GN | SEAT (mm) | DPI (mm/blow) | Max Allowable SEAT | Max Allowable DPI | Adequate Compaction based on DCP |
|---|---|---|---|---|---|---|---|---|---|---|---|
| 092U | 2459175 | 137 | 138 | 0.99 | 5.4 | 3.9 | 25 | 10 | 45 | 15 | Yes |
| 092U | 2459175 | 137 | 138 | 0.99 | 5.4 | 3.9 | 31 | 10 | 45 | 15 | Yes |
| 04FC | 2462110 | 118 | 119 | 0.99 | 12.1 | 3.9 | 25 | 7 | 55 | 19 | Yes |
| 035F | 2464060 | 132 | 136 | 0.97 | 3.4 | 4 | 19 | 6 | 40 | 10 | Yes |
| 06TD | 2465833 | 127 | 131 | 0.97 | 7.1 | 4.1 | 35 | 13 | 60 | 17 | Yes |
| 05F8 | 2395515 | 131 | 132 | 0.99 | 7.1 | 4 | 30 | 17 | 45 | 15 | No |
| 05F8 | 2396567 | 140 | 138 | 1.02 | 5.9 | 4 | 2 | 3 | 45 | 15 | Yes |
| 06UM | 2397634 | 130 | 134 | 0.97 | 6.1 | 3.8 | 40 | 15 | 45 | 15 | Yes |
| 021G | 2398830 | 139 | 138 | 1.01 | 5.7 | 3.9 | 26 | 7 | 45 | 15 | Yes |
| 021G | 2399132 | 138 | 138 | 1.01 | 5.3 | 3.9 | 35 | 8 | 45 | 15 | Yes |
| 06UM | 2402461 | 133 | 134 | 0.99 | 5 | 3.8 | 34 | 13 | 45 | 15 | Yes |
| 081J | 2403816 | 125 | 139 | 0.90 | 2.8 | 3.5 | 64 | 21 | 40 | 10 | No |
| 081J | 2404363 | 149 | 138 | 1.08 | 5.6 | 3.8 | 18 | 10 | 45 | 15 | Yes |
| 08LD | 2404863 | 141 | 138 | 1.02 | 5.4 | 4.2 | 36 | 13 | 60 | 17 | Yes |
| 06R3 | 2405409 | 143 | 135 | 1.06 | 4.3 | 4 | 22 | 9 | 40 | 10 | Yes |
| 021G | 2406495 | 138 | 136 | 1.02 | 4.9 | 3.8 | 35 | 13 | 40 | 10 | No |
| 08LD | 2406755 | 137 | 133 | 1.03 | 4.2 | 4.2 | 31 | 8 | 50 | 13 | Yes |
| 06FK | 2406749 | 138 | 142 | 0.97 | 3.6 | 4.2 | 12 | 5 | 50 | 13 | Yes |
| 08P3 | 2409196 | 134 | 124 | 1.08 | 11.4 | 3.5 | 25 | 7 | 40 | 16 | Yes |
| 07ME | 2409511 | 137 | 142 | 0.97 | 3.9 | 3.5 | 22 | 8 | 40 | 10 | Yes |

## 2019 SDDOT DCP Database - MDUW Based on SDDOT Curves

| Base Type | In-Situ Density (pcf) | MDUW based on SDDOT Curve (pcf) | Relative Density | MC (%) | GN | SEAT (mm) | PIV (mm/ blow) | Max Allowable SEAT | Max Allowable DPI | Adequate Compaction based on DCP Specification |
|---|---|---|---|---|---|---|---|---|---|---|
| 03RQ | 110.2 | 122 | 0.90 | 7.10 | 3.6 | 67 | 15 | 45 | 15 | No |
| | 111.8 | 122 | 0.92 | 7.40 | 3.6 | 59 | 17 | 45 | 15 | No |
| | 122.9 | 122 | 1.01 | 8.20 | 3.6 | 43 | 15 | 55 | 19 | Yes |
| | 106.3 | 122 | 0.87 | 7.10 | 3.6 | 61 | 13 | 45 | 15 | No |
| | 118.3 | 122 | 0.97 | 7.40 | 3.6 | 55 | 13 | 45 | 15 | No |
| | 119.9 | 122 | 0.98 | 5.80 | 3.6 | 49 | 14 | 45 | 15 | No |
| | 111.6 | 122 | 0.91 | 7.30 | 3.6 | 60 | 15 | 45 | 15 | No |
| | 118.8 | 122 | 0.97 | 7.60 | 3.6 | 56 | 14 | 45 | 15 | No |
| | 117.2 | 122 | 0.96 | 6.20 | 3.6 | 62 | 13 | 45 | 15 | No |
| 5777 | 132 | 136 | 0.97 | 4.70 | 4.2 | 63 | 8 | 50 | 13 | No |
| | 133.9 | 136 | 0.98 | 4.90 | 4.2 | 53 | 12 | 50 | 13 | No |
| | 141.2 | 136 | 1.04 | 4.40 | 4.2 | 33 | 10 | 50 | 13 | Yes |
| | 144.1 | 136 | 1.06 | 5.20 | 4.2 | 42 | 8 | 60 | 17 | Yes |
| | 132 | 136 | 0.97 | 4.20 | 4.2 | 49 | 10 | 50 | 13 | Yes |
| | 152.1 | 136 | 1.12 | 4.50 | 4.2 | 32 | 10 | 50 | 13 | Yes |
| | 139.2 | 136 | 1.02 | 5.20 | 4.2 | 34 | 9 | 60 | 17 | Yes |
| | 147.8 | 136 | 1.09 | 5.50 | 4.2 | 38 | 10 | 60 | 17 | Yes |
| | 145.8 | 136 | 1.07 | 4.30 | 4.2 | 27 | 9 | 50 | 13 | Yes |
| 025D | 119.7 | 131 | 0.91 | 6.80 | 4 | 51 | 17 | 45 | 15 | No |
| | 119.6 | 131 | 0.91 | 7.90 | 4 | 60 | 17 | 45 | 15 | No |
| | 117.8 | 131 | 0.90 | 6.80 | 4 | 58 | 14 | 45 | 15 | No |
| | 115.1 | 131 | 0.88 | 7.10 | 4 | 70 | 14 | 45 | 15 | No |
| | 111.3 | 131 | 0.85 | 6.80 | 4 | 57 | 13 | 45 | 15 | No |
| | 110.4 | 131 | 0.84 | 6.80 | 4 | 58 | 14 | 45 | 15 | No |
| | 116.3 | 131 | 0.89 | 7.50 | 4 | 45 | 14 | 45 | 15 | Yes |
| | 120.4 | 131 | 0.92 | 7.60 | 4 | 58 | 17 | 45 | 15 | No |
| | 118.7 | 131 | 0.91 | 6.00 | 4 | 62 | 15 | 45 | 15 | No |
| 06DJ | 119.7 | 128 | 0.94 | 6.80 | 4.3 | 49 | 16 | 60 | 17 | Yes |
| | 119.6 | 128 | 0.93 | 7.90 | 4.3 | 55 | 16 | 60 | 17 | Yes |
| | 117.8 | 128 | 0.92 | 6.80 | 4.3 | 55 | 14 | 60 | 17 | Yes |
| | 115.1 | 128 | 0.90 | 7.10 | 4.3 | 44 | 16 | 60 | 17 | Yes |
| | 111.3 | 128 | 0.87 | 6.80 | 4.3 | 70 | 21 | 60 | 17 | No |
| | 110.4 | 128 | 0.86 | 6.80 | 4.3 | 56 | 16 | 60 | 17 | Yes |

## 2019 SDDOT DCP Database - MDUW Based on SDDOT Curves

| Base Type | In-Situ Density (pcf) | MDUW based on SDDOT Curve (pcf) | Relative Density | MC (%) | GN | SEAT (mm) | PIV (mm/ blow) | Max Allowable SEAT | Max Allowable DPI | Adequate Compaction based on DCP Specification |
|---|---|---|---|---|---|---|---|---|---|---|
| | 116.3 | 128 | 0.91 | 7.50 | 4.3 | 67 | 15 | 60 | 17 | No |
| | 120.4 | 128 | 0.94 | 7.60 | 4.3 | 73 | 18 | 60 | 17 | No |
| | 118.7 | 128 | 0.93 | 6.00 | 4.3 | 95 | 12 | 60 | 17 | No |
| 04JY | 119 | 128 | 0.93 | 3.30 | 4.3 | 70 | 19 | 50 | 13 | No |
| | 123.5 | 128 | 0.96 | 3.50 | 4.3 | 42 | 13 | 50 | 13 | Yes |
| | 128.8 | 128 | 1.01 | 3.80 | 4.3 | 28 | 9 | 50 | 13 | Yes |
| | 119.6 | 128 | 0.93 | 3.20 | 4.3 | 63 | 16 | 50 | 13 | No |
| | 123.2 | 128 | 0.96 | 4.10 | 4.3 | 43 | 13 | 50 | 13 | Yes |
| | 129.8 | 128 | 1.01 | 4.20 | 4.3 | 30 | 10 | 50 | 13 | Yes |
| | 115.5 | 128 | 0.90 | 3.80 | 4.3 | 53 | 16 | 50 | 13 | No |
| | 120.7 | 128 | 0.94 | 3.60 | 4.3 | 44 | 12 | 50 | 13 | Yes |
| | 121.6 | 128 | 0.95 | 3.50 | 4.3 | 31 | 10 | 50 | 13 | Yes |
| 04D7 | 107.9 | 133 | 0.81 | 4.00 | 3.9 | 71 | 23 | 40 | 10 | No |
| | 110.5 | 133 | 0.83 | 4.70 | 3.9 | 66 | 19 | 40 | 10 | No |
| | 117.2 | 133 | 0.88 | 5.00 | 3.9 | 48 | 16 | 45 | 15 | No |
| | 106.4 | 133 | 0.80 | 4.60 | 3.9 | 73 | 17 | 40 | 10 | No |
| | 111.6 | 133 | 0.84 | 4.70 | 3.9 | 70 | 18 | 40 | 10 | No |
| | 123.5 | 133 | 0.93 | 4.60 | 3.9 | 53 | 19 | 40 | 10 | No |
| | 112.4 | 133 | 0.85 | 4.90 | 3.9 | 72 | 18 | 40 | 10 | No |
| | 117.2 | 133 | 0.88 | 4.80 | 3.9 | 54 | 19 | 40 | 10 | No |
| | 117.6 | 133 | 0.88 | 4.40 | 3.9 | 44 | 16 | 40 | 10 | No |
| 4E7 | 124.8 | 124 | 1.01 | 8.40 | 4.1 | 54 | 14 | 70 | 21 | Yes |
| | 126.5 | 124 | 1.02 | 9.10 | 4.1 | 48 | 13 | 70 | 21 | Yes |
| | 127.6 | 124 | 1.03 | 8.10 | 4.1 | 58 | 12 | 70 | 21 | Yes |
| | 123.4 | 124 | 1.00 | 7.50 | 4.1 | 54 | 13 | 60 | 17 | Yes |
| | 124 | 124 | 1.00 | 7.50 | 4.1 | 57 | 13 | 60 | 17 | Yes |
| | 127.9 | 124 | 1.03 | 7.60 | 4.1 | 51 | 13 | 60 | 17 | Yes |
| | 120.6 | 124 | 0.97 | 7.40 | 4.1 | 57 | 14 | 60 | 17 | Yes |
| | 123.7 | 124 | 1.00 | 8.60 | 4.1 | 54 | 15 | 70 | 21 | Yes |
| | 127.9 | 124 | 1.03 | 7.80 | 4.1 | 42 | 12 | 60 | 17 | Yes |
| | 135 | 131 | 1.03 | 6.20 | 4 | 61 | 13 | 45 | 15 | No |
| | 133.4 | 131 | 1.02 | 6.10 | 4 | 62 | 14 | 45 | 15 | No |
| | 139 | 131 | 1.06 | 6.60 | 4 | 42 | 12 | 45 | 15 | Yes |

# 2019 SDDOT DCP Database - MDUW Based on SDDOT Curves

| Base Type | In-Situ Density (pcf) | MDUW based on SDDOT Curve (pcf) | Relative Density | MC (%) | GN | SEAT (mm) | PIV (mm/ blow) | Max Allowable SEAT | Max Allowable DPI | Adequate Compaction based on DCP Specification |
|---|---|---|---|---|---|---|---|---|---|---|
| 04HK | 133.8 | 131 | 1.02 | 6.30 | 4 | 66 | 11 | 45 | 15 | No |
| | 133.2 | 131 | 1.02 | 5.90 | 4 | 61 | 12 | 45 | 15 | No |
| | 140.9 | 131 | 1.08 | 6.40 | 4 | 46 | 14 | 45 | 15 | No |
| | 138.2 | 131 | 1.05 | 6.40 | 4 | 59 | 13 | 45 | 15 | No |
| | 137.4 | 131 | 1.05 | 7.20 | 4 | 59 | 14 | 45 | 15 | No |
| | 136.2 | 131 | 1.04 | 6.90 | 4 | 62 | 14 | 45 | 15 | No |

## 2019 SDDOT DCP Database - MDUW Based on OHD Curves

| Base Type | In-Situ Density (pcf) | MDUW Based on Ohio Curve (pcf) | Relative Density OH | MC (%) | GN | SEAT (mm) | PIV (mm/ blow) | Max Allowable SEAT | Max Allowable DPI | Adequate Compaction based on DCP Specification |
|---|---|---|---|---|---|---|---|---|---|---|
| 5777 | 132 | 138 | 0.96 | 4.70 | 4.2 | 63 | 8 | 50 | 13 | No |
| | 133.9 | 138 | 0.97 | 4.90 | 4.2 | 53 | 12 | 50 | 13 | No |
| | 141.2 | 138 | 1.03 | 4.40 | 4.2 | 33 | 10 | 50 | 13 | Yes |
| | 144.1 | 138 | 1.05 | 5.20 | 4.2 | 42 | 8 | 60 | 17 | Yes |
| | 132 | 138 | 0.96 | 4.20 | 4.2 | 49 | 10 | 50 | 13 | Yes |
| | 152.1 | 138 | 1.10 | 4.50 | 4.2 | 32 | 10 | 50 | 13 | Yes |
| | 139.2 | 138 | 1.01 | 5.20 | 4.2 | 34 | 9 | 60 | 17 | Yes |
| | 147.8 | 138 | 1.07 | 5.50 | 4.2 | 38 | 10 | 60 | 17 | Yes |
| | 145.8 | 138 | 1.06 | 4.30 | 4.2 | 27 | 9 | 50 | 13 | Yes |
| 025D | 119.7 | 133 | 0.90 | 6.80 | 4 | 51 | 17 | 45 | 15 | No |
| | 119.6 | 133 | 0.90 | 7.90 | 4 | 60 | 17 | 45 | 15 | No |
| | 117.8 | 133 | 0.89 | 6.80 | 4 | 58 | 14 | 45 | 15 | No |
| | 115.1 | 133 | 0.87 | 7.10 | 4 | 70 | 14 | 45 | 15 | No |
| | 111.3 | 133 | 0.84 | 6.80 | 4 | 57 | 13 | 45 | 15 | No |
| | 110.4 | 133 | 0.83 | 6.80 | 4 | 58 | 14 | 45 | 15 | No |
| | 116.3 | 133 | 0.87 | 7.50 | 4 | 45 | 14 | 45 | 15 | Yes |
| | 120.4 | 133 | 0.91 | 7.60 | 4 | 58 | 17 | 45 | 15 | No |
| | 118.7 | 133 | 0.89 | 6.00 | 4 | 62 | 15 | 45 | 15 | No |
| 06DJ | 119.7 | 131 | 0.92 | 6.80 | 4.3 | 49 | 16 | 60 | 17 | Yes |
| | 119.6 | 131 | 0.92 | 7.90 | 4.3 | 55 | 16 | 60 | 17 | Yes |
| | 117.8 | 131 | 0.90 | 6.80 | 4.3 | 55 | 14 | 60 | 17 | Yes |
| | 115.1 | 131 | 0.88 | 7.10 | 4.3 | 44 | 16 | 60 | 17 | Yes |
| | 111.3 | 131 | 0.85 | 6.80 | 4.3 | 70 | 21 | 60 | 17 | No |
| | 110.4 | 131 | 0.84 | 6.80 | 4.3 | 56 | 16 | 60 | 17 | Yes |
| | 116.3 | 131 | 0.89 | 7.50 | 4.3 | 67 | 15 | 60 | 17 | No |
| | 120.4 | 131 | 0.92 | 7.60 | 4.3 | 73 | 18 | 60 | 17 | No |
| | 118.7 | 131 | 0.91 | 6.00 | 4.3 | 95 | 12 | 60 | 17 | No |
| 042U | 108.6 | 116 | 0.94 | 9.70 | 3.8 | 69 | 19 | 55 | 19 | No |
| | 111.6 | 116 | 0.96 | 9.50 | 3.8 | 57 | 18 | 55 | 19 | No |
| | 111 | 116 | 0.96 | 10.20 | 3.8 | 43 | 14 | 55 | 19 | Yes |
| | 109.8 | 116 | 0.95 | 9.80 | 3.8 | 72 | 19 | 55 | 19 | No |
| | 111.5 | 116 | 0.96 | 8.80 | 3.8 | 56 | 17 | 55 | 19 | No |
| | 112.8 | 116 | 0.97 | 9.40 | 3.8 | 47 | 15 | 55 | 19 | Yes |

## 2019 SDDOT DCP Database - MDUW Based on OHD Curves

| Base Type | In-Situ Density (pcf) | MDUW Based on Ohio Curve (pcf) | Relative Density OH | MC (%) | GN | SEAT (mm) | PIV (mm/ blow) | Max Allowable SEAT | Max Allowable DPI | Adequate Compaction based on DCP Specification |
|---|---|---|---|---|---|---|---|---|---|---|
| | 105 | 116 | 0.91 | 9.20 | 3.8 | 68 | 18 | 55 | 19 | No |
| | 111.5 | 116 | 0.96 | 8.60 | 3.8 | 53 | 15 | 55 | 19 | Yes |
| | 115.2 | 116 | 0.99 | 9.60 | 3.8 | 48 | 15 | 55 | 19 | Yes |
| 4E7 | 124.8 | 127 | 0.99 | 8.40 | 4.1 | 54 | 14 | 70 | 21 | Yes |
| | 126.5 | 127 | 1.00 | 9.10 | 4.1 | 48 | 13 | 70 | 21 | Yes |
| | 127.6 | 127 | 1.01 | 8.10 | 4.1 | 58 | 12 | 70 | 21 | Yes |
| | 123.4 | 127 | 0.97 | 7.50 | 4.1 | 54 | 13 | 60 | 17 | Yes |
| | 124 | 127 | 0.98 | 7.50 | 4.1 | 57 | 13 | 60 | 17 | Yes |
| | 127.9 | 127 | 1.01 | 7.60 | 4.1 | 51 | 13 | 60 | 17 | Yes |
| | 120.6 | 127 | 0.95 | 7.40 | 4.1 | 57 | 14 | 60 | 17 | Yes |
| | 123.7 | 127 | 0.98 | 8.60 | 4.1 | 54 | 15 | 70 | 21 | Yes |
| | 127.9 | 127 | 1.01 | 7.80 | 4.1 | 42 | 12 | 60 | 17 | Yes |
| 04HK | 135 | 133 | 1.02 | 6.20 | 4 | 61 | 13 | 45 | 15 | No |
| | 133.4 | 133 | 1.00 | 6.10 | 4 | 62 | 14 | 45 | 15 | No |
| | 139 | 133 | 1.05 | 6.60 | 4 | 42 | 12 | 45 | 15 | Yes |
| | 133.8 | 133 | 1.01 | 6.30 | 4 | 66 | 11 | 45 | 15 | No |
| | 133.2 | 133 | 1.00 | 5.90 | 4 | 61 | 12 | 45 | 15 | No |
| | 140.9 | 133 | 1.06 | 6.40 | 4 | 46 | 14 | 45 | 15 | No |
| | 138.2 | 133 | 1.04 | 6.40 | 4 | 59 | 13 | 45 | 15 | No |
| | 137.4 | 133 | 1.03 | 7.20 | 4 | 59 | 14 | 45 | 15 | No |
| | 136.2 | 133 | 1.02 | 6.90 | 4 | 62 | 14 | 45 | 15 | No |